AN INITIAL INVESTIGATION INTO METHODS OF COMPUTING TRANSONIC AERODYNAMIC SENSITIVITY COEFFICIENTS

aerospace engineering department

Final Report

TEXAS A&M UNIVERSITY

TAMRF Report No. 5802-94-01
March 1994

NASA Grant No. NAG-1-793

Leland A. Carlson
Professor of Aerospace Engineering
Texas A&M University
College Station, TX 77843-3141

TEXAS ENGINEERING EXPERIMENT STATION

AN INITIAL INVESTIGATION INTO METHODS OF COMPUTING TRANSONIC AERODYNAMIC SENSITIVITY COEFFICIENTS

Final Report

TAMRF Report No. 5802-94-01
March 1994

NASA Grant No. NAG-1-793

Leland A. Carlson
Professor of Aerospace Engineering
Texas A&M University
College Station, TX 77843-3141

AN INITIAL INVESTIGATION INTO METHODS OF COMPUTING TRANSONIC AERODYNAMIC SENSITIVITY COEFFICIENTS

I. Introduction

This final report will attempt to concisely summarize the activities and accomplishments associated with NASA Grant NAG-1-793. The project started on July 1, 1987 and officially terminated on December 31, 1994. While the total funding for the project was $110,395, many lengthy periods existed in which little or no funds were available for expenditure by the project; and all grant funds were essentially expended by August 31, 1993. Fortunately, the effort was maintained by significant financial support by the Aerospace Engineering Department in the form of Graduate Assistantship funds and faculty salary support and by moral and technical support from NASA Langley. In spite of these difficulties, significant accomplishments were achieved by the project; and these are summarized below.

II. Personnel

The individuals who have been associated with the project are as follows:

Leland A. Carlson, Professor of Aerospace Engineering -- Dr. Carlson served as the principal investigator for the project. At various times, Dr., Carlson was partially supported by the project.

Hesham M. El-banna, Graduate Research Assistant and Graduate Assistant Non-Teaching (GANT) -- Hesham El-banna joined the project at its inception. During the project, he earned his Masters' and Ph.D. degrees using research associated with the project for his thesis and dissertation. Dr. El-banna was partially supported by the project at various times. He was also extensively supported by the Aerospace Engineering Department as a GANT.

Alan Arslan -- Graduate Research Assistant Non-Teaching -- Alan Arslan joined the project in Fall 1992. He was supported by the Aerospace Engineering Department as a GANT. He used research associated with the project for his masters' thesis.

III. Accomplishments

The primary accomplishments of the project are as follows:

1. Using the transonic small perturbation equation as a flowfield model, the project demonstrated that the quasi-analytical method could be used to obtain aerodynamic sensitivity coefficients for airfoils at subsonic, transonic, and supersonic conditions for design variables such as Mach number, airfoil thickness, maximum camber, angle of attack, and location of maximum camber. The approach

was validated by comparison to results obtained using the finite difference technique. It was established that the quasi-analytical approach was an accurate method for obtaining aerodynamic sensitivity derivatives for airfoils at transonic conditions and usually more efficient than the finite difference approach. These initial results were among the first aerodynamic sensitivity results obtained by the quasi-analytical approach for transonic conditions.

2. The usage of symbolic manipulation software to determine the appropriate expressions and computer coding associated with the quasi-analytical method for sensitivity derivatives was investigated. Using the three dimensional fully conservative full potential flowfield model, it was determined that symbolic manipulation along with a chain rule approach was extremely useful in developing a combined flowfield and quasi-analytical sensitivity derivative code capable of considering a large number of realistic design variables. Various methods of solving the resulting large system of quasi-analytical equations were investigated. It was concluded that for the direct solver approach, that the iterative conjugate gradient method was accurate, capable of handling a large number of design variables, and more efficient than the finite difference approach.

3. Using the three dimensional fully conservative full potential flowfield model, the quasi-analytical method was applied to swept wings (i.e. three dimensional) at transonic flow conditions. The study included as basic design variables freestream Mach number, wing angle of attack, airfoil thickness, airfoil camber, location of airfoil maximum camber, wing twist angles at four spanwise locations, and the coordinates of the wing tip. From sensitivity derivatives for these design variables, sensitivities were also obtained for other variables of interest such as wing area, aspect ratio, wing sweep, and taper ratio. The resultant sensitivity derivative results were verified by comparison with finite difference computations. Sensitivity derivatives were obtained chordwise for $\partial C_p/\partial X_D$, spanwise for $\partial C_l/\partial X_D$, and overall for $\partial C_L/\partial X_D$, where X_D is any design variable. The sensitivity derivatives were also use to predict pressure distributions and aerodynamic coefficients at conditions different from those at which the derivatives were obtained. These predicted results demonstrated that sensitivity derivatives could be used over limited ranges for predictive purposes. Sensitivity derivatives were also obtained over a range of Mach numbers ranging from 0.8 up to 1.2 and for a variety of wing airfoil sections. These results demonstrated the feasibility and usefulness of the quasi-analytical approach for obtaining aerodynamic sensitivity derivatives about wings. It is believed that they were among the first sensitivity results to be obtained using the quasi-analytical method for wings at transonic conditions.

4. The incremental iterative technique has been applied to the three dimensional transonic nonlinear small perturbation flowfield formulation, an equivalent plate deflection model, and the associated aerodynamic and structural discipline sensitivity equations; and coupled aeroelastic results for an aspect ratio three wing in transonic flow have been obtained. This approach permitted the use

of finer grids and inclusion of both aerodynamic and structural sensitivity derivatives with the final results including full aeroelastic coupling. In addition, system sensitivity derivatives were obtained. Results were obtained for nine aerodynamic design variables and four structural design variables. The results demonstrated the usefulness and feasibility of combining the incremental iterative approach with the quasi-analytical formulation for obtaining both discipline and system sensitivity derivatives. Again, these are among the first results to utilize the quasi-analytical approach to obtain aerodynamic-structural coupled sensitivity derivatives and system sensitivity derivatives. However, it appears that further studies are needed in methods associated with determining system sensitivities and of utilizing this information in optimization procedures. This effort is discussed in Section IV below.

IV. Progress in the Last Six Months

During the past six months, Arslan and Carlson as part of a pilot study have applied the incremental iterative technique to the transonic nonlinear small perturbation formulation, an equivalent plate deflection model, and the associated discipline sensitivity equations, to obtain coupled aeroelastic results for an AR=3 wing in transonic flow. This integrated approach allows the use of finer grids and simultaneously yields the aerodynamic and structural deflection solutions, the aerodynamic sensitivity derivatives for nine aerodynamic design variables, the structural sensitivities for four design variables, and the coupling derivatives needed for the system derivatives, which are computed subsequently. It is outlined in Fig. 1.

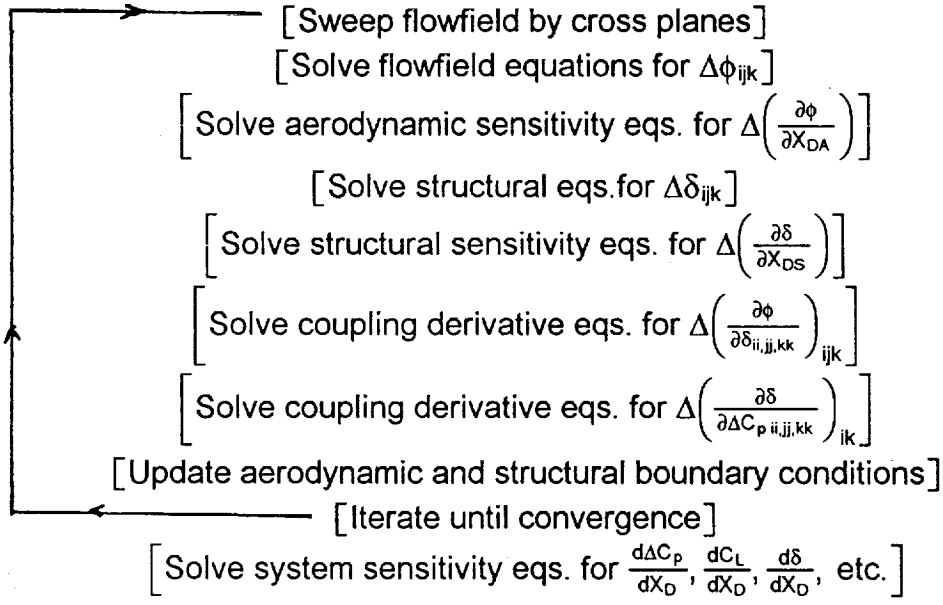

Fig. 1 -- Integrated Solution Approach

Basic aerodynamic sensitivities were obtained at all 97x16x16 flowfield points while aerodynamic coefficient and structural deflection derivatives were computed

at 980 wing surface points, comprising ten half-span stations each having 49 points on top and 49 on the lower surface. System derivatives were obtained with the Global System Equation Method 2 (GSE2). Since Sobieski has suggested that system derivatives can be obtained using condensed information, system sensitivities were computed from the fine grid aerodynamic, structures, and discipline sensitivity results for two condensed cases. The first computed system sensitivities at eight half-span stations each with 13 chordwise locations and the second used five half-span stations each with 25 chordwise values. Limiting the number of system sensitivities is desirable since the coupling derivatives required to compute them treat each δ and ΔC_p considered in the system formulation as a design variable. Thus, even for the condensed problem using a 25x5 system grid, the number of design variables was effectively 138; and 125 lengthy coupling vectors $\partial\delta/\partial\Delta C_{pk}$ and $\partial\Delta C_p/\partial\delta_k$ had to be computed. Obviously, the inclusion of system sensitivities greatly increases the problem complexity. While results were obtained at each wing station, representative results for the 97x16x16 flowfield, 49x10 structural, and 25x5 system case are shown on Fig. 2. The wing was at $M_\infty = 0.82$, $\alpha = 2^0$, had 1^0 of twist (T_{tip}), and the airfoil sections varied from a NACA 2406 at the root to a NACA 1706 at the tip. The deflected wing position is shown dotted, the $\partial C_p/\partial T_{tip}$ curves are for the upper and lower surfaces, and in the two lower plots the discipline derivatives are dotted while the system sensitivities are solid. Note that the flow is supercritical, that the wing has significant deflection and twist due to aerodynamic loading, and the upper surface shock wave strongly affects the aerodynamic derivatives. Also, note that the system derivative $d\Delta C_p/dT_{tip}$ is significantly different from the discipline value near the trailing edge due to twist induced by aerodynamic-structural coupling, and that $d\delta/dt$, where t is a wing structural thickness parameter, differs in magnitude and sign from the corresponding discipline result, $\partial\delta/\partial t$.

Unfortunately, comparison of the 13x8 and 25x5 system derivative results indicates differences in values, magnitudes, and sometimes signs. Since these sensitivities were obtained from the same fine grid aerodynamic, structural, and discipline sensitivity solutions and since the differences do not appear to be due to numerical error, they must be associated with the system derivative solution approach, the number and location of condensed points considered, etc.

Since accurate system derivatives are required before the optimization portion of a MDDO process can be applied to transonic wing design, the methodology and approach for computing system derivatives for a transonic aeroelastic wing needs to be further investigated. In addition, since the present study utilized a pilot code and was primary a research investigation of feasibility, further work is needed to develop an aerodynamics flowfield solver and sensitivity module that is suitable for engineering applications and studies.

A copy of Mr. Arslan's masters' thesis and an abstract of a proposed AIAA paper, which discuss this effort and include many of the details, will be sent under separate cover to the project monitor.

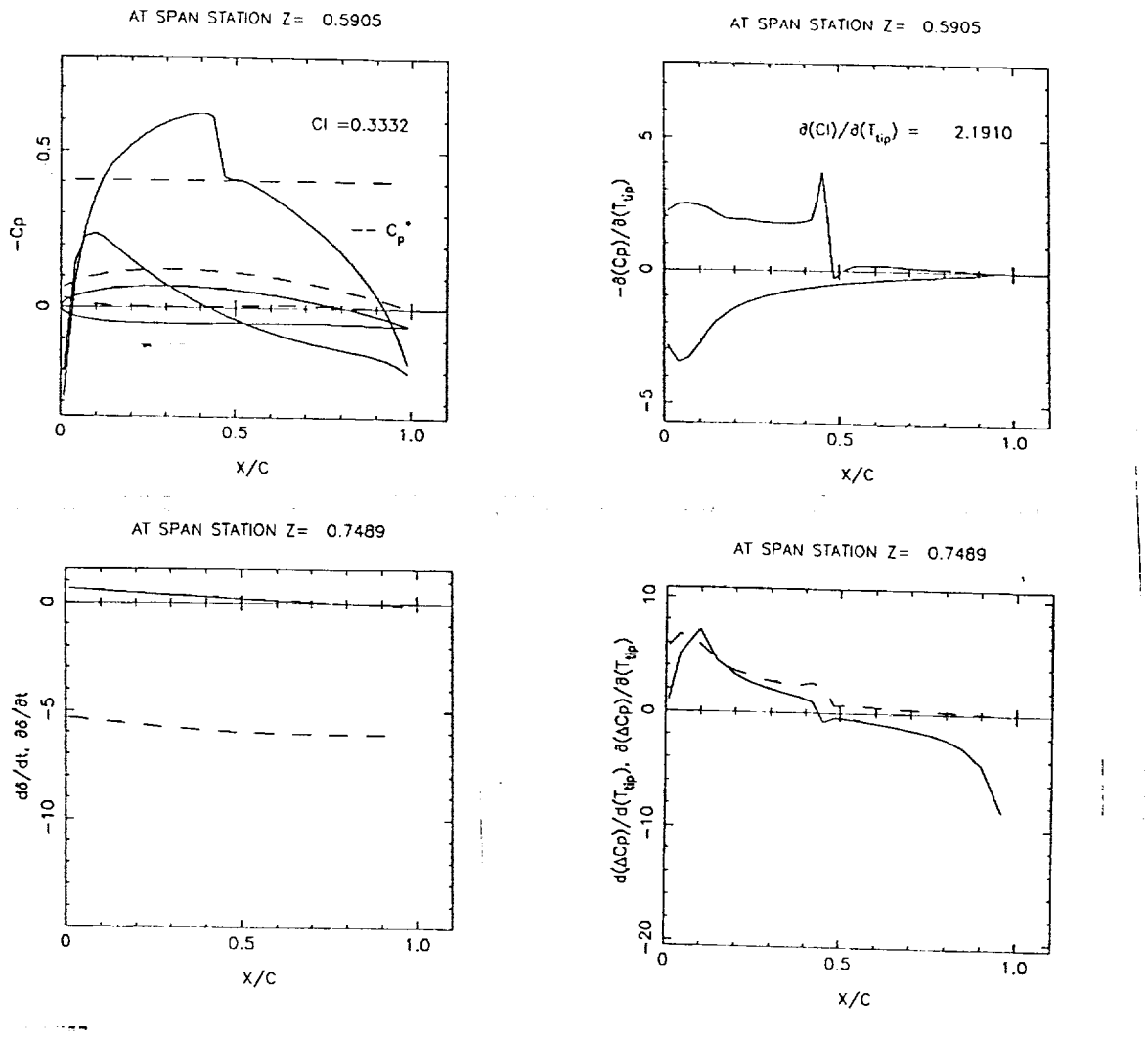

Fig. 2 -- Representative Results from Pilot Study

V. Publications and Degrees

The following degrees were earned at Texas A&M University by individuals associated with this research project:

El-banna, Hesham M., Master of Science (Aerospace Engineering), May 1988.

El-banna, Hesham M., Doctor of Philosophy (Aerospace Engineering), August 1992.

Arslan, Alain, Master of Science (Aerospace Engineering), December 1993.

The following publications resulted from research associated with this project:

El-banna, H. M., "Numerical Computation of Aerodynamic Sensitivity Coefficients in the Transonic and Supersonic Regimes," Master of Science Thesis, Aerospace Engineering Department, Texas A&M University, College Station, Texas, May 1988.

El-banna, H. M. and Carlson, L. A., "Determination of Aerodynamic Sensitivity Coefficients in the Transonic and Supersonic Regimes," AIAA Paper 89-0532, January 1989.

El-banna, H. M. and Carlson, L. A., "Determination of Aerodynamic Sensitivity Coefficients Based on the Transonic Small Perturbation Formulation," ***Journal of Aircraft***, Vol. 27, No. 6, June 1990, pp. 507-515.

El-banna, H. M. and Carlson, L. A., "Determination of Aerodynamic Sensitivity Coefficients Based on the Three-Dimensional Full Potential Equation," AIAA Paper 92-2671, June 1992.

El-banna, H. M. and Carlson, L. A., "A Compendium of Transonic Aerodynamic Sensitivity Coefficient Data," TAMRF Rept. 5802-9203, Texas A&M Research Foundation, College Station, TX, July 1992.

El-banna, H. M., "Aerodynamic Sensitivity Analysis in the Transonic Regime," Doctor of Philosophy Dissertation, Aerospace Engineering Department, Texas A&M University, College Station, Texas, August 1992.

Carlson, L. A. and El-banna, H. M., "Determination of Aerodynamic Sensitivity Coefficients Based on the Three Dimensional Full Potential Equation: Users Guide for Analysis/Sensitivity Program and Graphics Program, " Aerospace Engineering Department, Texas A&M University, College Station, Texas, August 1992.

Carlson, L. A. and El-banna, H. M., "Determination of Aerodynamic Sensitivity Coefficients for Wings in Transonic Flow," ***Proceedings of the 3rd Pan American Congress of Applied Mechanics***, D. T. Mook, editor, Sao Paulo, Brazil, January 1993, pp. 13-16.

Arslan, A. E. "Analysis and Numerical Computation of Sensitivity Derivatives in the Transonic Regime," Master of Science Thesis, Aerospace Engineering, Texas A&M University, College Station, Texas, December 1993.

El-banna, H. M. and Carlson, L. A., "Aerodynamic Sensitivity Coefficients Using the 3-D Full Potential Equation," accepted for publication in the ***Journal of Aircraft,*** 1994.

Arslan, A. E. and Carlson, L. A., "Integrated Determination of Sensitivity Derivatives for an Aeroelastic Transonic Wing," Submitted to the 5th AIAA/USAF/NASA/ISSMO Symposium on Multidisciplinary Analysis and Optimization, September 1994.

Copies of some of these publications are included in the appendix of this report.

VI. Acknowledgments

The original technical monitor for this grant was Dr. E. Carson Yates, Jr. After his retirement, Dr. Woodrow Whitlow, Jr., Unsteady Aerodynamics Branch, MS 173, NASA Langley Research Center, became the Technical Monitor. Dr. Perry A. Newman of the Computational Sciences Branch of NASA Langley also assisted the project with many helpful suggestions and comments. All the individuals associated with this project wish to express their heartfelt appreciation to Drs. Yates, Whitlow, and Newman for helpful support and assistance.

APPENDIX

Relevant Publications

from the Project

AIAA '89

AIAA 89-0532
Determination of Aerodynamic Sensitivity Coefficients in the Transonic and Supersonic Regimes

H. Elbanna and L. Carlson, Texas A&M Univ., College Station, TX

27th Aerospace Sciences Meeting
January 9–12, 1989/Reno, Nevada

DETERMINATION OF AERODYNAMIC SENSITIVITY COEFFICIENTS IN THE TRANSONIC AND SUPERSONIC REGIMES

AIAA-89-0532

Hesham M. Elbanna* and Leland A. Carlson**
Texas A&M University
College Station, Texas 77843

Abstract

The quasi-analytical approach is developed to compute airfoil aerodynamic sensitivity coefficients in the transonic and supersonic flight regimes. Initial investigation verifies the feasibility of this approach as applied to the transonic small perturbation residual expression. Results are compared to those obtained by the direct (finite difference) approach and both methods are evaluated to determine their computational accuracies and efficiencies. The quasi-analytical approach is shown to be superior and worth further investigation.

Nomenclature

A1, A2	Coordinate stretching constants
C	Maximum camber in fraction of chord
Cp	Pressure coefficient
IM, JM	Grid dimensions
JB	Row above airfoil
L	Chordwise location of maximum camber
M	Mach number
R	Residual expression
T	Maximum thickness in fraction of chord
XD	Design variable
f, g	Cartesian coordinate stretching functions
x, y	Cartesian coordinates
α	Angle of attack
γ	Ratio of specific heats
Γ	Circulation
φ	Perturbation potential function
ΔCp	$Cp_l - Cp_u$

Subscripts

∞	Free stream condition
b	Body
p	Pressure
u, l	Upper, lower
TE	Trailing edge

Introduction

Over the past few years, computational fluid dynamics has evolved rapidly as a result of the immense advancements in the computational field and the impact of the use of computers on obtaining numerical solutions to complex problems. Accordingly, researchers are now capable of calculating aerodynamic forces on wing-body-nacelle-empennage configurations subject to subsonic or transonic flows. A next logical step would be to compute the sensitivity of these forces to configuration geometry.

In order to improve the design of transonic vehicles, design codes are being developed which use optimization techniques; and, in order to be successful, these codes require aerodynamic sensitivity coefficients, which are defined as the derivatives of the aerodynamic functions with respect to the design variables. Obviously, it is desirable that such sensitivity coefficients be easily obtained. Consequently, the primary objective of this effort is to investigate the feasibility of using the quasi-analytical method[1-5] for calculating the aerodynamic sensitivity derivatives in the transonic and supersonic flight regimes. As part of this work, the resulting sensitivity coefficients are compared to those obtained from the finite difference approach. Finally, both methods are evaluated to determine their computational accuracies and efficiencies.

In the transonic regime, a variety of flowfield solution methods exist. These range from full Navier-Stokes solvers to transonic small perturbation equation solvers. The complexity of the equations that need to be solved depends upon the flow phenomena in question and the objective of the analysis. Since it is not the objective of this work to develop flowfield algorithms, the present research uses the nonlinear transonic small perturbation equation to determine and verify efficient methods for calculating the aerodynamic sensitivity derivatives. In addition, only two dimensional results will be presented in this initial work.

Background

Most recently, sensitivity methodology has been successfully used in structural design[2] and optimization programs[3] primarily to assess the effects of the variation of various fundamental properties relative to the important physical design variables. Moreover, researchers have developed and applied sensitivity analysis for analytical model improvement and assessment of design trends. In most cases, a predominant contributor to the cost and time in the optimization procedures is the calculation of derivatives. For this reason it is desirable in aerodynamic optimization to have efficient methods of determining the aerodynamic sensitivity coefficients and, wherever possible, to develop appropriate numerical methods for such computations.

Currently, most methods for calculating transonic aerodynamic sensitivity coefficients are based upon the finite difference approximation to the derivatives. In this approach, a design variable is perturbed from its previous value, a new complete solution is obtained, and the differences between the new and the old solutions are used to obtain the

* Graduate Research Asst., Student Member AIAA
** Professor, Aerospace Engr., Assoc. Fellow AIAA

sensitivity coefficients. This direct, or brute force, technique has the disadvantage of being potentially very computer intensive, especially if the governing equations are expensive to solve. Accordingly, the need to eliminate these costly and repetitive analyses is the primary motivation for the development of alternative efficient computational methods to determine the aerodynamic sensitivity coefficients.

Problem Statement

Based on the foregoing discussion, the current problem is formulated starting from the generic quasi-analytical approach and manipulated according to the rules given in Appendix A of Ref.1 for the derivation of the general sensitivity equation. This general sensitivity equation is then applied to the residual expression (R) of the transonic small perturbation equation, which is a simple and adequate description of the nonlinear phenomena occurring in the transonic regime. Although this expression is nonlinear in the perturbation potential (φ), the general sensitivity equation, Eq.(1), is linear with respect to the unknown sensitivity ($\partial\varphi/\partial XD_i$). It is to be noticed that the practical implementation of the above step is not achieved until the residual expression is approximated on a finite domain and the mathematical form of the problem rendered to that of one in linear algebra. This discretization process is explained in detail in Ref.6.

Thus, the quasi-analytical method, as applied to the residual expression of the transonic small perturbation equation, yields the sensitivity equations,

$$\left[\frac{\partial R}{\partial \varphi}\right]\left\{\frac{\partial \varphi}{\partial XD_i}\right\} = -\left\{\frac{\partial R}{\partial XD_i}\right\} \qquad (1)$$

where

$$R = (B_1+B_2\varphi_x)\,\varphi_{xx} + \varphi_{yy} = 0 \qquad (2)$$

$$B_1 = 1 - M_\infty^2$$

$$B_2 = -(\gamma+1)\,M_\infty^2$$

$$\varphi = \varphi\,(x,y,XD) \qquad (3)$$

XD = set of design variables

XD_i = i^{th} design variable

subject to the airfoil boundary condition,

$$\varphi_y(x_b,0) = \left[\frac{dy}{dx}\right]_b = F(x,XD) \qquad (4)$$

the infinity boundary condition,

for $M_\infty<1$

$$\varphi_\infty = -\Gamma\theta/(2\pi),\ \theta = n\pi/2,\ n = 0,1,2,3,4$$

or for $M_\infty>1$

$$\varphi_\infty = 0\ ,\ \theta = n\pi/2,\ n = 1,2,3$$
$$\varphi_x = 0\ ,\ \theta = n\pi/2,\ n = 0,4 \qquad (5)$$

and the Kutta Condition

$$\Delta P = 0\ \ (\Gamma = \Delta\varphi = \text{const.}),\ x_{TE} < x \le \infty \qquad (6)$$

Equation (1) is discretized into a system of linear equations to be solved for the unknown sensitivity vectors. The solution of this system is obtained efficiently by using either a direct or an iterative procedure that allows for multiple right hand sides. This approach is explained in the following section and has the advantage that several unknown vectors can be obtained simultaneously, each vector representing the sensitivity of the potential (φ) with respect to some design variable XD_i.

At this stage, it is convenient to define the vector of design variables

$$XD = \{\ XD_1,\ XD_2,\ \ldots,\ XD_n\ \} \qquad (7)$$

and to exactly determine which variables influence the solution of Eq.(2). In doing so, the relation between the sensitivity coefficients corresponding to these variables and the form of the optimization algorithm that utilizes this information needs to be considered. Notice that the derivatives computed in this study, namely, the first partial derivatives, are adequate for a typical optimization routine if it were to be applied to the present two dimensional problem. Notice also that some optimization studies might require higher derivatives.

For the transonic flow problem, an appropriate choice of the first design variable is the free stream Mach Number (M_∞). This variable appears in the governing Eq.(2) and has an important influence on the character of the equation via its influence on local Mach number (for M<1,the equation is elliptic, for M>1, the equation is hyperbolic) and thus on the nature of the solution. For this reason, it is desirable to have M_∞ as one of the design variables.

Next, it is appropriate to examine the boundary condition given by Eq.(5). In the transonic small perturbation formulation, the angle of attack (α) enters the problem through the boundary condition and thus,

$$F_{u_1} = \left[\frac{dy}{dx}\right]_b = y_{u_1}' - \alpha \qquad (8)$$

For simplicity, the function (F) should be easily differentiable with respect to the design variables defining the airfoil geometry. This desirable feature simplifies the computation of the right hand side term of the sensitivity equation. Therefore, it would seem plausible to have a simple analytical expression for modeling the upper and lower surfaces of the airfoil.

For the present studies, it was decided to limit consideration to two basic airfoil sections, namely parabolic-arc sections, and the NACA four-digit sections, whose families of wing sections are obtained by combining a mean line and a thickness distribution[7]. The resultant expressions possess the necessary features that suit the problem, mainly the concise description of the airfoil surfaces in terms of several geometric design variables. The expressions are as follows :

For parabolic-arc sections

$$y_{u_l} = \begin{cases} C(2Lx-x^2)/L^2 & \pm 2Tx(1-x), \quad x \le L \\ C[(1-L)+2Lx-x^2]/(1-L)^2 & \pm 2Tx(1-x), \quad x > L \end{cases} \tag{9}$$

For NACA four-digit sections

$$y_{u_l} = \begin{cases} C(2Lx-x^2)/L^2 \pm 5T(0.2969\sqrt{x}-0.126x \\ \quad -0.3516x^2+0.2843x^3-0.1015x^4), \quad x \le L \\ \\ C[(1-2L)+2Lx-x^2]/(1-L)^2 \pm 5T(0.2969\sqrt{x} \\ \quad -0.126x-0.3516x^2+0.2843x^3-0.1015x^4), \quad x > L \end{cases} \tag{10}$$

Each of the quantaties C, L, and T is expressed as a fraction of the chord (e.g. if T is 6% chord then T = 0.06). Differentiating Eqs.(9) and (10) with respect to x and substituting the results into Eq.(8) yields :

For parabolic-arc sections

$$F_{u,l} = 2C(L-x)/LL \pm 2T(1-2x) - \alpha \tag{11}$$

For NACA four-digit sections

$$F_{u,l} = 2C(L-x)/LL \pm 5T(0.14845/\sqrt{x}-0.126 \\ -0.7032x+0.8529x^2-0.406x^3) - \alpha \tag{12}$$

where

$$LL = \begin{cases} L^2, & x \le L \\ (1-L)^2, & x > L \end{cases} \tag{13}$$

Eqs.(11) and (12) are simple analytical expressions in terms of the four variables T, L, C, and α. Thus,

$$XD = (T, M_\infty, \alpha, L, C) \tag{14}$$

represents the complete set of design variables that define the present two-dimensional airfoil sensitivity problem. Notice that these variables are completely uncoupled and, thus the sensitivity equation can be solved independently with respect to each variable[8].

Mathematical Treatment and Solution Procedure

Problem Discretization

Equation (1) represents the general sensitivity equation applied to the residual R. Now, in order to solve the problem numerically, Eq.(2) is formulated computationally on a finite domain. This transformation is achieved by using a stretched Cartesian grid that maps the infinite physical domain onto a finite computational grid. In this study, the grid used is based upon a hyperbolic tangent transformation that places the outer boundaries at infinity. Accordingly, the computational variables used are given by,

$$\xi = \tanh A_2 x \tag{15}$$
$$\eta = \tanh A_1 y \tag{16}$$

In addition, the stretching functions are defined as,

$$f = (d\xi/dx) = A_2(1-\xi^2) \tag{17}$$
$$g = (d\eta/dy) = A_1(1-\eta^2) \tag{18}$$

so that,

$$\varphi_x = f\varphi_\xi \tag{19}$$
$$\varphi_y = g\varphi_\eta \tag{20}$$
$$\varphi_{xx} = f\,(f\varphi_\xi)_\xi \tag{21}$$
$$\varphi_{yy} = g\,(g\varphi_\eta)_\eta \tag{22}$$

Substituting from Eqs.(19)-(22) into Eq.(2), yields the transformed residual expression,

$$R = [B_1+B_2 f\varphi_\xi]\, f(f\varphi_\xi)_\xi + g(g\varphi_\eta)_\eta = 0 \tag{23}$$

This equation is solved numerically by an approximate factorization scheme[9] in which the objective is to force the residual to zero at each point of the computational domain. In finite difference form, Eq.(23) can be written as,

$$\begin{aligned} R_{i,j} = {} & [B_1 + B_2(\varphi_{i+1,j}-\varphi_{i-1,j})/(2\Delta\xi)]\, f_i/\Delta\xi^2 \\ & [\nu_{i,j} f_{i+\frac{1}{2}}(\varphi_{i+1,j}-\varphi_{i,j}) \\ & -(2\nu_{i,j}-1) f_{i-\frac{1}{2}}(\varphi_{i,j}-\varphi_{i-1,j}) \\ & -(1-\nu_{i,j}) f_{i-3/2}(\varphi_{i-1,j}-\varphi_{i-2,j})] \\ & + [g_{j+\frac{1}{2}}(\varphi_{i,j+1}-\varphi_{i,j}) \\ & -g_{j-\frac{1}{2}}(\varphi_{i,j}-\varphi_{i,j-1})]\, g_j/\Delta\eta^2 \end{aligned} \tag{24}$$

where

$\nu_{i,j} = 1$ if point (i,j) is subsonic
$\nu_{i,j} = 0$ if point (i,j) is supersonic

Eq.(24) is the discretized form of the residual at a general point (i,j) in terms of φ values at surrounding points. Consequently, R at i,j can be viewed as a function of the φ values at neighboring points; and, therefore, the differentiation of the residual expression is straight forward.

Differentiation of the Residual

Rearranging Eq.(24) yields

$$\begin{aligned} R_{i,j} = {} & c_1\varphi_{i,j} + c_2\varphi_{i+1,j}\varphi_{i-1,j} + c_3\varphi_{i+1,j}\varphi_{i,j} \\ & + c_4\varphi_{i-1,j}\varphi_{i,j} + c_5\varphi_{i+1,j}\varphi_{i-2,j} \\ & + c_6\varphi_{i-1,j}\varphi_{i-2,j} + c_7\varphi_{i-1,j}^2 + c_8\varphi_{i+1,j}^2 \\ & + c_9\varphi_{i+1,j} + c_{10}\varphi_{i-1,j} + c_{11}\varphi_{i,j+1} \\ & + c_{12}\varphi_{i,j-1} + c_{13}\varphi_{i-2,j} \end{aligned} \tag{25}$$

For a fixed computational grid, the coefficients $c_1, c_2, \ldots, c_{13}$ are functions only of B_1 and B_2 which in turn are functions of M_∞. This fact is used when differentiating Eq.(25) with respect to M_∞ in order to obtain the right hand side $(\partial R/\partial M_\infty)$. It is also necessary to consider the treatment of various types of grid points and examine the effect on the general residual expression. Several groups of points, such as those adjacent to the airfoil, to the wake cut, and to infinity boundaries, need special treatment. Accordingly, it is necessary

to revise the residual expression at these boundary points to include the boundary conditions. The resulting updates are used to modify the residual equation, Eq.(25), and yield a set of expressions, each being valid for a group of boundary points. The details of these operations are found in Ref.6.

In setting up the complete quasi-analytical problem the circulation and its dependence upon trailing edge potentials must be carefully included. Since the circulation is determined by the difference in potentials at the trailing edge,

$$\Gamma = \varphi_{uTE} - \varphi_{lTE} \tag{26}$$

or, by interpolating the trailing edge values

$$\begin{aligned}\Gamma = T_1 [\ 1.5\ (\varphi_{ITE-1,JB} - \varphi_{ITE-1,JB-1}) \\ - 0.5\ (\varphi_{ITE-1,JB+1} - \varphi_{ITE-1,JB-2})\ ] \\ + T_2 [\ 1.5\ (\varphi_{ITE,JB} - \varphi_{ITE,JB-1}\ ) \\ - 0.5\ (\varphi_{ITE,JB+1} - \varphi_{ITE,JB-2}\ )\ ]\end{aligned} \tag{27}$$

where

$$T_2 = [\ \xi(x-0.5) - \xi(ITE-1)\ ] / \Delta\xi \tag{28}$$

$$T_1 = [\ 1 - T_2\ ] \tag{29}$$

and since a branch cut extends from the trailing edge to downstream infinity, the trailing edge potentials appear in the residual expressions for points along the branch cut. In addition, since in the two dimensional case the infinity boundary conditions are proportional to the circulation, the trailing edge potentials also appear in the residual expressions at points adjacent to the outer boundaries. Consequently, the resultant matrix ($\partial R/\partial\varphi$), while banded, also contains many nonzero elements far from the central band. Notice that the presence of these elements greatly complicates the rapid and efficient solution of the sensitivity equation, Eq.(1).

The resulting residual expressions are differentiated analytically with respect to the potential (φ). To be more specific, each equation is differentiated with respect to the potential at neighboring points and trailing edge points (the later enters as a result of the implicit nature of the circulation effects). These points are denoted by the counters (ii,jj) and are given by,

(i,j-1), (i,j), (i,j+1), (i-2,j), (i-1,j), (i+1,j), (ITE-1,JB-2), (ITE-1,JB-1), (ITE-1,JB), (ITE-1,JB+1), (ITE,JB-2), (ITE,JB-1), (ITE,JB), (ITE,JB+1).

Solution about a Fixed Design Point

Once the residual relations are obtained, the actual coefficients are assembled by evaluating the appropriate analytical expresssions using a flowfield solution obtained from Eq.(2) for a given set of conditions (i.e. about a fixed design point). Similarly, the right hand sides are evaluated by differentiating the analytical expressions for the residual with respect to each design variable. Again, the details and results of these steps are found in Ref.7.

The end result is that the coefficient matrix ($\partial R_{i,j}/\partial\varphi_{ii,jj}$) is of size (IM-2)*(JM-2)x(IM-2)*(JM-2) for a general (IM*JM) grid. This system is large, of block structure, diagonally dominant, and sparse; and, while banded, also contains many nonzero elements far from the central band. As a result of this size and structure, it is obvious that a reasonably fast scheme for solving Eq.(1) is needed.

Currently, it is very difficult to single out an optimum routine that handles a general large sparse system of linear equations for which the coefficient matrix is unsymmetric. This is due to the fact that, unlike the theory of symmetric matrices, the theory of general unsymmetric matrices is more involved and has yet to be developed. Since research in the above areas is currently very active and specialized, any attempt to cover these topics in detail would be laborious. For this reason, it was decided to use a few general approaches that were available in the literature and that could be integrated into the sensitivity codes with adjustments. This approach would allow an evaluation of the overall cost involved in solving the current two-dimensional problem and would give a crude estimate of the effort involved in solving a three dimensional problem.

The first solver is based on standard Gaussian Elimination with partial pivoting and full storage. The second is based on triangular decomposition[10] and uses a compact storage scheme that avoides handling the zero entries and therefore should be more efficient than standard Guassian Elimination. The third solver is based on a Gauss-Seidel iterative scheme[11] and was not optimized for speed (through the choice of optimum acceleration parameters) but uses sparse matrix technology in processing only the nonzero elements. The fourth and last solver used is based on the conjugate gradient method[12]. Handling the sparsity pattern for the third and fourth solvers is achieved by assembling the symbolic part of the coefficient matrix only once for a given grid size and given free-stream (subsonic versus supersonic). The resultant structure is then stored on a diskfile. Before the numerical part is executed, the symbolic information is read into the code and used directly to assemble the new matrix. This procedure is followed in order to reduce the time consumed in assembling the coefficient matrix. Notice also that in the Gauss-Seidel and conjugate-gradient solvers that the error tolerances for the coefficients involving maximum thickness, free stream Mach number, and location of maximum camber were 1.E-06 while those on angle of attack and maximum camber were 1.E-04.

Once the sensitivities of the potentials, and thus the Cp distribution, to the design variables are known, the sensitivity of the lift coefficients to the design variables can be easily computed. To minimize errors, these coefficients are computed using

$$C_L = 2\ \Gamma = 2\ (\varphi_{uTE} - \varphi_{lTE}) \tag{30}$$

and hence,

$$\partial C_L/\partial XD_i = 2\ (\partial\varphi_{uTE}/\partial XD_i - \partial\varphi_{lTE}/\partial XD_i) \tag{31}$$

Finally, all methods used for computing the derivatives are compared to the finite-difference approach and the results are presented and evaluated to determine the computational accuracy and efficiency (with regards to time) of each method.

Test Cases

In this study, the quasi-analytical method has been used to determine the aerodynamic sensitivity coefficients at three freestream Mach numbers (M_∞ = 0.2, 0.8, 1.2) for two arbitrarily selected airfoils, each at one degree angle of attack. The first is a cambered parabolic arc section having 1% camber at 40% chord, a maximum thickness of 6% at 50% chord, and which is designated P1406; and the second is a NACA 1406 airfoil. Since most of the interesting captured phenomena were found to be identical for both airfoils, only results for the NACA 1406 airfoil are presented in this paper.

In the following, two types of results will be presented. The first will be plots of Cp versus chord for the three chosen Mach numbers. The second will be the corresponding plots of $(\partial Cp/\partial T)$, $(\partial Cp/\partial M_\infty)$, $(\partial Cp/\partial \alpha)$, $(\partial Cp/\partial C)$, and $(\partial Cp/\partial L)$ obtained by the quasi-analytical method. In addition, all of the figures will also contain results obtained using the direct (finite difference) approach in which each design variable was individually perturbed by a small amount, typically 0.001, and a new flowfield solution obtained. Then the sensitivities were computed using $\Delta Cp/\Delta XD$ and are shown via dashed lines. In many cases the lines are coincident with the quasi-analytical results and cannot be observed. Table I compares results obtained by the two methods, and in most cases the agreement is within one percent.

In all cases, an 81*20 stretched Cartesian grid was utilized. In addition, for these studies, the flowfield was normally computed using double precision arithmetic and the maximum residual reduced eight orders of magnitude. It was felt that this level of convergence was necessary in order to accurately evaluate sensitivity coefficients using a finite difference approach, although such convergence may not be required in the flowfield solver for the quasi-analytical method.

Results and Discussion

Subsonic Case (M_∞ = 0.2)

Initial studies concentrated on subsonic cases since at least approximate results would be known from thin airfoil theory. Figure 1 shows the pressure distribution for the NACA 1406 airfoil while Figs.2a and 2b show the sensitivity of the pressure to thickness for the same airfoil. As expected from thin airfoil theory, the upper and lower surface values are essentially identical and the difference is very small everywhere. Also shown on the same figure (and on subsequent figures) by the dashed line is the result obtained by using the finite difference approach; and as can be seen, the agreement betweeen the two approaches is excellent.

The sensitivity of pressure to freestream Mach number is plotted on Figs.3a and 3b. It is noticed that while the profiles for the upper and lower surfaces are similar, they are not equal in magnitude, indicating a nonlinear variation with Mach number as predicted by simple Prandtl-Glauret Theory. However, as indicated by the results on Fig.3b, the magnitudes for this subsonic Mach number are very low.

The sensitivity of the pressure coefficients to angle of attack are shown for this case on Figs.4a and 4b. As expected from linear thin airfoil theory, the upper and lower surface curves are essentially equal in magnitude but of opposite sign. Not surprisingly, the sensitivity of the delta Cp variation, Fig.4b, has the shape of the pressure difference curve for a flat plate at angle of attack; and its magnitude, particularly near the leading edge is quite large.

On Figs.5a and 5b is plotted the sensitivity of the pressure coefficient to the amount of maximum camber. Since camber contributes to lift, it is expected from thin airfoil theory that these values should be "equal but opposite in sign" for the upper and lower surfaces. In addition, the pressure difference curve has the correct shape for that associated with a 14 mean line with the peak occuring at 30% chord[7] and has magnitude comparable to those for the $(\partial Cp/\partial \alpha)$ curves.

Finally, the sensitivity of pressure to the location of the maximum camber point is portrayed on Figs.6a and 6b, and to say the least the results are interesting. Since maximum camber location affects the camber profile and hence lift, the equal and opposite behavior of the upper and lower surface coefficients is expected. In addition, the pressure difference sensitivity is primarily negative forward of the point of maximum camber and positive aft of it. This result indicates that if the location of maximum camber were moved rearward slightly (i.e. a positive ΔL) that lift would be decreased on the forward portion of the airfoil and increased on the aft portion of the airfoil, which is in agreement with the results presented in Ref.7.

Transonic Case (M_∞ = 0.8)

At M_∞ = 0.8, the flow about the NACA 1406 airfoil has a strong shock at 40% chord, Fig.7; and the lower surface is entirely subcritical. As a consequence, the variation with chord of the sensitivity coefficients is considerably different than in the subsonic case.

Figs.8a and 8b show the sensitivity of pressure to the maximum thickness; and while the lower surface profile is similar to that obtained at subsonic conditions, the upper surface curve and the pressure difference coefficient plot show the effect of the upper surface shock wave. The large peak on the curves corresponds to the location of the shock wave and indicates that the shock wave location is very sensitive to maximum thickness. Notice on Figs.8a and 8b the excellent agreement of the quasi-analytical results indicated by the solid lines with those obtained using the finite-differece approach (dashed lines).

The results for $(\partial Cp/\partial M_\infty)$, which are shown on Figs.9a and 9b, are similar. The lower surface curve is typical of a subsonic flow, while the

upper surface and the pressure difference coefficients reflect the presence of the upper surface shock wave. Similar comments can be made for the remaining design variable coeficients, which are plotted on Figs.10, 11, and 12.

Examination of the curves in the vicinity of the shock wave location indicates that the pressure sensitivity and indirectly the shock wave location is about equally influenced by the maximum thickness, freestream Mach number, and angle of attack. However, in comparison it is relatively insensitive to location of maximum camber; but, perhaps surprisingly so, the pressure is twice as sensitive to the amount of maximum camber as it is to the other design variables. It should also be noticed that the lift is most sensitive to angle of attack and to maximum camber.

In addition, Fig.11 shows a discrepancy between the results obtained by the direct approach and those obtained thru the quasi-analytical method. It will be shown in the following section that this discrepancy is related to the choice of the step size used in computing the finite-difference solution, thus revealing a significant deficiency in computing the sensitivity derivatives in nonlinear regimes via the finite-difference approach.

Supersonic Case (M_∞ = 1.2)

In order to investigate the applicability of the quasi-analytical method at supersonic freestream Mach numbers, solutions were obtained for the NACA 1406 airfoil at Mach 1.2. At this condition, the flow is transonic in that the bow shock is detached, and there is a region of subsonic flow extending to approximately the quarter chord, Fig.13. Figures 14-18 show the pressure sensitivities for these cases, and Table I lists the lift sensitivities.

Examination of the plots shows that the pressure sensitivity coefficients have different trends and magnitudes from those computed for subsonic freestream supercritical conditions, and that they are approaching the form expected from supersonic linear theory. These changes are particularly evident in the lift derivatives presented in Table I. Notice that the derivatives with respect to the design variables maximum thickness, Mach number, and location of maximum camber have switched sign. In addition, as expected from linear theory, the influence of camber on lift has decreased significantly; and at M_∞ = 1.2 is only about 15% of the angle of attack effect as compared to a factor of about two at M_∞ = 0.8. Notice also that Fig.15 shows a discrepancy similar to that found in Fig.11.

Time Comparisons

Obviously, in the development of the quasi-analytical method it was hoped that not only would this approach yield accurate values for the aerodynamic sensitivity coefficients but also that it would be more efficient than the brute force finite difference approach. Table II presents some comparisons concerning the amount of computational effort required to obtain solutions by the two approaches.

In comparing the values, several items should be kept in mind. First, it has been assumed that the finite difference approach will require six independent solutions. In practice it might be possible to start each finite difference solution from a previous solution and, thus, decrease the time to convergence. However, to be accurate, the finite difference approach will probably require double precision and will have to be extremely well converged (i.e.1.E-08). Nevertheless, the values for the finite difference approach probably should be viewed as maximum values.

Second, the methods used for obtaining the sensitivity coefficients have not been optimized and, as mentioned earlier, may not even be optimum; and the flowfield solution required for the quasi-analytical approach may not need double precision and may not have to be as tightly converged. Thus the values shown for the quasi-analytical approach should also be viewed as maximum values.

In spite of these limitations, results obtained by direct methods do indicate, that the quasi-analytical method is at transonic conditions potentially more computationally efficient than the brute force finite difference approach.

Notice that in this study, the initial guess used in computing the sensitivity derivatives via iterative methods was arbitrarily chosen as the zero-vector. In addition, time comparisons presented in Table II show that iterative methods are in general less efficient than direct methods if the derivatives for the current two-dimensional problem were sought about some general design point. However, if the objective is to incorporate the sensitivity derivatives in an optimization loop (i.e. to use the derivatives in a continuation problem), then, a good initial guess (which in this case would be available) would enhance convergence and the overall cost of computing the derivatives using iterative methods might be reduced. These points should be taken into consideration when a sensitivity study is to be integrated into an optimization procedure.

Additional Test Cases

The first group of cases are carried out to investigate the performance of the NACA 1406 airfoil for a range of Mach numbers from 0.79 to 0.86 in increments of 0.01. As shown in Fig.19, this range of transonic Mach numbers encompasses the development of the shock wave on the upper surface of the airfoil. Also, as shown on Figs.20 and 21 for the cases involving thickness, Mach number, and maximum camber, the quasi-analytical derivatives are in the vicinity of the shockwave frequently different from those obtained by the finite-difference approach. This discrepancy raises two questions -- What is the cause of the disagreement and which set of derivatives is more accurate ? Examination of the variation of the integrated coefficient, $\partial CL/\partial XD_i$ with M_∞, which is portrayed on Fig.22, shows that the quasi-analytical results are smooth and follow a definite trend while the finite difference values are at best "discontinuous". Consequently, it is concluded that the finite-difference results are less accurate. In order to observe the performance of the finite-difference approach in the transonic regime, it is necessary to examine the effect of changing the step size (delta of

the design variable) on the computed derivatives. Four different values for the step size (1.E-03, 1.E-04, 1.E-05, and 1.E-06) were chosen and applied to the NACA 1406 at a Mach number of 0.84. Examination of the results (Table III) show that as the step size is decreased, the finite difference lift coefficient sensitivity derivatives approach the values computed by the quasi-analytical method. However, in some cases, for small ΔXD_i values, oscillations in the pressure coefficient sensitivity derivatives have been observed depending upon the machine used and the method of storing and retrieving the data. These oscillations combined with the difficulty of properly choosing a suitable finite difference ΔXD_i a priori indicates that the finite difference approach is probably not a practical method of efficiently computing sensitivity coefficients. On the other hand, the present results demonstrate that the quasi-analytical method can be used accurately to obtain such coefficients in the transonic flight regime.

Conclusion

Based upon these investigations and results, it is concluded that the quasi-analytical method is a feasible approach for accurately obtaining transonic aerodynamic sensitivity coefficients in two dimensions. The results obtained from the quasi-analytical method are almost identical to those obtained by the brute force (finite difference) technique. Furthermore, the study indicates that obtaining the quasi-analytical transonic derivates using a direct solver is more efficient than computing the derivatives by the finite difference method.

Acknowledgment

This effort was primarily supported by the National Aeronautics and Space Administration under Grant No. NAG 1-793, with Dr. E. Carson Yates, Jr., NASA Langley Research Center, as technical monitor. A very warm and special thank-you goes to Dr. M.S. Pilant, Professor of Mathematics, Texas A&M University, for helpful ideas and comments.

References

1. Sobieski, J."The Case for Aerodynamic Sensitivity Analysis", Paper presented to NASA/VPI$-SY Symposium on Sensitivity Analysis in Engineering, September 25-26, 1986.
2. Adelman, H.M.; and Haftka, R.T.: "Sensitivity Analysis and Discrete Structural Systems", AIAA Journal, Vol.24, No.5, May 1986, pp.823-832.
3. Bristow, D.R.; and Hawk, J.D.: Subsonic Panel Method for Designing Wing Surfaces from Pressure Distributions. NASA CR-3713, 1983.
4. Sobieszczanski-Sobieski, J.; Barthelemy, J.-F.M.; and Riley, M.F.: Sensitivity of Optimum Solutions of Problem Parameters. AIAA Paper No.81-0548 R. AIAA Journal, Vol.20, No.9, September 1982, pp.1291-1299.
5. Barthelemy, J.-F.M.; and Sobieszczanski-Sobieski, J.: Optimum Sensitivity Derivatives of Objective Functions in Nonlinear Programming. AIAA Journal, Vol.21, No.6, June 1983, pp.913-915.
6. Elbanna, H.M., Numerical Computation of Aerodynamic Sensitivity Coefficients In the Transonic and Supersonic Regimes, M.S. Thesis, Texas A&M University, May 1988.
7. Abbott, I.H. and Von Doenhoff, A.E., Theory of Wing Sections, Dover, NewYork., 1959.
8. Vanderplaats, G.N.; Hicks, R.M.; and Murman, E.M.: "Application of Numerical Optimization Techniques To Airfoil Design", NASA SP-047, Part II, March, 1975, pp.745-768.
9. Ballhaus, W.F.;Jameson, A; and Albert, J.: Implicit Approximate Factorization Schemes for Steady Transonic Flow Problems. AIAA Journal, Vol.16, No.6,June 1978, pp.573-579.
10. Gupta S.K. and Tanji K.K., Computer Program for Large, Sparse, Unsymmetric Systems of Linear Equations, International Journal for Numerical Methods in Engineering, Vol.11, 1251-1259(1977).
11. Sergio Pissanetzky: Sparse Matrix Technology, Academic Press, Inc., New York, 1984.
12. Press, W.H., Flannery, B.P., Tenkolsky S.A., Vetterling W.T., Numerical Recipes, Cambridge, University Press, Cambridge, 1986.

Table I

Accuracy of Quasi-Analytical Method
for Computing
Lift Coefficient Sensitivity Derivatives

NACA 1406, GRID 81*20

XD_i	METHOD	M_∞=0.2	M_∞=0.8	M_∞=1.2
T	FD	0.0044	0.5232	-0.2949
	QA	0.0044	0.5447	-0.3376
M_∞	FD	0.0471	0.9708	1.0235
	QA	0.0470	0.9905	-0.0703
α	FD	6.1385	10.5229	4.8758
	QA	6.1386	10.5229	4.8726
C	FD	9.9380	19.5767	0.7695
	QA	9.9381	18.6154	0.7356
L	FD	0.0696	0.1499	-0.0348
	QA	0.0693	0.1496	-0.0349

FD Finite-Difference
QA Quasi -Analytical

Table II

Time* Comparisons
for Obtaining Sensitivity Coefficients
for Five Design Variables

NACA 1406, GRID 81*20

METHOD	M_∞=0.2	M_∞=0.8	M_∞=1.2
FD	1.0000	1.0000	1.0000
TD	2.5187	0.9962	0.3929
GE	2.4089	0.9927	0.5165
GS	0.9971	1.5410	------
CG	35.2264	10.6199	------

P1406, GRID 81*20

METHOD	M_∞=0.2	M_∞=0.8	M_∞=1.2
FD	1.0000	1.0000	1.0000
TD	1.8808	0.8550	0.3930
GE	1.7891	0.9397	0.5202
GS	0.7153	1.5526	------
CG	26.3326	10.0323	------

FD Finite-Difference
TD Triangular-Decomposition
GE Gauss-Elimination
GS Guass-Seidel
CG Conjugate-Gradient
* All CPU times were normalized by the time taken to compute FD derivatives

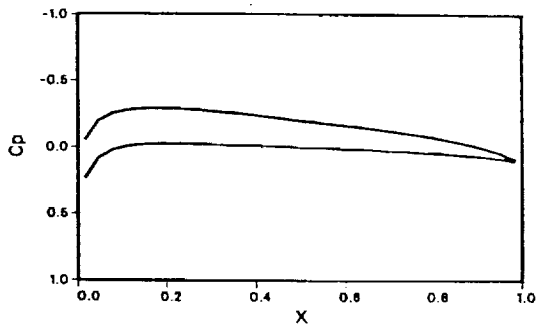

Fig.1 Pressure Coefficient, M_∞=0.2

Table III

Effect of Changing Step Size Delta
on Finite Difference
Lift Coefficient Sensitivity Derivatives

NACA 1406, GRID 81*20, M_∞=0.84

DELTA XD_t	XD_t=T	XD_t=M_∞	XD_t=C
1.E-03	7.7603	7.8715	24.0912
1.E-04	-0.8493	-0.6340	83.9853
1.E-05	-0.8497	-0.6364	14.7719
1.E-06	-0.8498	-0.6366	14.7695
QA	-0.8498	-0.6367	14.7692

QA Quasi-Analytical Lift Coefficient
Sensitivity Derivatives

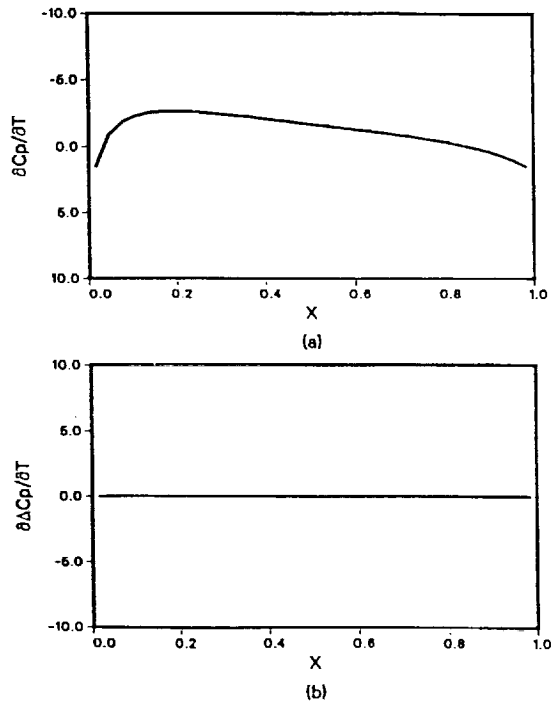

Fig.2 Sensitivity of Pressure to Maximum Thickness, M_∞=0.2

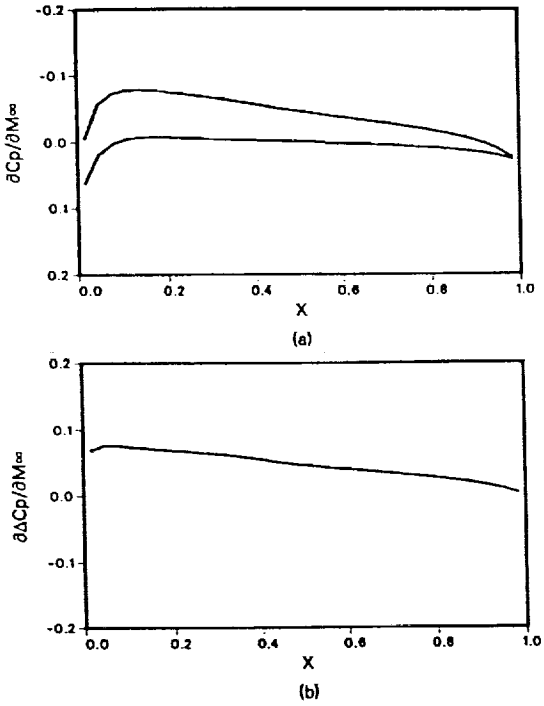

Fig.3 Sensitivity of Pressure to Mach Number, M∞=0.2

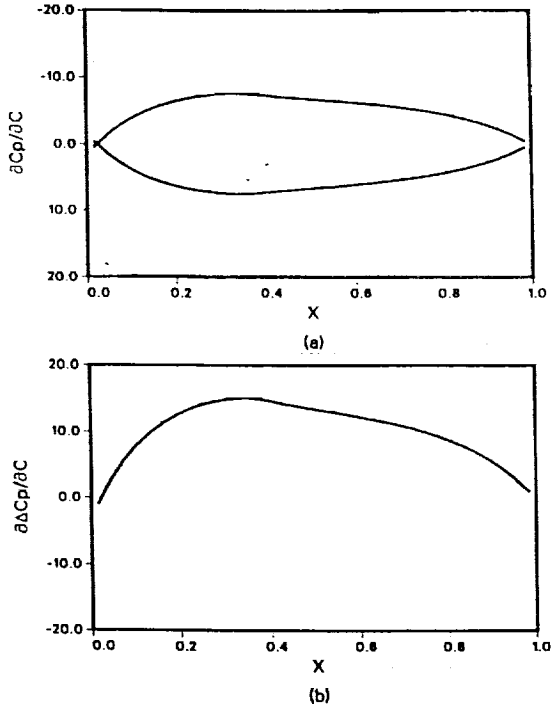

Fig.5 Sensitivity of Pressure to Maximum Camber, M∞=0.2

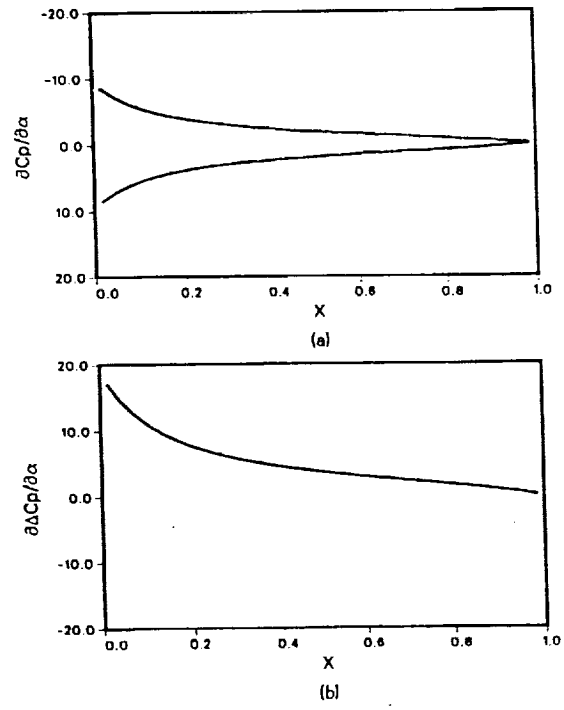

Fig.4 Sensitivity of Pressure to Angle of Attack, M∞=0.2

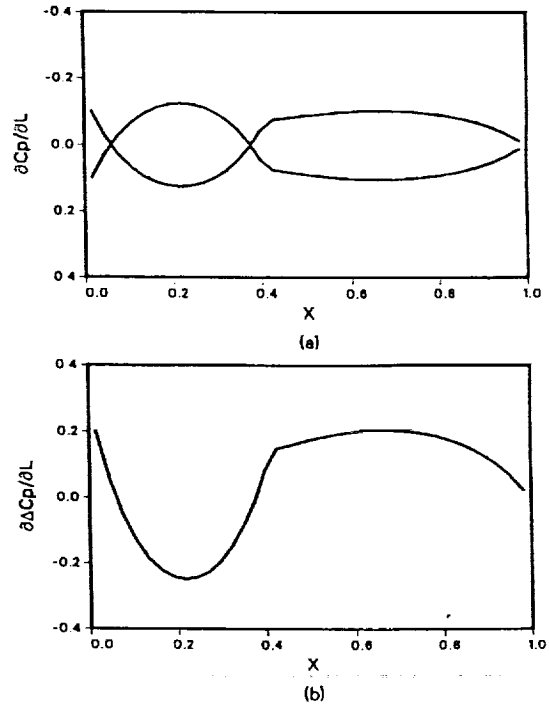

Fig.6 Sensitivity of Pressure to Location of Max Camber, M∞=0.2

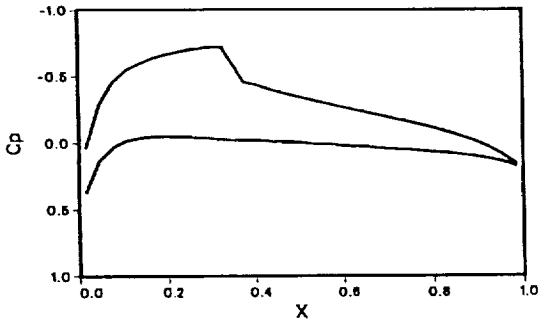

Fig.7 Pressure Coefficient, M_∞=0.8

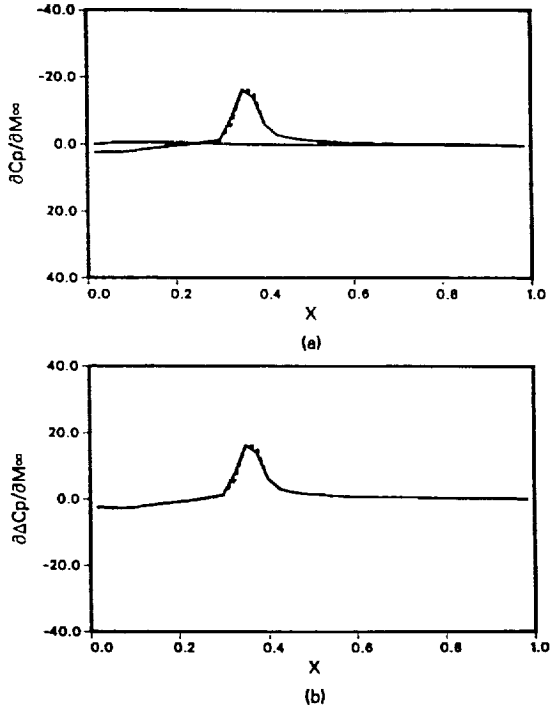

Fig.9 Sensitivity of Pressure to Mach Number, M_∞=0.8

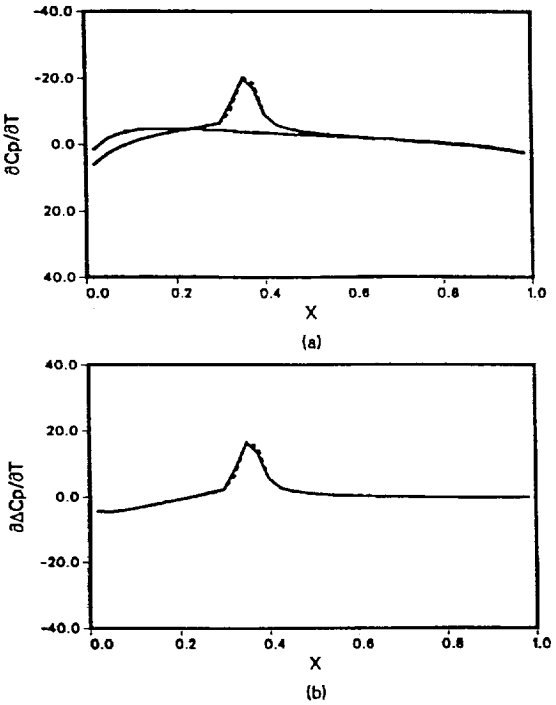

Fig.8 Sensitivity of Pressure to Maximum Thickness, M_∞=0.8

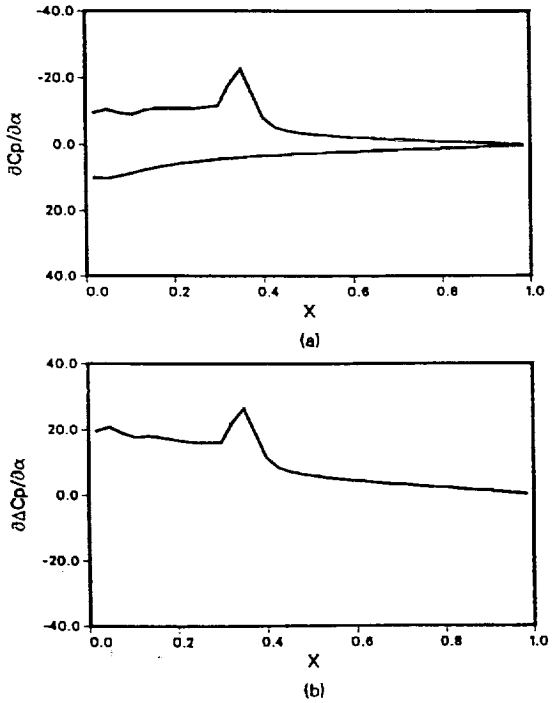

Fig.10 Sensitivity of Pressure to Angle of Attack, M_∞=0.8

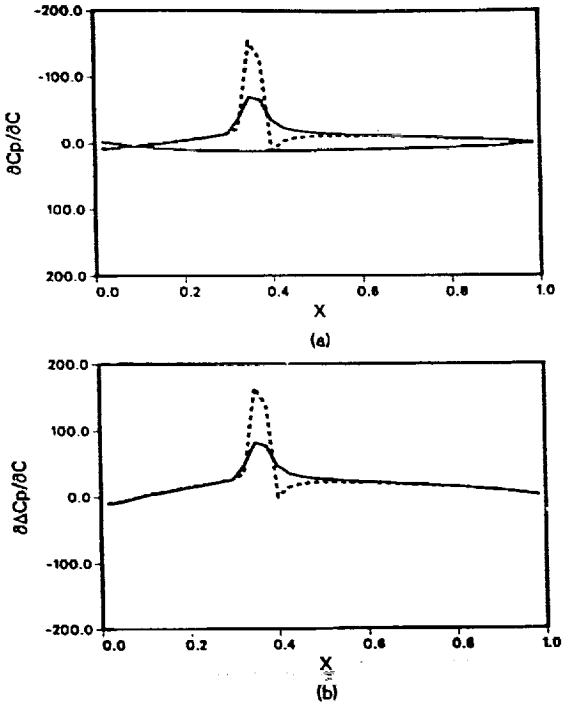

Fig.11 Sensitivity of Pressure to Maximum Camber, M∞=0.8

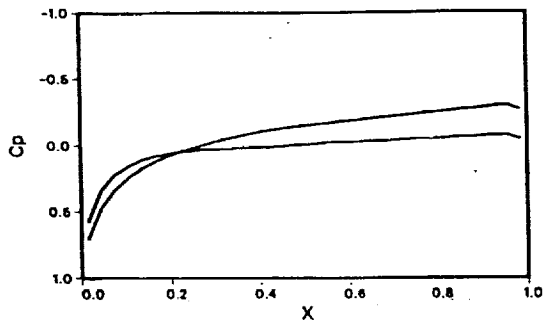

Fig.13 Pressure Coefficient, M∞=1.2

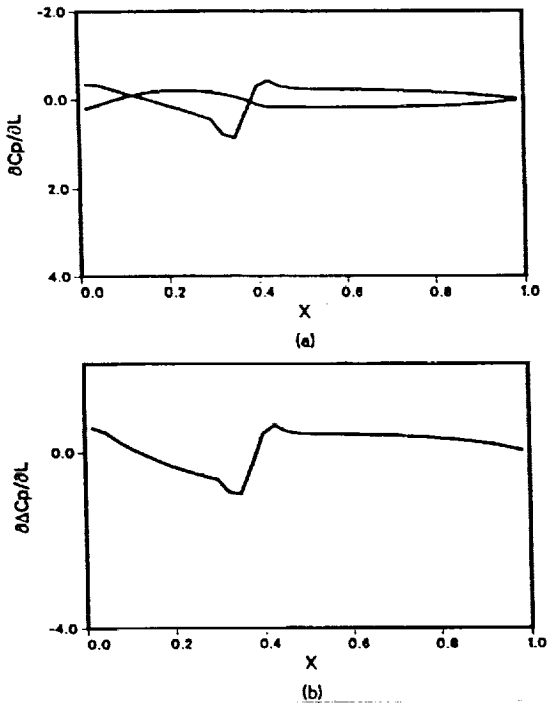

Fig.12 Sensitivity of Pressure to Location of Max Camber, M∞=0.8

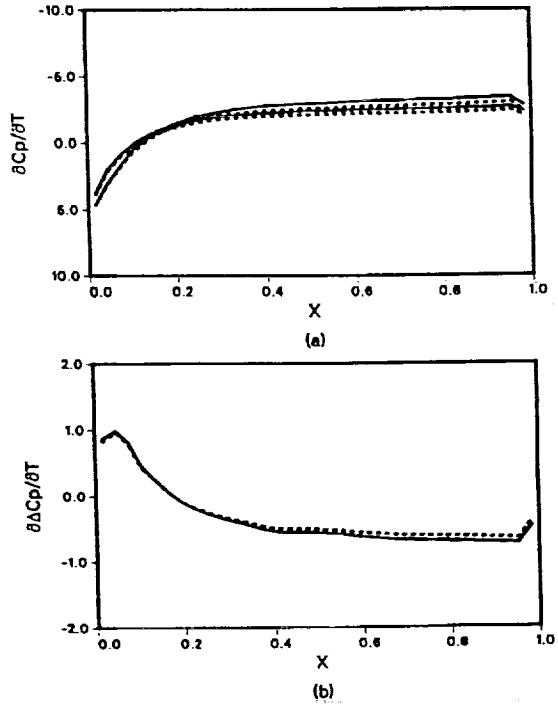

Fig.14 Sensitivity of Pressure to Maximum Thickness, M∞=1.2

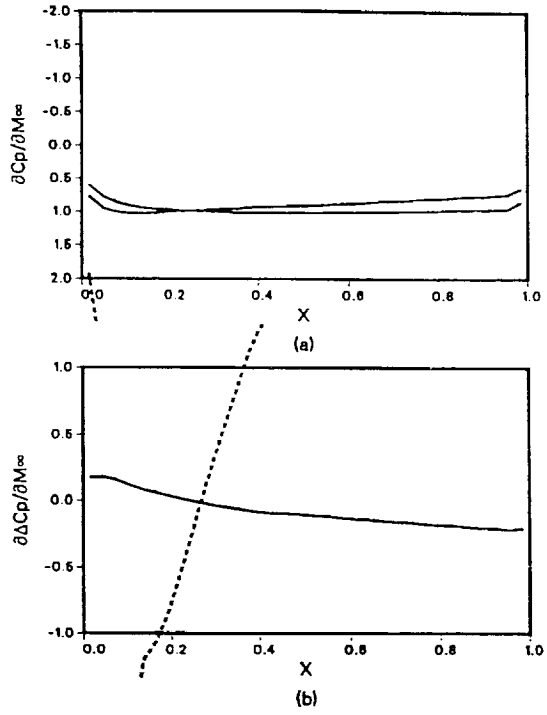

Fig.15 Sensitivity of Pressure to Mach Number, M∞=1.2

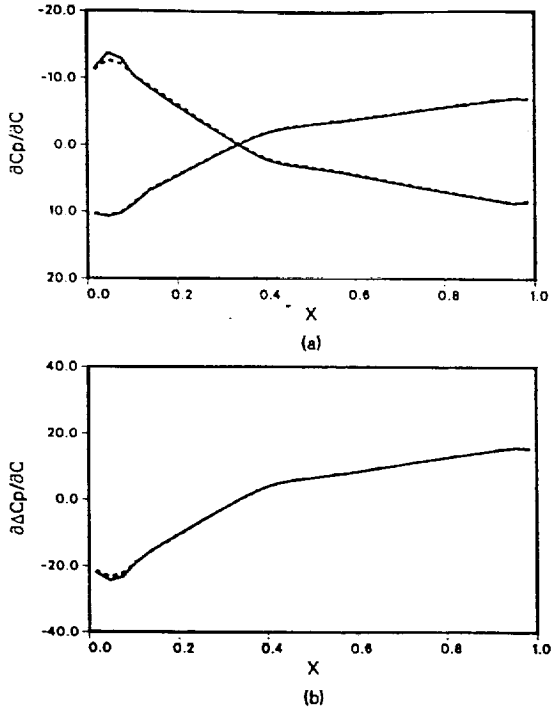

Fig.17 Sensitivity of Pressure to Maximum Camber, M∞=1.2

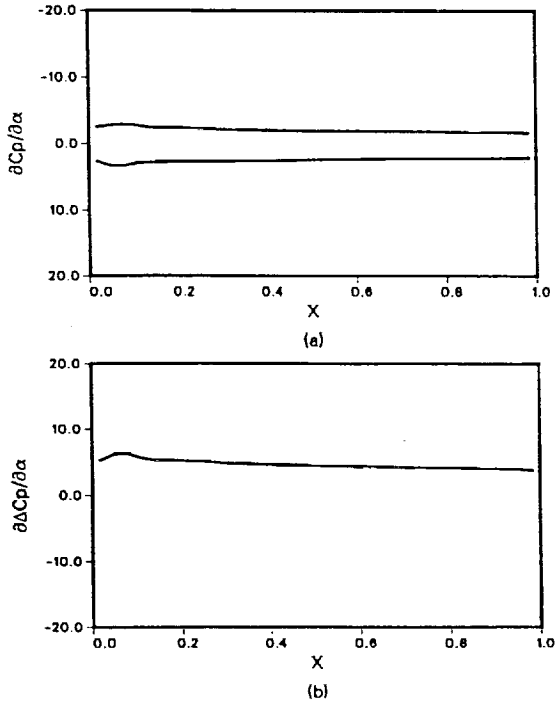

Fig.16 Sensitivity of Pressure to Angle of Attack, M∞=1.2

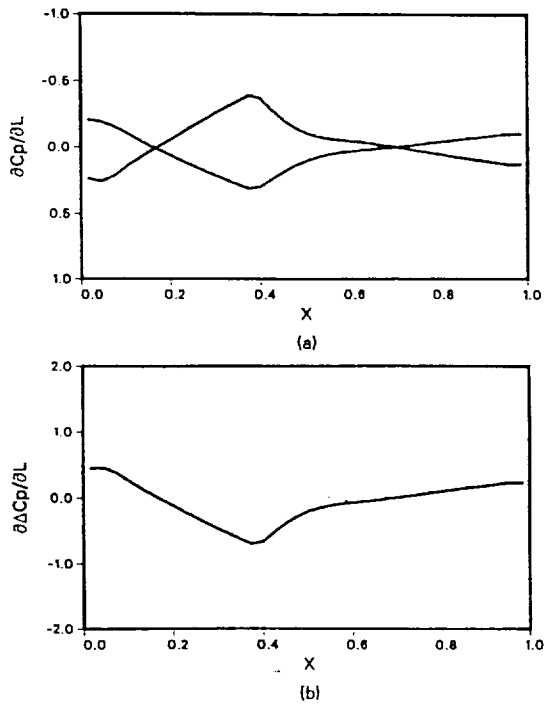

Fig.18 Sensitivity of Pressure to Location of Max Camber, M∞=1.2

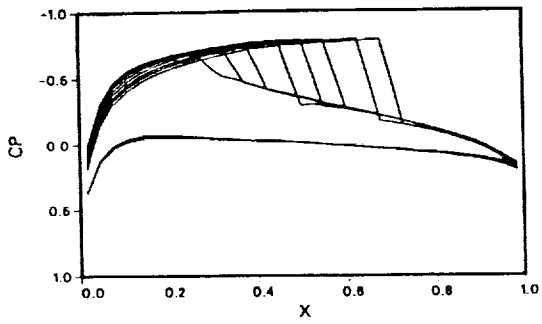

Fig.19 Pressure Coefficient

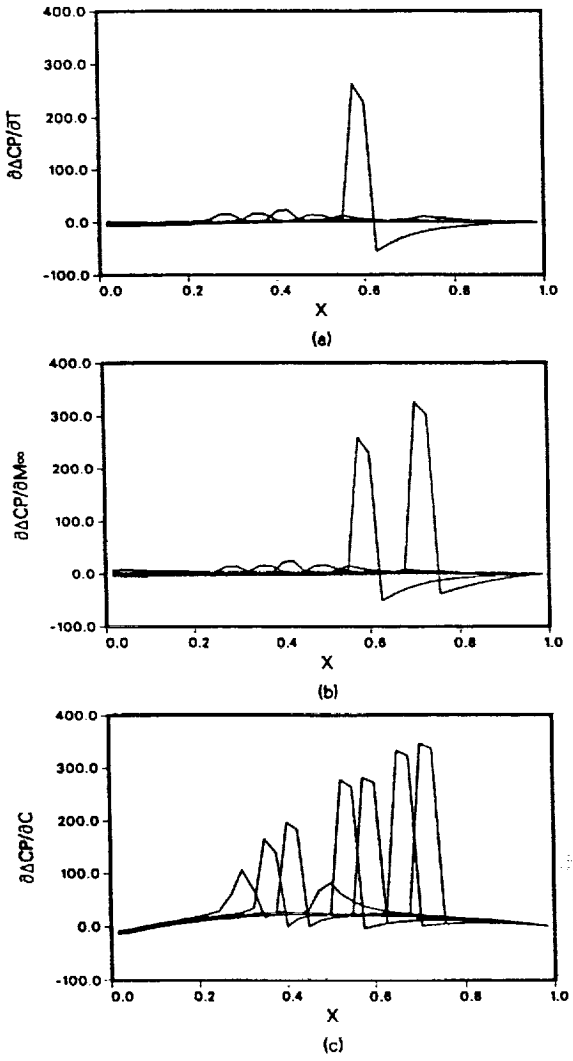

Fig.20 F-D Pressure Difference Coefficient Sensitivity Derivatives

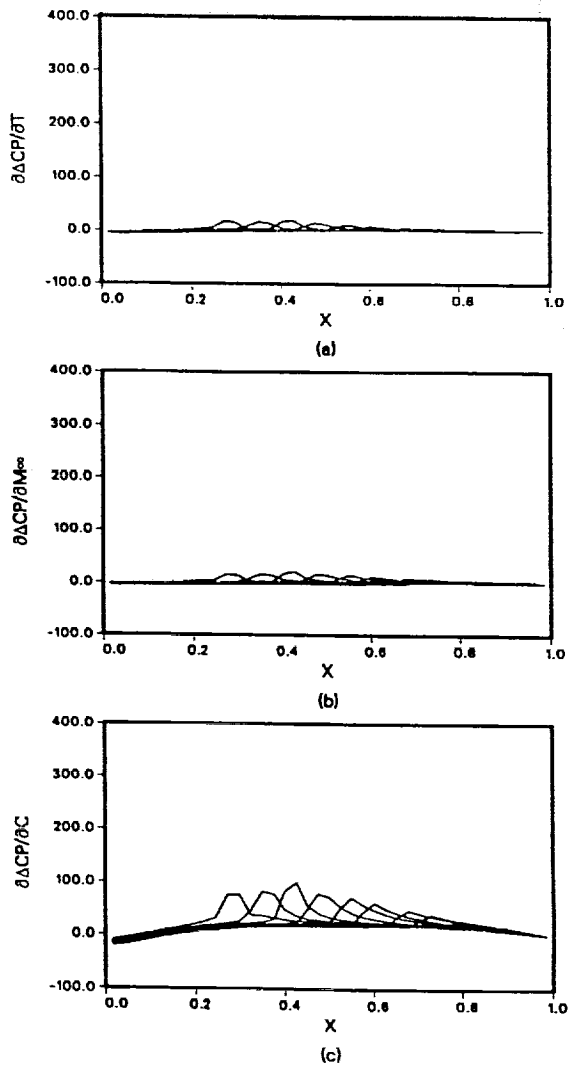

Fig.21 Q-A Pressure Difference Coefficient Sensitivity Derivatives

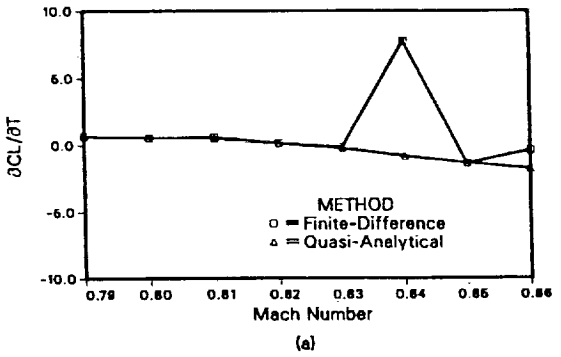

(a)

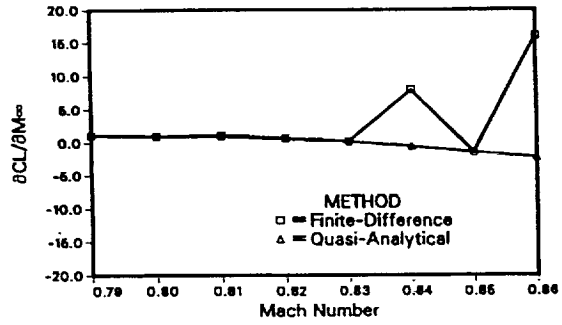

(b)

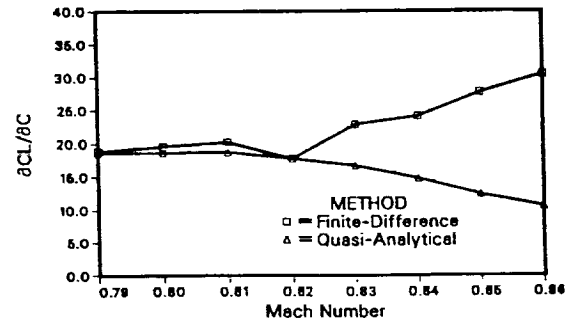

(c)

Fig.22 Lift Coefficient Sensitivity Derivatives

Determination of Aerodynamic Sensitivity Coefficients Based on the Transonic Small Perturbation Formulation

H. M. Elbanna and L. A. Carlson

Reprinted from

Journal of Aircraft

Volume 27, Number 6, June 1990, Pages 507-515

AMERICAN INSTITUTE OF AERONAUTICS AND ASTRONAUTICS, INC.
370 L'ENFANT PROMENADE, SW • WASHINGTON, DC 20024

Determination of Aerodynamic Sensitivity Coefficients Based on the Transonic Small Perturbation Formulation

Hesham M. Elbanna* and Leland A. Carlson†
Texas A&M University, College Station, Texas 77843

The quasianalytical approach is developed to compute airfoil aerodynamic sensitivity coefficients in the transonic and supersonic flight regimes. Initial investigation verifies the feasibility of this approach as applied to the transonic small perturbation residual expression. Results are compared to those obtained by the direct (finite difference) approach, and both methods are evaluated to determine their computational accuracies and efficiencies. The quasianalytical approach is shown to yield more accurate coefficients and is potentially more efficient and worth further investigation.

Nomenclature

C	= maximum camber in fraction of chord
Cp	= pressure coefficient
IM, JM	= grid dimensions
JB	= row above airfoil
L	= chordwise location of maximum camber
M	= Mach number
R	= residual expression
T	= maximum thickness in fraction of chord
XD	= design variable
f, g	= Cartesian coordinate stretching functions
x, y	= Cartesian coordinates
ξ, η	= computational variables
α	= angle of attack
γ	= ratio of specific heats
Γ	= circulation
φ	= perturbation potential function
ΔCp	= $Cp_l - Cp_u$

Subscripts

∞	= freestream condition
b	= body
p	= pressure
u, l	= upper, lower
TE	= trailing edge

Introduction

OVER the past few years, computational fluid dynamics has evolved rapidly as a result of the immense advancements in the computational field and the impact of the use of computers on obtaining numerical solutions to complex problems. Accordingly, researchers are now capable of calculating aerodynamic forces on wing-body-nacelle-empennage configurations. A next logical step would be to compute the sensitivity of these forces to configuration geometry.

In order to improve the design of transonic vehicles, design codes are being developed that use optimization techniques; and, in order to be successful, these codes require aerodynamic sensitivity coefficients, which are defined as the derivatives of the aerodynamic functions with respect to the design variables. Obviously, it is desirable that such sensitivity coefficients be easily obtained. Consequently, the primary objective of this effort is to investigate the feasibility of using the quasi-analytical method[1-3] for calculating the aerodynamic sensitivity derivatives in the transonic and supersonic flight regimes. As part of this work, the resulting sensitivity coefficients are compared to those obtained from the finite difference approach. Finally, both methods are evaluated to determine their computational accuracies and efficiencies.

In the transonic regime, a variety of flowfield solution methods exist. These range from full Navier-Stokes solvers to transonic small perturbation equation solvers. The complexity of the equations that need to be solved depends upon the flow phenomena in question and the objective of the analysis. Since it is not the objective of this work to develop flowfield algorithms, the present research uses the nonlinear transonic small perturbation equation to determine and verify efficient methods for calculating the aerodynamic sensitivity derivatives. In addition, only two-dimensional results will be presented in this initial work.

Background

Most recently, sensitivity methodology has been successfully used in structural design[2] and optimization programs[3] primarily to assess the effects of the variation of various fundamental properties relative to the important physical design variables. Moreover, researchers have developed and applied sensitivity analysis for analytical model improvement and assessment of design trends. In most cases, a predominant contributor to the cost and time in the optimization procedures is the calculation of derivatives. For this reason, it is desirable in aerodynamic optimization to have efficient methods of determining the aerodynamic sensitivity coefficients and, wherever possible, to develop appropriate numerical methods for such computations.

Currently, most methods for calculating transonic aerodynamic sensitivity coefficients are based upon the finite difference approximation to the derivatives. In this approach, a design variable is perturbed from its previous value, a new complete solution is obtained, and the differences between the new and the old solutions are used to obtain the sensitivity coefficients. This direct, or brute force, technique has the disadvantage of being potentially very computer intensive, especially if the governing equations are expensive to solve. In addition, it is difficult to guarantee the accuracy of the derivatives obtained by the finite difference method. Accordingly, the need to eliminate these costly and repetitive analyses is the primary motivation for the development of alternative, efficient computational methods to determine the aerodynamic sensitivity coefficients.

Presented as Paper 89-0532 at the AIAA 27th Aerospace Sciences Meeting, Reno, NV, Jan. 9-12; received March 15, 1989; revision received Oct. 2, 1989.

*Graduate Research Assistant. Student Member AIAA.
†Professor, Aerospace Engineering. Associate Fellow AIAA.

Problem Statement

Based on the foregoing discussion, the current problem is formulated starting from the generic quasianalytical approach and manipulated according to the rules given in Appendix A of Ref. 1 for the derivation of the general sensitivity equation. This general sensitivity equation is then applied to the residual expression R of the transonic small perturbation equation, which is a simple and adequate description of the nonlinear phenomena occurring in the transonic regime. Although this expression is nonlinear in the perturbation potential φ, the general sensitivity equation, Eq. (1), is linear with respect to the unknown sensitivity $(\partial\varphi/\partial XD_i)$. It is to be noticed that the practical implementation of the above step is not achieved until the residual expression is approximated on a finite domain and the mathematical form of the problem rendered to that of one in linear algebra. This discretization process is explained in detail in Ref. 4.

Thus, the quasianalytical method, as applied to the residual expression of the transonic small perturbation equation, yields the sensitivity equations,

$$\left[\frac{\partial R}{\partial \varphi}\right]\left\{\frac{\partial \varphi}{\partial XD_i}\right\} = -\left\{\frac{\partial R}{\partial XD_i}\right\} \tag{1}$$

where

$$R \equiv (B_1 + B_2\varphi_x)\varphi_{xx} + \varphi_{yy} = 0 \tag{2}$$

$$B_1 = 1 - M_\infty^2$$

$$B_2 = -(\gamma + 1)M_\infty^2$$

$$\varphi \equiv \varphi(x, y, XD) \tag{3}$$

$XD \equiv$ set of design variables

$XD_i \equiv i$th design variable

subject to the airfoil boundary condition,

$$\varphi_y(x_b, 0) = \left[\frac{dy}{dx}\right]_b = F(x, XD) \tag{4}$$

the infinity boundary condition, for $M_\infty < 1$

$$\varphi_\infty = -\Gamma\theta/(2\pi), \qquad \theta = n\pi/2, \qquad n = 0,1,2,3,4$$

or for $M_\infty > 1$

$$\varphi_\infty = 0, \qquad \theta = n\pi/2, \qquad n = 1,2,3$$

$$\varphi_x = 0, \qquad \theta = n\pi/2, \qquad n = 0,4 \tag{5}$$

and the Kutta condition

$$\Delta P = 0 \qquad (\Gamma = \Delta\varphi = \text{const}), \qquad x_{TE} < x \le \infty \tag{6}$$

Equation (1) is discretized into a system of linear equations to be solved for the unknown sensitivity vectors. In carrying out this step, the expressions for both the right side vector and the left side matrix are generated analytically. The solution of this system is obtained efficiently by using either a direct or an iterative procedure that allows for multiple right sides. This approach is explained in the following section and has the advantage that several unknown vectors can be obtained simultaneously, each vector representing the sensitivity of the potential φ with respect to some design variable XD_i.

At this stage, it is convenient to define the vector of design variables

$$XD = \{XD_1, XD_2, \ldots, XD_n\} \tag{7}$$

and to exactly determine which variables influence the solution of Eq. (2). In doing so, the relation between the sensitivity coefficients corresponding to these variables and the form of the optimization algorithm that utilizes this information needs to be considered. Notice that the derivatives computed in this study, namely, the first partial derivatives, are adequate for a typical optimization routine if it were to be applied to the present two-dimensional problem. Notice also that some optimization studies might require higher derivatives.

For the transonic flow problem, an appropriate choice of the first design variable is the freestream Mach number (M_∞). This variable appears in the governing Eq. (2) and has an important influence on the character of the equation via its influence on local Mach number (for $M < 1$, the equation is elliptic, for $M > 1$, the equation is hyperbolic) and thus on the nature of the solution. For this reason, it is desirable to have M_∞ as one of the design variables.

Next, it is appropriate to examine the boundary condition given by Eq. (4). In the transonic small perturbation formulation, the angle of attack (α) enters the problem through the boundary condition and thus,

$$F_u = \left[\frac{dy}{dx}\right]_b = y_u' - \alpha \tag{8}$$

For simplicity, the function F should be easily differentiable with respect to the design variables defining the airfoil geometry. This desirable feature simplifies the computation of the right side term of the sensitivity equation. Therefore, it would seem plausible to have a simple analytical expression for modeling the upper and lower surfaces of the airfoil.

For the present studies, it was decided to limit consideration to one basic airfoil section, namely the NACA four-digit section, whose families of wing sections are obtained by combining a mean line and a thickness distribution.[5] The resultant expressions possess the necessary features that suit the problem, mainly the concise description of the airfoil surfaces in terms of several geometric design variables. The expressions are as follows:

$$y_u = \begin{cases} C(2Lx - x^2)/L^2 \pm 5T(0.2969\sqrt{x} - 0.126x \\ \quad -0.3516x^2 + 0.2843x^3 - 0.1015x^4), \quad x \le L \\ C\left[(1-2L) + 2Lx - x^2\right]/(1-L)^2 \\ \quad \pm 5T(0.2969\sqrt{x} - 0.126x - 0.3516x^2 \\ \quad +0.2843x^3 - 0.1015x^4), \quad x > L \end{cases} \tag{9}$$

Each of the quantities C, L, and T is expressed as a fraction of the chord. Differentiating Eq. (9) with respect to x and substituting the result into Eq. (8) yields

$$F_u = 2C(L - x)/LL \pm 5T(0.14845/\sqrt{x} - 0.126 - 0.7032x + 0.8529x^2 - 0.406x^3) - \alpha \tag{10}$$

where

$$LL = \begin{cases} L^2, & x \le L \\ (1-L)^2, & x > L \end{cases} \tag{11}$$

Eq. (10) is a simple analytical expression in terms of the four variables T, L, C, and α. Thus,

$$XD = \{T,\ M_\infty,\ \alpha,\ L,\ C\} \tag{12}$$

represents the complete set of design variables that define the present two-dimensional airfoil sensitivity problem. Notice that these variables are completely uncoupled; and, thus, the sensitivity equation can be solved independently with respect to each variable.[6]

Mathematical Treatment and Solution Procedure

Problem Discretization

Equation (1) represents the general sensitivity equation applied to the residual R. Now, in order to solve the problem numerically, Eq. (2) is formulated computationally on a finite domain. This transformation is achieved by using a stretched Cartesian grid that maps the infinite physical domain onto a finite computational grid. In this study, the grid used is based upon a hyperbolic tangent transformation that places the outer boundaries at infinity. Accordingly, the transformed residual expression is given by

$$R \equiv [B_1 + B_2 f \varphi_\xi] f(f\varphi_\xi)_\xi + g(g\varphi_\eta)_\eta = 0 \tag{13}$$

This equation is solved numerically by an approximate factorization scheme.[7] In finite-difference form, Eq. (13) can be written as

$$\begin{aligned} R_{i,j} \equiv & \left[B_1 + B_2(\varphi_{i+1,j} - \varphi_{i-1,j}/(2\Delta\xi)\right] f_i/\Delta\xi^2 \\ & \times \left[\nu_{i,j} f_{i+\frac{1}{2}}(\varphi_{i+1,j} - \varphi_{i,j}) - (2\nu_{i,j} - 1) f_{i-\frac{1}{2}}(\varphi_{i,j} - \varphi_{i-1,j})\right. \\ & \left. - (1 - \nu_{i,j}) f_{i-3/2}(\varphi_{i-1,j} - \varphi_{i-2,j})\right] \\ & + \left[g_{j+\frac{1}{2}}(\varphi_{i,j+1} - \varphi_{i,j}) - g_{j-\frac{1}{2}}(\varphi_{i,j} - \varphi_{i,j-1})\right] g_j/\Delta\eta^2 \end{aligned} \tag{14}$$

where

$\nu_{i,j} = 1$ if point (i,j) is subsonic

$\nu_{i,j} = 0$ if point (i,j) is supersonic

Eq. (14) is the discretized form of the residual at a general point (i,j) in terms of φ values at surrounding points. Consequently, R at i,j can be viewed as a function of the φ values at neighboring points; and, therefore, the differentiation of the residual expression is straightforward.

Differentiation of the Residual

Rearranging Eq. (14) yields

$$\begin{aligned} R_{i,j} = & c_1\varphi_{i,j} + c_2\varphi_{i+1,j}\varphi_{i-1,j} + c_3\varphi_{i+1,j}\varphi_{i,j} + c_4\varphi_{i-1,j}\varphi_{i,j} \\ & + c_5\varphi_{i+1,j}\varphi_{i-2,j} + c_6\varphi_{i-1,j}\varphi_{i-2,j} + c_7\varphi_{i-1,j}^2 + c_8\varphi_{i+1,j}^2 \\ & + c_9\varphi_{i+1,j} + c_{10}\varphi_{i-1,j} + c_{11}\varphi_{i,j+1} + c_{12}\varphi_{i,j-1} + c_{13}\varphi_{i-2,j} \end{aligned} \tag{15}$$

The coefficients $c_1, c_2, \ldots, c_{13}$ are functions only of the stretching factors and of B_1 and B_2, which are functions of M_∞. This fact is used when differentiating Eq. (15) with respect to M_∞ in order to obtain the right side $(\partial R/\partial M_\infty)$. It is also necessary to consider the treatment of various types of grid points and examine the effect on the general residual expression. Several groups of points, such as those adjacent to the airfoil, to the wake cut, and to infinity boundaries, need special treatment. Accordingly, it is necessary to revise the residual expression at these boundary points to include the boundary conditions. The resulting updates are then used to modify the residual equation, Eq. (15), and to yield a set of expressions, each being valid for a group of boundary points. The details of these operations and the expressions for the coefficients c_1–c_{13} are found in Ref. 4.

In setting up the complete quasianalytical problem, the circulation and its dependence upon trailing-edge potentials must be carefully included. Since the circulation is determined by the difference in potentials at the trailing edge,

$$\Gamma = \varphi_{\text{uTE}} - \varphi_{\text{lTE}} \tag{16}$$

or, by interpolating the trailing-edge values

$$\begin{aligned} \Gamma = & T_1\left[1.5(\varphi_{\text{ITE}-1,JB} - \varphi_{\text{ITE}-1,JB-1})\right. \\ & \left. - 0.5(\varphi_{\text{ITE}-1,JB+1} - \varphi_{\text{ITE}-1,JB-2})\right] \\ & + T_2\left[1.5(\varphi_{\text{ITE},JB} - \varphi_{\text{ITE},JB-1})\right. \\ & \left. - 0.5(\varphi_{\text{ITE},JB+1} - \varphi_{\text{ITE},JB-2})\right] \end{aligned} \tag{17}$$

where

$$T_2 = \left[\xi(x = 0.5) - \xi(\text{ITE} - 1)\right]/\Delta\xi \tag{18}$$

$$T_1 = [1 - T_2] \tag{19}$$

and since a branch cut extends from the trailing edge to downstream infinity, and trailing-edge potentials appear in the residual expressions for points along the branch cut. In addition, since in the two-dimensional case the infinity boundary conditions are proportional to the circulation, the trailing-edge potentials also appear in the residual expressions at points adjacent to the outer boundaries. Consequently, the resultant matrix $(\partial R/\partial\varphi)$, while banded, also contains many nonzero elements far from the central band. Notice that the presence of these elements greatly complicates the rapid and efficient solution of the sensitivity equation, Eq. (1).

The resulting residual expressions are differentiated analytically with respect to the potential φ. Specifically, each equation is differentiated with respect to the potential at neighboring points and trailing-edge points. The latter enter as a result of the implicit nature of the circulation effects. These points are denoted by the counters (ii,jj) and are given by

$$(i,j-1),\ (i,j),\ (i,j+1),\ (i-2,j),\ (i-1,j),\ (i+1,j)$$

$$(\text{ITE}-1,JB-2),\ (\text{ITE}-1,JB-1),\ (\text{ITE}-1,JB)$$

$$(\text{ITE}-1,JB+1),\ (\text{ITE},JB-2),\ (\text{ITE},JB-1)$$

$$(\text{ITE},JB),\ (\text{ITE},JB+1)$$

Solution about a Fixed Design Point

Once the residual relations are obtained, the actual coefficients are assembled by evaluating the appropriate analytical expressions using a flowfield solution obtained from Eq. (2) for a given set of conditions (i.e., about a fixed design point). Similarly, the right sides are evaluated by differentiating the analytical expressions for the residual with respect to each design variable. Again, the details and results of these steps are found in Ref. 4.

The end result is that the coefficient matrix $(\partial R_{i,j}/\partial\varphi_{ii,jj})$ is of size $(IM-2)\times(JM-2)\times(IM-2)\times(JM-2)$ for a general $(IM \times JM)$ grid. This system is large, of block structure, diagonally dominant, and sparse and, while banded, also contains many nonzero elements far from the central band. As a result of this size and structure, it is obvious that a reasonably fast scheme for solving Eq. (1) is needed.

Currently, it is very difficult to single out an optimum routine that handles a general, large, sparse system of linear equations for which the coefficient matrix is unsymmetric. This is because, unlike the theory of symmetric matrices, the theory of general unsymmetric matrices is more involved and has yet to be developed. Since research in the above areas is currently very active and specialized, any attempt to cover these topics in detail would be laborious. For this reason, it was decided to use a few general but not necessarily the most efficient approaches that were available in the literature and that could be integrated into the sensitivity codes with adjustments. This approach would allow an evaluation of the overall cost involved in solving the current two-dimensional problem.

The first solver is based on standard Gaussian elimination with partial pivoting and full storage. The second is based on triangular decomposition[8] and uses a compact storage scheme that avoids handling the zero entries and therefore should be more efficient than standard Gaussian elimination. The third solver is based on a Gauss-Seidel iterative scheme[9] and was not optimized for speed (through the choice of optimum acceleration parameters) but uses sparse matrix technology in processing only the nonzero elements. The fourth and last solver used is based on the conjugate gradient method.[10] Handling the sparsity pattern for the third and fourth solvers is achieved by assembling the symbolic part of the coefficient matrix only once for a given grid size and given freestream (subsonic vs supersonic). The resultant structure is then stored on a disk file. Before the numerical part is executed, the symbolic information is read into the code and used directly to assemble the new matrix. This procedure is followed to reduce the time consumed in assembling the coefficient matrix. Notice also that in the Gauss-Seidel and conjugate-gradient solvers that the error tolerances for the coefficients involving maximum thickness, freestream Mach number, and location of maximum camber were 1.E-06, while those on angle of attack and maximum camber were 1.E-04.

Once the sensitivities of the potentials, and thus the Cp distribution, to the design variables are known, the sensitivity of the lift coefficients to the design variables can be easily computed. To minimize errors, these coefficients are computed using

$$C_L = 2\Gamma = 2(\varphi_{uTE} - \varphi_{lTE}) \tag{20}$$

and hence,

$$\partial C_L/\partial XD_i = 2(\partial\varphi_{uTE}/\partial XD_i - \partial\varphi_{lTE}/\partial XD_i) \tag{21}$$

Finally, all methods used for computing the derivatives are compared to the finite-difference approach, and the results are presented and evaluated to determine the computational accuracy and efficiency of each method.

Test Cases

In this study, the quasianalytical method has been used to determine the aerodynamic sensitivity coefficients at two freestream Mach numbers ($M_\infty = 0.2, 0.8$) for the NACA 1406 airfoil at 1-deg angle of attack. Results were also obtained[4,11] for a supersonic case at $M_\infty = 1.2$. Notice that further studies are needed to examine the results for a wider range of design parameter variation.

In the following, two types of results will be presented. The first will be plots of Cp vs chord for the three chosen Mach numbers. The second will be the corresponding plots of $(\partial Cp/\partial T)$, $(\partial Cp/\partial M_\infty)$, $(\partial Cp/\partial\alpha)$, $(\partial Cp/\partial C)$, and $(\partial Cp/\partial L)$ for the upper and lower surfaces and plots of $(\partial\Delta Cp/\partial T), \ldots$, etc., involving the difference, all will be obtained by the quasianalytical method. In addition, all of the figures will also contain results obtained using the direct (finite difference) approach in which each design variable was individually perturbed by a small amount, typically 0.001, and a new flowfield solution obtained. Then the sensitivities were computed using $\Delta Cp/\Delta XD$ and are shown via dashed lines. In many cases, the lines are coincident with the quasianalytical results and cannot be observed. Table 1 compares results obtained by the two methods, and in most cases the agreement is within 1%.

In all cases, an 81×20 stretched Cartesian grid was utilized. While finer grid studies are needed, they were not performed as part of this initial study. In addition, for these studies, the flowfield was normally computed using double precision arithmetic and the maximum residual reduced eight orders of magnitude. It was felt that this level of convergence was necessary in order to accurately evaluate sensitivity coefficients using a finite-difference approach, although such convergence may not be required in the flowfield solver for the quasi-analytical method.

Table 1 Accuracy of quasianalytical method for computing lift coefficient sensitivity derivatives for NACA 1406, GRID 81×20

XD_i	Method[a]	$M_\infty = 0.2$	$M_\infty = 0.8$	$M_\infty = 1.2$
T	FD	0.0044	0.5232	−0.2949
	QA	0.0044	0.5447	−0.3376
M_∞	FD	0.0471	0.9708	1.0235
	QA	0.0470	0.9905	−0.0703
α	FD	6.1385	10.5229	4.8758
	QA	6.1386	10.5229	4.8726
C	FD	9.9380	19.5767	0.7695
	QA	9.9381	18.6154	0.7356
L	FD	0.0696	0.1499	−0.0348
	QA	0.0693	0.1496	−0.0349

[a]FD, finite difference. QA, quasianalytical.

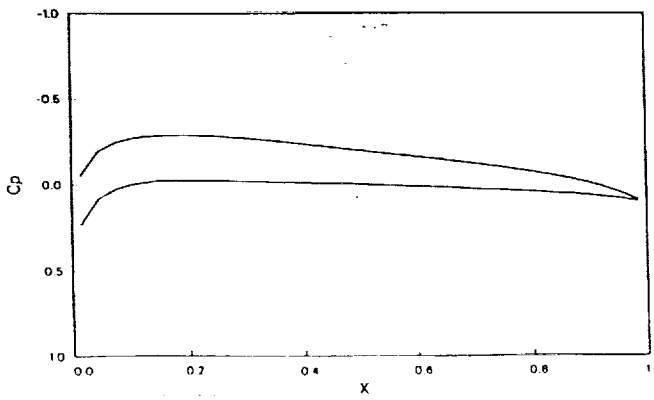

Fig. 1 Pressure coefficient distribution at $M_\infty = 0.2$.

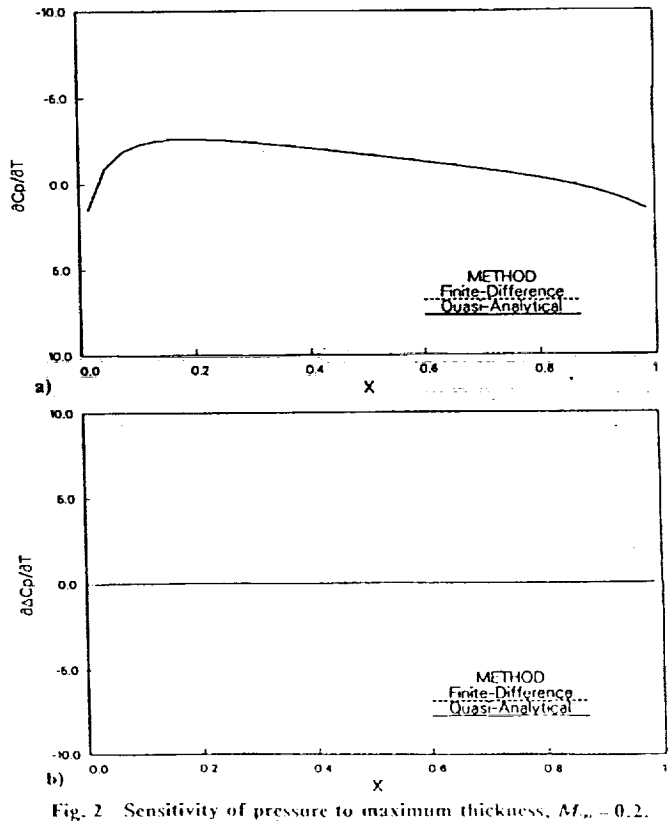

Fig. 2 Sensitivity of pressure to maximum thickness, $M_\infty = 0.2$.

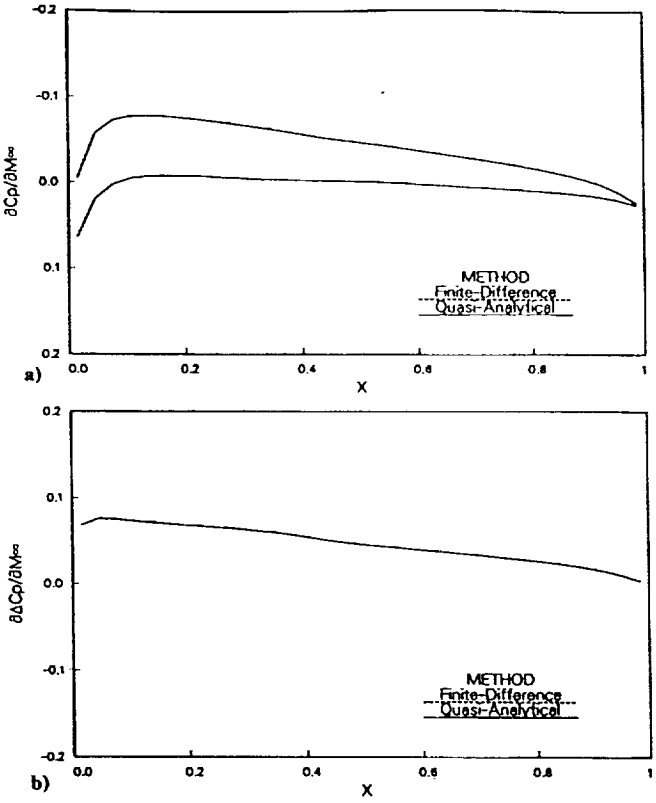

Fig. 3 Sensitivity of pressure to freestream Mach number, $M_\infty = 0.2$.

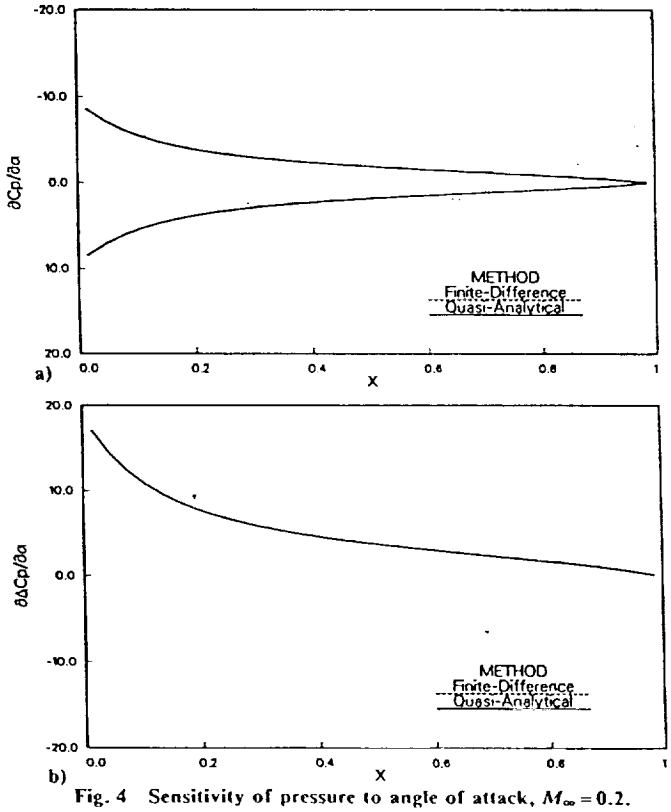

Fig. 4 Sensitivity of pressure to angle of attack, $M_\infty = 0.2$.

Results and Discussion

Subsonic Case – $M_\infty = 0.2$

Initial studies concentrated on subsonic cases since at least approximate results would be known from thin airfoil theory.[5] Figure 1 shows the pressure distribution for the NACA 1406 airfoil, while Figs. 2a and 2b show the sensitivity of the pressure to thickness for the same airfoil. As expected from thin

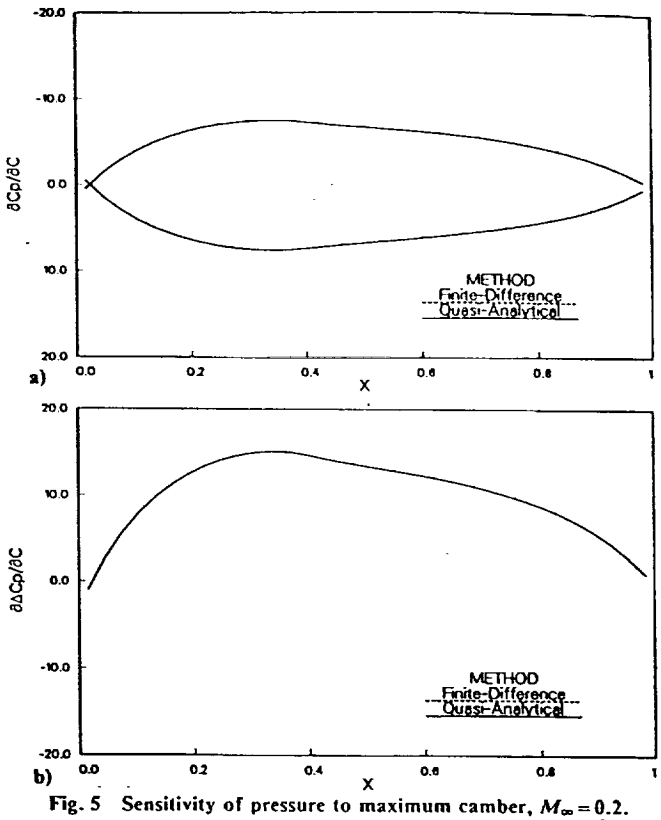

Fig. 5 Sensitivity of pressure to maximum camber, $M_\infty = 0.2$.

airfoil theory, the upper and lower surface values are essentially identical, and the difference is very small everywhere. Also shown on the same figure (and on subsequent figures) by the dashed line is the result obtained by using the finite-difference approach; and as can be seen, the agreement between the two approaches is excellent.

The sensitivity of pressure to freestream Mach number is plotted on Figs. 3a and 3b. It is noticed that while the profiles for the upper and lower surfaces are similar, they are not equal in magnitude, indicating a nonlinear variation with Mach number as predicted by simple Prandtl-Glauert theory. However, as indicated by the results plotted on Fig. 3b, the magnitudes for this subsonic Mach number are very low.

The sensitivity of the pressure coefficients to angle of attack are depicted for this case in Figs. 4a and 4b. As expected from linear thin airfoil theory, the upper and lower surface curves are essentially equal in magnitude but of opposite sign. Not surprisingly, the sensitivity of the delta Cp variation, Fig. 4b, has the shape of the pressure difference curve for a flat plate at angle of attack; and its magnitude, particularly near the leading edge, is quite large.

On Figs. 5a and 5b is plotted the sensitivity of the pressure coefficient to the amount of maximum camber. Since camber contributes to lift, it is expected from the thin airfoil theory that these values should be "equal but opposite in sign" for the upper and lower surfaces. In addition, the pressure difference curve has the correct shape for that associated with a 14 mean line with the peak occurring at 30% chord[5] and has a magnitude comparable to those for the $(\partial Cp/\partial\alpha)$ curves.

Finally, the sensitivity of pressure to the location of the maximum camber point is portrayed in Figs. 6a and 6b and, to say the least, the results are interesting. Since maximum camber location affects the camber profile and hence lift, the equal and opposite behavior of the upper and lower surface coefficients is expected. In addition, the pressure difference sensitivity is primarily negative forward of the point of maximum camber and positive aft of it. This result indicates that if the location of maximum camber were moved rearward slightly (i.e., a positive ΔL), that lift would be decreased on the forward portion of the airfoil and increased on the aft portion of

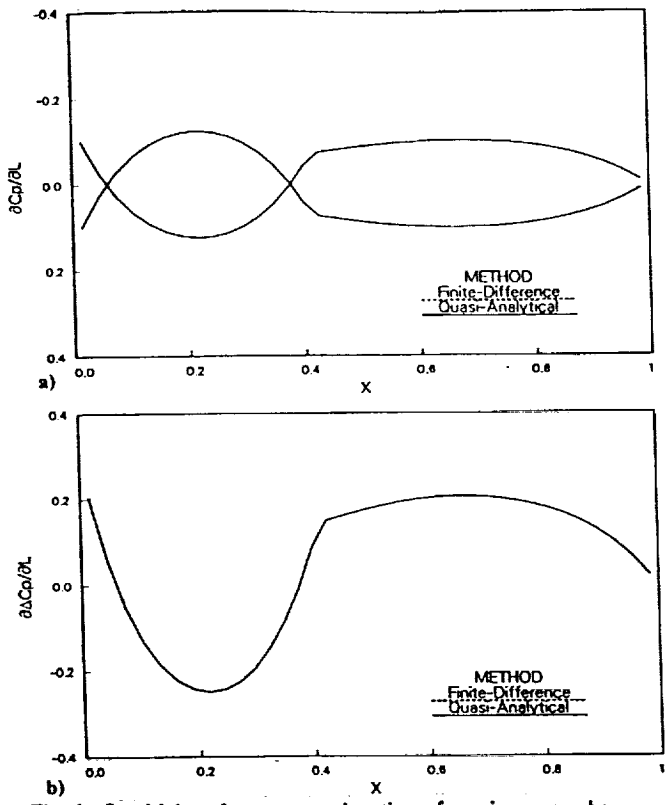

Fig. 6 Sensitivity of pressure to location of maximum camber, $M_\infty = 0.2$.

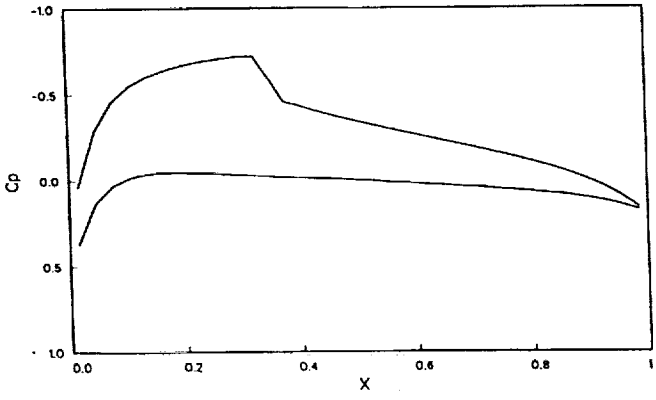

Fig. 7 Pressure coefficient distribution at $M_\infty = 0.8$.

the airfoil, which is in agreement with the results presented in Ref. 5.

Transonic Case – $M_\infty = 0.8$

At $M_\infty = 0.8$, the flow about the NACA 1406 airfoil has a strong shock at 40% chord, see Fig. 7, and the lower surface is entirely subcritical. As a consequence, the variation with chord of the sensitivity coefficients is considerably different than in the subsonic case.

Figs. 8a and 8b show the sensitivity of pressure to the maximum thickness; and while the lower surface profile is similar to that obtained at subsonic conditions, the upper surface curve and the pressure difference coefficient plot show the effect of the upper surface shock wave. The large peak on the curves corresponds to the location of the shock wave and indicates that the shock-wave location is very sensitive to maximum thickness. Notice on Figs. 8a and 8b the excellent agreement of the quasianalytical results indicated by the solid lines with those obtained using the finite-difference approach (dashed lines).

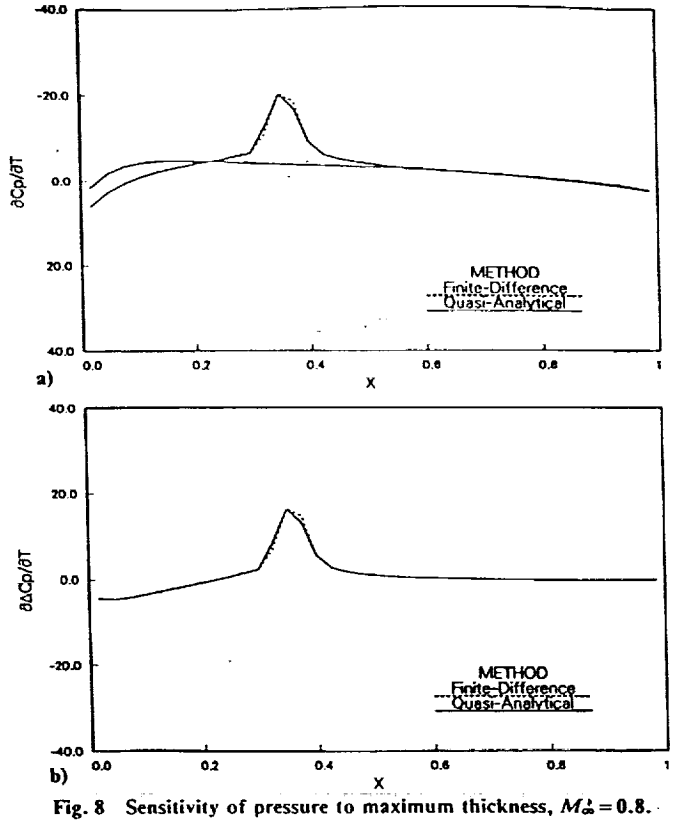

Fig. 8 Sensitivity of pressure to maximum thickness, $M_\infty = 0.8$.

The results for $(\partial Cp/\partial M_\infty)$, which are shown on Figs. 9a and 9b, are similar. The lower surface curve is typical of a subsonic flow, whereas the upper surface and the pressure difference coefficients reflect the presence of the upper surface shock wave. Similar comments can be made for the remaining design variable coefficients, which are plotted on Figs. 10, 11, and 12.

Examination of the curves in the vicinity of the shock wave location indicates that the pressure sensitivity and indirectly the shock wave location is about equally influenced by the maximum thickness, freestream Mach number, and angle of attack. However, in comparison it is relatively insensitive to the location of maximum camber; but, perhaps surprisingly so, the pressure is twice as sensitive to the amount of maximum camber as it is to the other design variables. It should also be noticed that the lift is most sensitive to angle of attack and to maximum camber.

In addition, Fig. 11 shows a discrepancy between the results obtained by the direct approach and those obtained through the quasianalytical method. It will be shown in the following section that this discrepancy is related to the choice of the step size used in computing the finite-difference solution, thus, revealing a significant deficiency in computing the sensitivity derivatives in nonlinear regimes via the finite-difference approach.

Time Comparisons

Obviously, in the development of the quasianalytical method, it was hoped that not only would this approach yield accurate values for the aerodynamic sensitivity coefficients, but also that it would be more efficient than the brute-force, finite-difference approach. Table 2 presents some comparisons concerning the amount of computational effort required to obtain solutions by the two approaches including results for the supersonic case.[4,11]

In comparing the values, several items should be kept in mind. First, it has been assumed that the finite-difference approach will require six independent solutions. In practice, it might be possible to start each finite-difference solution from

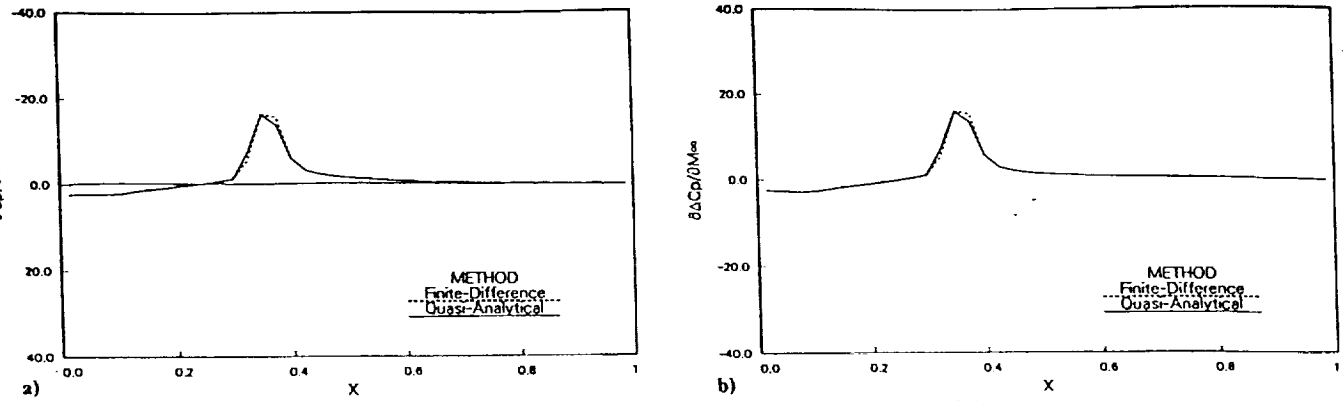

Fig. 9 Sensitivity of pressure to freestream Mach number, $M_\infty = 0.8$.

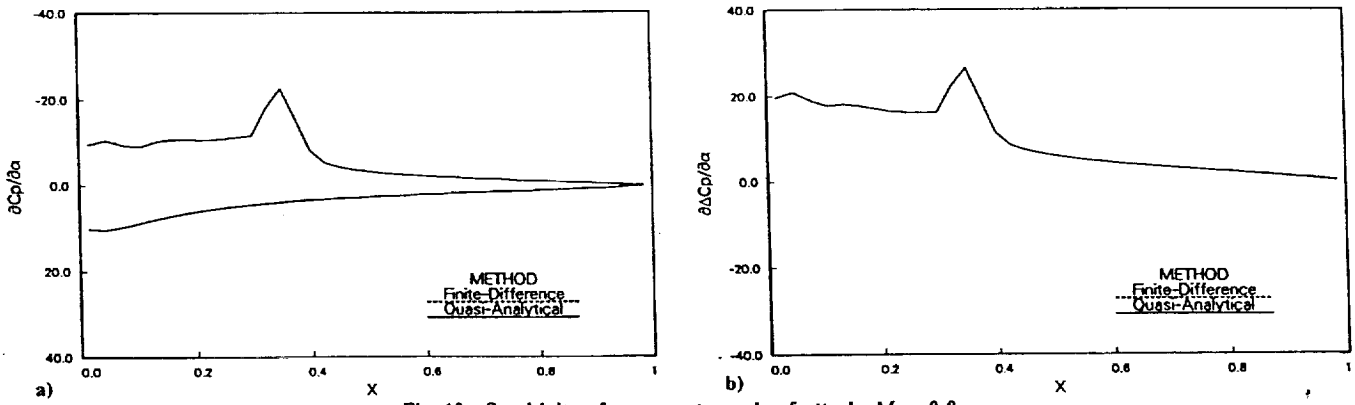

Fig. 10 Sensitivity of pressure to angle of attack, $M_\infty = 0.8$.

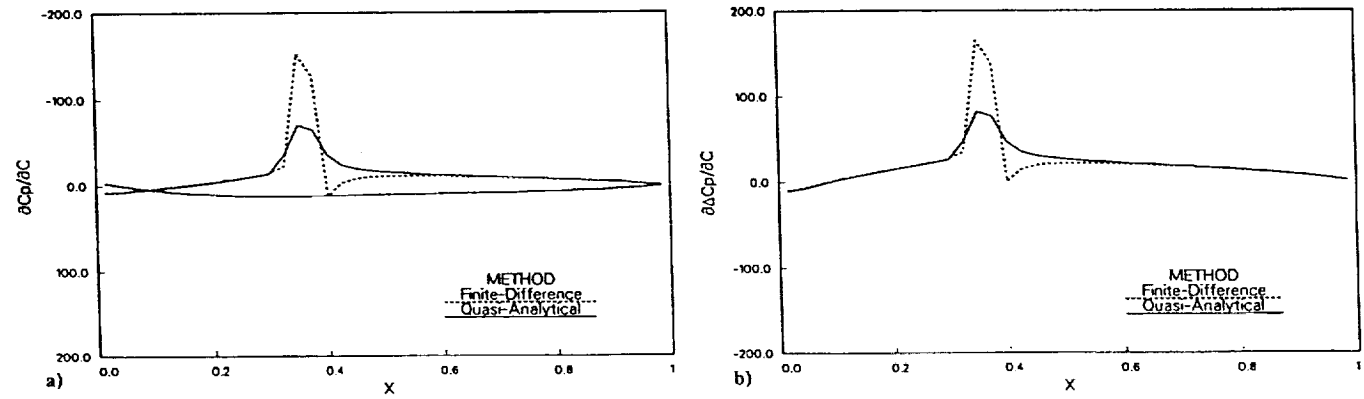

Fig. 11 Sensitivity of pressure to maximum camber, $M_\infty = 0.8$.

a previous solution and, thus, decrease the time to convergence. However, to be accurate, the finite-difference approach will probably require double precision and will have to be extremely well converged (i.e., 1.E-08). Nevertheless, the values for the finite-difference approach probably should be viewed as maximum values.

Second, the methods used for obtaining the sensitivity coefficients have not been optimized and, as mentioned earlier, may not even be optimum; and the flowfield solution required for the quasianalytical approach may not need double precision and may not have to be as tightly converged. Thus, the values shown for the quasianalytical approach should also be viewed as maximum values.

In spite of these limitations, results obtained by direct methods do indicate that the quasianalytical method is more computationally efficient at supersonic conditions and potentially efficient at transonic conditions than the brute-force, finite-difference approach.

Notice that in this study, the initial guess used in computing the sensitivity derivatives via iterative methods was arbitrarily chosen as the zero vector. In addition, time comparisons presented in Table 2 show that iterative methods are in general less efficient than direct methods if the derivatives for the current two-dimensional problem were sought about some general design point. However, if the objective is to incorporate the sensitivity derivatives into an optimization loop (i.e., to use the derivatives in a continuation problem), then, a good initial guess (which in that case would be available) would enhance convergence, and the overall cost of computing the derivatives using iterative methods might be reduced. These points should be taken into consideration when a sensitivity study is to be integrated into an optimization procedure.

Additional Test Cases

The first group of cases are carried out to investigate the performance of the NACA 1406 airfoil for a range of Mach numbers from 0.79 to 0.86 in increments of 0.01. As shown in Fig. 13, this range of transonic Mach numbers encompasses the development of the shock wave on the upper surface of the airfoil. Also, as shown on Figs. 14 and 15 for the cases involving thickness, Mach number, and maximum camber, the quasianalytical derivatives are in the vicinity of the shock wave frequently different from those obtained by the finite-difference approach. This discrepancy raises two questions—what is

Table 2 Time[a] comparisons for obtaining sensitivity coefficients for five design variables for NACA 1406, GRID 81×20

Method[b]	$M_\infty = 0.2$	$M_\infty = 0.8$	$M_\infty = 1.2$
FD	1.0000	1.0000	1.0000
TD	2.5187	0.9962	0.3929
GE	2.4089	0.9927	0.5165
GS	0.9971	1.5410	—
CG	35.2264	10.6199	—

[a]All CPU times were normalized by the time taken to compute FD derivatives.
[b]FD, finite difference; TD, triangular decomposition; GE, Gauss elimination; GS, Gauss-Seidel; CG, conjugate gradient.

Table 3 Effect of changing step size delta on finite-difference lift coefficient sensitivity derivatives for NACA 1406, GRID 81×20, $M_\infty = 0.84$

Delta XD_i	$XD_i = T$	$XD_i = M_\infty$	$XD_i = C$
1.E-03	7.7603	7.8715	24.0912
1.E-04	−0.8493	−0.6340	83.9853
1.E-05	−0.8497	−0.6364	14.7719
1.E-06	−0.8498	−0.6366	14.7695
QA[a]	−0.8498	−0.6367	14.7692

[a]QA, quasianalytical lift coefficient sensitivity derivatives.

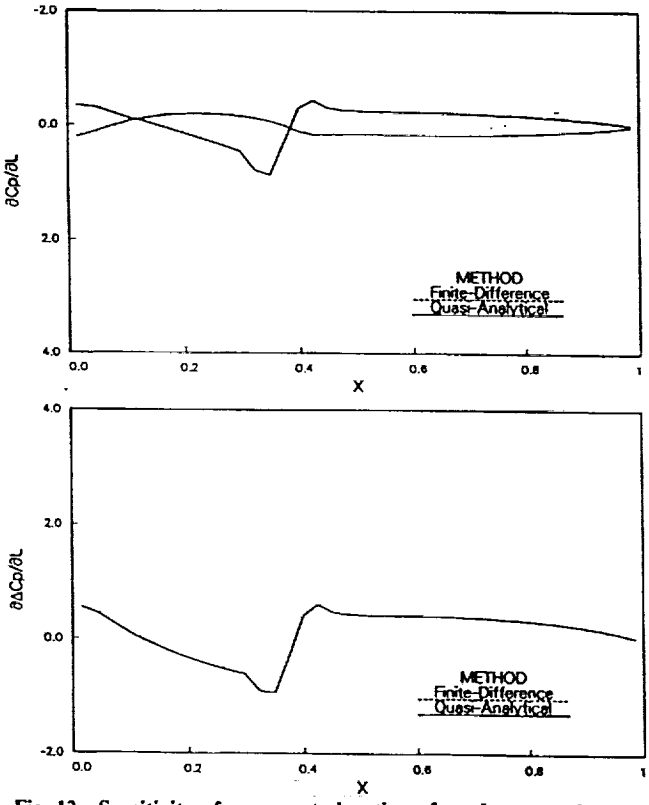

Fig. 12 Sensitivity of pressure to location of maximum camber, $M_\infty = 0.8$.

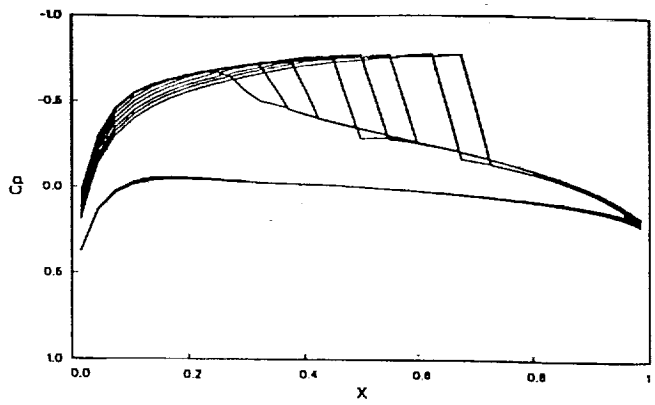

Fig. 13 Pressure coefficient distributions at various Mach numbers.

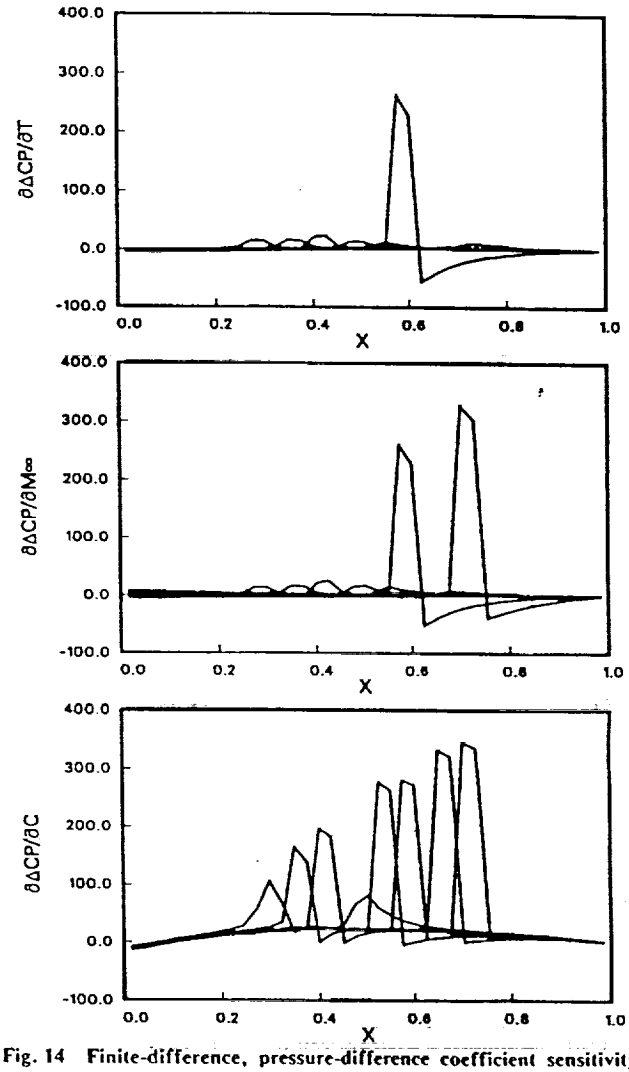

Fig. 14 Finite-difference, pressure-difference coefficient sensitivity derivatives at various Mach numbers.

the cause of the disagreement and which set of derivatives is more accurate? Examination of the variation of the integrated coefficient, $\partial CL/\partial XD_i$ with M_∞, which is portrayed on Fig. 16, shows that the quasianalytical results are smooth and follow a definite trend, whereas the finite-difference values are at best "discontinuous." Consequently, it is concluded that the finite-difference results are less accurate.

In order to observe the performance of the finite-difference approach in the transonic regime, it is necessary to examine the effect of changing the step size (delta of the design variable) on the computed derivatives. Four different values for the step size (1.E-03, 1.E-04, 1.E-05, and 1.E-06) were chosen and applied to the NACA 1406 at a Mach number of 0.84. Examination of this second group of results (see Table 3) show that as the step size is decreased, the finite-difference lift coefficient sensitivity derivatives approach the values computed by the quasianalytical method. However, in some cases, for small ΔXD_i values, oscillations in the pressure coefficient sensitivity derivatives have been observed depending upon the machine used and the method of storing and retrieving the data. These oscillations combined with the difficulty of properly choosing a suitable finite-difference ΔXD_i a priori indicates that the finite-difference approach is probably not a practical method of efficiently computing sensitivity coefficients. On the other

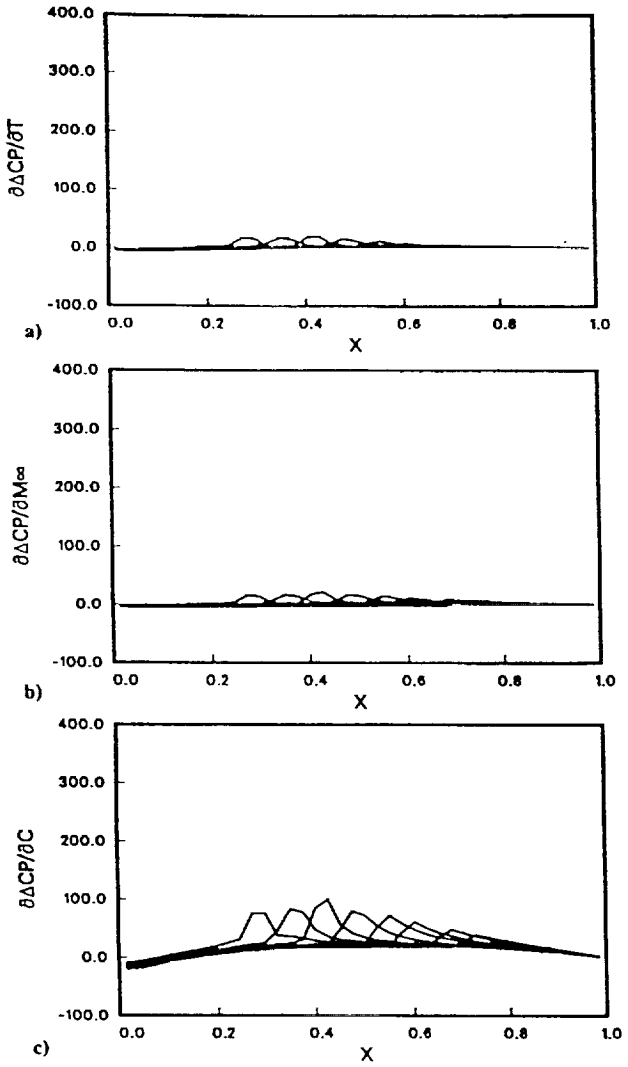

Fig. 15 Quasianalytical pressure-difference coefficient sensitivity derivatives at various Mach numbers.

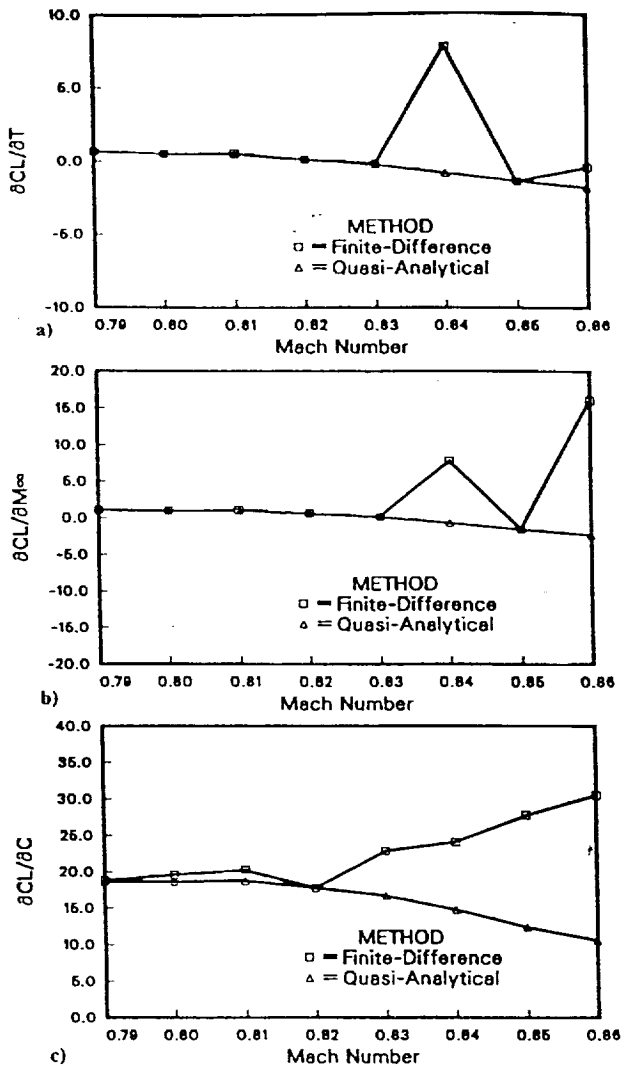

Fig. 16 Lift coefficient sensitivity derivatives.

hand, the present results demonstrate that the quasianalytical method can be used accurately to obtain such coefficients in the transonic flight regime.

Conclusion

Based upon these investigations and results, it is concluded that the quasianalytical method is a feasible approach for accurately obtaining transonic aerodynamic sensitivity coefficients in two dimensions. The results obtained from the quasianalytical method are almost identical to those obtained by the brute-force (finite-difference) technique. Furthermore, the study indicates that the computation of sensitivity derivatives at transonic conditions is generally more accurate using the quasianalytical direct solver approach than the finite-difference approach. In addition, the quasianalytical method is more efficient at supersonic Mach numbers and is potentially more efficient than the brute-force approach at transonic speeds. However, further studies to determine the effects of grid refinement and to examine the results over a wider range of design parameter variation are needed.

Acknowledgments

This effort was primarily supported by the National Aeronautics and Space Administration under Grant NAG 1-793 with E. Carson Yates, Jr. of the NASA Langley Research Center as Technical Monitor. A very warm and special thank you goes to M. S. Pilant, Professor of Mathematics, Texas A&M University, for helpful ideas and comments.

References

[1]Sobieski, J., "The Case for Aerodynamic Sensitivity Analysis," NASA/VPI&SY Symposium on Sensitivity Analysis in Engineering, Sept. 1986.

[2]Adelman, H. M., and Haftka, R. T., "Sensitivity Analysis and Discrete Structural Systems," *AIAA Journal*, Vol. 24, No. 5, May 1986, pp. 823-832.

[3]Bristow, D. R., and Hawk, J. D., "Subsonic Panel Method for Designing Wing Surfaces from Pressure Distributions," NASA CR-3713, 1983.

[4]Elbanna, H. M., "Numerical Computation of Aerodynamic Sensitivity Coefficients in the Transonic and Supersonic Regimes," M.S. Thesis, Texas A&M University, College Station, TX, May 1988.

[5]Abbott, I. H., and Von Doenhoff, A. E., *Theory of Wing Sections*, Dover, New York, 1959.

[6]Vanderplaats, G. N., Hicks, R. M., and Murman, E. M., "Application of Numerical Optimization Techniques To Airfoil Design," NASA SP-047, Pt. II, March 1975, pp. 745-768.

[7]Ballhaus, W. F., Jameson, A., and Albert, J., "Implicit Approximate Factorization Schemes for Steady Transonic Flow Problems," *AIAA Journal*, Vol. 16, No. 6, 1978, pp. 573-579.

[8]Gupta, S. K., and Tanji, K. K., "Computer Program for Large, Sparse, Unsymmetric Systems of Linear Equations," *International Journal for Numerical Methods in Engineering*, Vol. 11, 1977, pp. 1251-1259.

[9]Pissanetzky, S., *Sparse Matrix Technology*, Academic, New York, 1984.

[10]Press, W. H., Flannery, B. P., Tenkolsky, S. A., and Vetterling, W. T., *Numerical Recipes*, Cambridge Univ., Cambridge, MA, 1986.

[11]Elbanna, H. M., and Carlson, L. A., "Determination of Aerodynamic Sensitivity Coefficients in the Transonic and Supersonic Regimes," AIAA Paper 89-0532, Jan. 1989.

AIAA Paper No. 92-2670

DETERMINATION OF AERODYNAMIC SENSITIVITY COEFFICIENTS BASED ON THE THREE-DIMENSIONAL FULL POTENTIAL EQUATION

Hesham M. El-banna and Leland A. Carlson
Texas A&M University
College Station, TX 77843

AIAA 10th Applied Aerodynamics Conference
June 22-24, 1992, Palo Alto, CA

AIAA 92-2670

DETERMINATION OF AERODYNAMIC SENSITIVITY COEFFICIENTS BASED ON THE THREE-DIMENSIONAL FULL POTENTIAL EQUATION

Hesham M. Elbanna* and Leland A. Carlson**
Texas A & M University
College Station, Texas 77843

Abstract

The quasianalytical approach is applied to the three-dimensional full potential equation to compute wing aerodynamic sensitivity coefficients in the transonic regime. Symbolic manipulation is used to reduce the effort associated with obtaining the sensitivity equations, and the large sensitivity system is solved using "state of the art" routines. Results are compared to those obtained by the direct finite difference approach and both methods are evaluated to determine their computational accuracy and efficiency. The quasianalytical approach is shown to be accurate and efficient for large aerodynamic systems.

Nomenclature

C	Maximum camber in fraction of chord
CG	Conjugate gradient
Cl	Local lift coefficient
CL	Total lift coefficient
Cp	Pressure coefficient
c(y)	Chord function
FD	Finite difference
GMRES	Generalized minimum residual
L	Chordwise location of maximum camber
M	Local Mach number $M_{i,j,k}$
M_c	Cutoff Mach number $0.94 \leq M_c \leq 1.0$
M_∞	Freestream Mach number
P_∞	Freestream pressure, nondimensionalized by $[2\gamma/(\gamma+1)]P_0$
P_0	Stagnation pressure
QA	Quasianalytical
q_∞	Freestream velocity, nondimensionalized by V^*
T	Maximum thickness in fraction of chord
$T_{1..4}$	Twist angles
U,V,W	Contravariant velocity components
V^*	Critical speed
x,y,z	Physical grid system
X,Y,Z	Computational coordinates
xle(y)	Leading edge function
XL_T	X-Coordinate of leading edge corner point
XT_T	X-Coordinate of trailing edge corner point
Y_T	Y-Coordinate of wing tip
XD	Vector of design variables
ρ	Density, nondimensionalized by ρ_0
ρ_∞	Freestream density, nondimensionalized by ρ_0
ρ_0	Stagnation density
$\bar{\rho}$	Retarded density coefficient
$\delta()$	First order backward difference operator
ν	Switching function
α	Angle of attack
γ	Ratio of specific heats
ϕ	Reduced potential function
Φ	Full potential function
Γ	Circulation

* Graduate Research Asst.
** Professor, Aerospace Engr., Associate Fellow AIAA

Introduction

To design transonic vehicles using optimization techniques requires aerodynamic sensitivity coefficients, which are defined as the derivatives of the aerodynamic functions with respect to the design variables. In most cases, the main contributor to the optimization effort is the calculation of these derivatives; and, thus, it is desirable to have numerical methods which easily, efficiently, and accurately determine these coefficients for large complex problems. At present[1-6], there are two primary approaches for calculating transonic aerodynamic sensitivity derivatives. In the first approach, the sensitivities are calculated by perturbing a design variable from its previous value, a new complete solution is obtained, and the differences between the new and the old solutions are used to obtain the sensitivity derivatives. This brute force direct technique is computer intensive for complex governing equations that include a large number of design variables. In the second approach, termed the quasianalytical method, the sensitivities are obtained by solving a large sparse system of algebraic sensitivity equations in which the Jacobian matrix and right-hand-side vectors are obtained by differentiating the discretized form of the governing equations. The differentiations, while being staightforward in principle, are usually lengthy and tedious. However, once obtained, the

sensitivity equations can be very efficient and accurate for computing large numbers of sensitivity coefficients.

In the first phase of this research[2], the quasi-analytical approach was developed and applied to two-dimensional airfoils. Based upon these proof-of-concept investigations, it was concluded that the quasianalytical method was a feasible approach for accurately obtaining transonic aerodynamic sensitivity derivatives in two dimensions, and was often more accurate and efficient than the finite difference method as the number of design variables was increased. Further, the algebraic forms of the matrix elements in the two-dimensional sensitivity equations were determined by hand, which involved extensive effort associated with differentiating the discretized residual with respect to the various design variables and the dependent unknowns. Today, such operations could be carried out using Symbolic Manipulation Programs (SMs)[7], such as MACSYMA[8,9], but present SMs are incapable of automatically performing all the necessary simplification, combinations, and cancellations of terms associated with algorithmic simplification of expressions. Consequently, the user must be familiar with the commands available for the organization of expressions and conduct various trials and experiments to identify a symbolic procedure which is efficient. As a result of these two-dimensional studies, it was decided to extend the quasianalytical approach to three dimensions and to investigate the use of Symbolic Manipulation Programs (SMs)[10,11] for obtaining the matrix elements.

For this extended effort, it was decided to use for the flow solver a modified version of the three-dimensional direct-inverse analysis-design transonic full potential fully conservative code, ZEBRA[12-15]. The full potential equation was selected because it can be solved rapidly and is robust, and accurate for engineering purposes[15]. Further, it can be formulated using a stretched Cartesian grid system that can be rapidly generated and which has simple metrics. Also, such a grid permits the variation of several design parameters without changing the physical or computational grids. For the present work, the analysis portions of ZEBRA have been rearranged and unneeded portions deleted. In addition, the capability of calculating the sensitivity derivatives via the finite difference approach has been added.

Problem Statement

Application of the quasianalytical method to the full potential equation yields the sensitivity equation

$$\left[\frac{\partial R_{i,j,k}}{\partial \phi_{ii,jj,kk}}\right]\left(\frac{\partial \phi_{ii,jj,kk}}{\partial XD}\right) = -\left(\frac{\partial R_{i,j,k}}{\partial XD}\right) \qquad (1)$$

where the residual expression in the computational plane in terms of backward differences is

$$R_{i,j,k} = \delta_X(\frac{\bar{\rho}U}{J})_{i+1/2,j,k} + \delta_Y(\frac{\bar{\rho}V}{J})_{i,j+1/2,k} + \delta_Z(\frac{\bar{\rho}W}{J})_{i,j,k+1/2} \qquad (2)$$

The retarded density coefficients in Eq.(2) are

$$\bar{\rho}_{i+1/2,j,k} = (1-\nu_{i+1/2,j,k})\rho_{i+1/2,j,k} + \nu_{i+1/2,j,k}\rho_{i-1/2,j,k} \qquad (3)$$

$$\bar{\rho}_{i,j+1/2,k} = \frac{1}{2}(\rho_{i,j,k} + \bar{\rho}_{i,j+1,k}) \qquad (4)$$

$$\bar{\rho}_{i,j,k+1/2} = \frac{1}{2}(\bar{\rho}_{i,j,k} + \bar{\rho}_{i,j,k+1}) \qquad (5)$$

where

$$\rho_{i,j,k} = \left[1 - \frac{\gamma-1}{\gamma+1}(U\Phi_X + V\Phi_Y + W\Phi_Z)\right]^{\frac{1}{\gamma-1}}_{i,j,k} \qquad (6)$$

and

$$\nu_{i,j,k} = min[1, max(1 - \frac{M_c}{M^2_{i,j,k}}, 0)] \qquad (7)$$

In Eq.(7), the Mach number is obtained from

$$\frac{1}{\rho_{i,j,k}} = (\frac{T_0}{T})^{\frac{1}{\gamma-1}} = (1 + \frac{\gamma-1}{2}M^2_{i,j,k})^{\frac{1}{\gamma-1}} \qquad (8)$$

and thus

$$M^2_{i,j,k} = \frac{2}{\gamma-1}(\rho^{1-\gamma}_{i,j,k} - 1) \qquad (9)$$

where $\rho_{i,j,k}$ is nondimensionalized by ρ_0. From Eqs.(7) and (9),

$$\nu_{i,j,k} = \begin{cases} 0, & M_{i,j,k} < 1 \\ 1 - \frac{(\gamma-1)M_c/2}{\rho^{1-\gamma}_{i,j,k}-1}, & M_{i,j,k} > 1 \end{cases} \qquad (10)$$

The contravariant velocities are

$$U = (X_x^2 + X_y^2)\Phi_X + X_y\Phi_Y \quad (11)$$

$$V = X_y\Phi_X + \Phi_Y \quad (12)$$

$$W = \Phi_Z \quad (13)$$

where the full potential is split into perturbation and freestream components as

$$\Phi_{i,j,k} = \phi_{i,j,k} + Xq_\infty Cos(\alpha) + Zq_\infty Sin(\alpha) \quad (14)$$

Note that the angle of attack enters the formulation thru the above equation. Also note that the physical grid system (x,y,z) is transformed into the wing aligned computational grid (X,Y,Z) by

$$X(x,y) = \frac{x - xle(y)}{c(y)} \quad (15)$$

$$Y(y) = y \quad (16)$$

$$Z(z) = z \quad (17)$$

The boundary conditions are the surface boundary condition,

$$W = U\frac{\partial z}{\partial X} + V\frac{\partial z}{\partial Y} \quad (18)$$

the Kutta condition along the wing semispan,

$$\Gamma = \Delta\phi, \quad x_{TE} < x \leq \infty \quad (19)$$

and the far field boundary condition. Additional conditions include updating the potential on the downstream boundary ($\phi_x = 0$) and implementing the wing symmetry condition by setting $V = 0$.

Once the unknown sensitivities $\partial\phi/\partial XD$ are obtained, the sensitivities of the pressure coefficient, Cp, with respect to the design variables can be computed. From the pressure coefficient expression

$$Cp = \frac{P - P_\infty}{\rho q_\infty^2/2} \quad (20)$$

substitution for the pressure using the isentropic relation yields

$$Cp = \frac{(\gamma+1)/\gamma}{\rho q_\infty^2}(\rho^\gamma - \rho_\infty^\gamma) \quad (21)$$

where

$$\rho = \left[1 - \frac{\gamma-1}{\gamma+1}(U\Phi_X + V\Phi_Y + W\Phi_Z)\right]^{\frac{1}{\gamma-1}} \quad (22)$$

and where the freestream values q_∞, ρ_∞, and P_∞ in Eqs.(20) and (21) are

$$q_\infty = [\frac{\gamma+1}{\gamma-1+2/M_\infty^2}]^{1/2} \quad (23)$$

$$\rho_\infty = [1 - \frac{\gamma-1}{\gamma+1}q_\infty^2]^{1/(\gamma-1)} \quad (24)$$

$$P_\infty = \frac{\gamma+1}{2\gamma}\rho_\infty^\gamma \quad (25)$$

Design Variables

Design variables can be classified according to whether or not they are coupled. Uncoupled design variables are termed basic variables, which are the independent variables that influence the solution of a problem; while coupled design variables are termed nonbasic and are obtained from the basic design variables usually using simple algebraic expressions. For example, in the current problem, wing planform sweepback angles are nonbasic design variables which are obtained knowing the basic variables or the coordinates of the corner points of the wing. Other examples of nonbasic variables are the wing semi-span, aspect ratio, and taper ratio.

The basic design variables for the current problem are:

(a) Freestream design variables: These include the freestream Mach number and the angle of attack. The Mach number enters the formulation thru Eq.(23) while the angle of attack shows up in Eq.(14).

(b) Cross section design variables: These include variables that define the airfoil section such as maximum thickness, maximum camber, and location of maximum camber for a NACA four-digit section and, variables that define each spanwise section such as geometric twist. For the current problem, these variables enter the problem via the boundary condition, Eq.(18).

(c) Planform design variables: These variables define the geometry of the wing planform. In this study, the coordinates of the wing corner points are used as the basic design variables. Knowing the sensitivities with respect to these basic variables allows evaluation of

the derivatives with respect to the nonbasic variables. The coordinates of the corner points enter the current formulation via Eq.(15).

Thus, for the current three-dimensional problem, the vector of design variables consists of twelve variables and six derived variables and is given by,

$$XD = \left[M, \alpha, T, C, L, T_1, T_2, T_3, T_4, XL_T, XT_T, Y_T\right] \tag{26}$$

These variables are used in obtaining the right hand side vectors in Eq.(1).

Symbolic and Numerical Treatment

The basic approach used to symbolically differentiate the residual expression was to treat the main expression in terms of smaller subexpressions, each of which was examined in terms of its constituents. This process was extended until the final subexpressions included the appropriate derivative argument, the reduced potential or the design variables, in a simple functional form. The best method to obtain these subexpressions was to consider the governing equation and the involved intermediate expressions in the original form given in Eqs.(2)-(14). This splitting or nesting of expressions with various intermediate dependencies declared in advance allowed each subexpression to be handled efficiently by the symbolic manipulator. This usage of the chain rule of differentiation together with MACSYMA's ability to keep track of various equations resulted in an efficient scheme of analytical differentiation. It is noted that an early attempt to obtain the derivatives from a residual expressed as an explicit function of the reduced potential thru appropriate substitutions, Eq.(14) into (11), (12) and (13) up to Eq.(2), proved to be a poor strategy since the rapid increase in expression size eventually caused MACSYMA to encounter limitations on memory and manipulative ability. The experience gained from this attempt, however, turned out to be useful in identifying the capabilities and limitations of various MACSYMA commands and assisted in the development of further symbolic aspects associated with the project.

During this study, various MACSYMA codes have been developed to assist in the application of the quasianalytical method. The first code, termed RMD.MAC, finds all residual reduced potential dependencies. This code is needed prior to carrying out the analytical differentiation of the residual, Eq.(2), with respect to the reduced potential function. Notice that the latter function shows up in Eq.(14), where the details of the dependence of the residual expression on this function are not obvious, since intermediate expressions Eqs.(3) to (13) are involved. As mentioned earlier, handling each intermediate subexpression separately simplifies the operations involved. The result of this code is a file which includes various intermediate dependencies obtained in the form of lists. The second code termed RMDER.MAC, uses these lists and starts the symbolic differentiation process in order to obtain the Jacobian and right hand side vectors. The result of this lengthy code is a large FORTRAN segment that includes three subroutines and is about 15000 lines long. As mentioned in the following section, this segment which is the heart of the quasianalytical method, is linked into the quasianalytical sensitivity driver. The third MACSYMA code is termed RCP.MAC, and generates FORTRAN source code for the derivatives of the pressure coefficient, Eqs.(21) to (25), with respect to the vector of design variables. This code uses the reduced potential sensitivity derivatives as input arrays. This segment of FORTRAN source code is also linked with the segment obtained from the second MACSYMA code. Finally, the fourth MACSYMA code is termed RESID.MAC and was created during debugging operations to test the evaluation of various residual terms. This program was very helpful in revealing logic and procedure errors in RMDER.MAC. Finally, it is important to emphasize that each of the above MACSYMA codes is executed only once followed by a transfer of the resulting FORTRAN segments to the QA sensitivity driver.

Direct solvers that were previously used in the two-dimensional problem[2] (i.e. tridiagonal decomposition and full Gaussian elimination) failed on the three-dimensional problem due to limitations on memory; while the iterative routines developed earlier worked properly but were very slow. However, library routines[16] available on the IBM-3090 were extremely efficient with respect to memory and execution speed; and two scientific library solvers based on the iterative conjugate gradient method and the generalized minimum residual approach have been used with success. For these solvers, the exact amount of storage needed depends on the sparsity and band width of the Jacobian matrix which in turn depends on the size of the three-dimensional grid. The present grid of 45*30*16 yields a large, sparse, banded, and unsymmetric Jacobian matrix of about 17500*17500

that is less than one percent dense. An incomplete LU factorization is applied only once to this large matrix, and the sensitivity equations are solved using the iterative CG or GMRES methods[16,17,18]. Following the factorization of the Jacobian matrix, back substitution using the known right hand side vectors generates the unknown sensitivity derivatives with a trivial computational cost. Recall that one crucial objective of this study is to exploit the efficiency of the QA method as the number of design variables is increased.

Program Structure

The analysis-sensitivity program consists of the modified analysis program, ZEBRA, the finite difference sensitivity driver, and the quasianalytical sensitivity driver. Execution of the main code starts with an analysis run followed by sensitivity derivative calculations for each point in the flowfield. These calculations are carried out either using the FD method or the QA approach. The FD portion of the code uses two consecutive ZEBRA runs to calculate a vector of sensitivity derivatives. This brute force technique, while straight-forward, has the disadvantage of being expensive to implement and exhibits problems when single precision variables are used. The QA driver consists of two main parts. The first part assembles the Jacobian matrix and the right-hand-side vectors. This assembly is achieved using calls to the large code segment generated via MACSYMA. This section of subroutines, as explained earlier, contains source code for the elements of the Jacobian matrix and right-hand-side vectors. Following the numerical assembly step, the second part of the sensitivity driver solves the sensitivity equations using one of the available linear sparse solvers and yields the unknown sensitivity vectors. Finally, the resulting sensitivity derivatives $\partial\phi/\partial XD$ are processed to obtain the pressure coefficient sensitivity derivatives, $\partial Cp/\partial XD$, at twenty-five chordwise locations at each of the twenty wing semispan stations. This process is performed using the subroutines generated via RCP.MAC, the MACSYMA file used to symbolically differentiate the the pressure coefficient with respect to the reduced potential.

Test Cases

The wing configuration considered is that for the four cornered ONERA M6 wing planform[13-15] with NACA 1406 airfoil sections. For this configuration, four test cases have been successfully conducted. The first case is subcritical at a freestream Mach number of 0.8 and an angle of attack of one degree. The second and third cases are supercritical at Mach number of 0.84 and 0.88 respectively and an angle of attack of three degrees, while the fourth case is supersonic at a Mach number of 1.2 and an angle of attack of three degrees. Due to space limitations, only results for the second case ($M_\infty = 0.84, \alpha = 3\,\mathrm{deg}$) are presented in this paper. This case is challenging since it includes a subcritical lower surface flow and exhibits an upper surface shock wave located at 70% chord at the root to 10% chord at the tip that increases in strength from the root to a point near the wing tip. Thus, results for this case are believed sufficient to demonstrate the capabilities of the present analysis-sensitivity program.

In the above cases, a coarse-medium grid sequence was used in computing the analysis information in order to speed up convergence. For the FD method, each design variable was individually perturbed by a small amount, typically $1 * 10^{-6}$, and a new flowfield solution obtained. In all cases, double precision arithmetic was utilized and the residual reduced eight orders of magnitude. In addition, the sensitivity information was computed by restarting each of the perturbed design states from the coarse grid then proceeding to the medium grid. Different strategies for grid sequencing together with various choices of a suitable starting solution are all valid options to speed up the FD approach. In the QA method, as mentioned earlier, the sensitivity equation was set up with multiple right hand sides (the current vector of design variables, Eq.(26), includes twelve basic parameters) and was solved using the CG routine.

Results and Discussion

For the subcritical test case, the results obtained by the quasianalytical method were found to be in excellent agreement with results obtained via the finite difference method. In addition, the results followed the trend of the two-dimensional study[2].

Typical results for the chordwise variation of the pressure coefficient sensitivity derivatives at the $M_\infty = 0.84, \alpha = 3\,\mathrm{deg}$ supercritical case are shown on Figs. 1 and 2 for a midspan station. Also displayed next to the legend in each case are the integrated coefficients $\partial C_l/\partial XD_i$. As expected, the sensitivity derivative profiles for the lower surface are typical of subcritical flow[2]; and the upper surface results exhibit large variations

in the vicinity of the shock wave. The latter reflect the influence on the aerodynamic coefficients of the sensitivity of the upper surface shock wave location to various design parameters. In addition, a comparison of the spanwise distribution of the integrated coefficients, $\partial C_l/\partial XD_i$, is shown on Fig. 3; and in general these section values are smaller in magnitude than corresponding values for the two-dimensional problem[2]. As can be seen on Figs. 1-2, the agreement between the FD and QA results is excellent, indicating that accurate results can be obtained using the quasianalytical approch for three-dimensional transonic cases.

Since both the FD and QA methods yield similar results, the question arises as to which is the least expensive. Current results obtained with the CG solver indicate that the QA method is computationally more efficient than the brute-force, finite difference approach. A representative CPU time ratio QA/FD of 0.46 was obtained for the above case with twelve design variables. It is recognized, however, that the potential exists for reducing the cost associated with the FD method. For example, the perturbed runs could be executed directly on the medium grid starting with the design point solution obtained on the coarse grid. Likewise, the QA method could be improved by speeding up the evaluation of the Jacobian and right hand sides and/or using various options related to the library solver. Therefore, the stated time ratio should only be considered as an estimate for comparing the two methods.

One application of sensitivity derivatives is solution prediction. Fig. 4 compares the pressure coefficent distributions predicted at midspan using a first order Taylor series expansion about a design point with the actual pressure coefficient variation. The predicted Cp's are calculated using

$$C_{p_{predicted}} = C_{p_{design}} + \frac{\partial Cp}{\partial XD_i}\Delta XD_i \qquad (27)$$

where the $\partial Cp/\partial XD_i$ values where obtained from the QA approach and ΔXD_i = (0.005, 0.1, 0.005, 0.001, 0.1, 0.1) for $(M_\infty, \alpha, T, C, L, T_1)$ respectively.

As can be seen, the agreement between the two distributions is very good, which indicates that the sensitivity derivatives calculated using the QA method can indeed be used in prediction. As mentioned earlier, another important application of sensitivity derivatives is in optimization routines. This application, however, is beyond the scope of the current project.

Conclusion and Recommendations

Based upon the above results, it is concluded that the quasianalytical method is a feasible and efficient approach for accurately obtaining transonic aerodynamic sensitivity coefficients in three dimensions. In addition, use of the symbolic manipulation package, MACSYMA, to carry out the symbolic evaluation of the elements of the sensitivity equations is crucial in this type of sensitivity study. The results obtained from the quasianalytical method are almost identical to those obtained by the finite difference approach. Furthermore, the study indicates that (a) obtaining the quasianalytical sensitivity derivatives using an iterative conjugate gradient method is more efficient than computing the derivatives by the finite difference method, especially as the number of design variables increases, and (b) the quasianalytical method shows promise with regard to analysis-sensitivity methodologies applied to large aerodynamic systems.

Acknowledgment

This project is supported by the National Aeronautics and Space Administration under grant No. NAG 1-793, Dr. E. Carson Yates, Jr., and Dr. Woodrow Whitlow, Jr., NASA Langley Research Center, as technical monitors. The authors also appreciate the helpful suggestions and discussions of Dr. Perry Newman of NASA Langley.

References

1. Sobieski, J.S. "The Case for Aerodynamic Sensitivity Analysis", Paper presented to NASA/ VPI&SU Symposium on Sensitivity Analysis in Engineering, September 25-26, 1986.
2. Elbanna, H.M. and Carlson, L.A., "Determination of Aerodynamic Sensitivity Coefficients Based on the Transonic Small Perturbation Formulation", *Journal of Aircraft*, Vol 27, No.6, June 1990, pp 507-515.
3. Baysal, O., Eleshaky, M.E., Burgreen, G.W., "Aerodynamic Design Optimization Using Sensitivity Analysis and Computational Fluid Dynamics", AIAA paper No.91-0471.
4. Dulikravich, G.S.,"Aerodynamic Shape Design and Optimization", AIAA paper No.91-0476.
5. Taylor III, A.C., Korivi, V.M., Hou, G.W., "Approximate Analysis and Sensitivity Anal-

ysis Methods for Viscous Flow Involving Variation of Geometric Shape", AIAA paper No.91-1569.

6. Baysal, O., Eleshaky, M.E., Burgreen, G.W., "Aerodynamic Shape Optimization Using Sensitivity Analysis on Third-Order Euler Equations", AIAA paper No.91-1577.
7. Bau, H.H., "Symbolic Computation - An Introduction for the Uninitiated", Symbolic Computation in Fluid Mechanics and Heat Transfer, The American Society of Mechanical Engineers, Vol 97, 1988, pp 1-10.
8. Macsyma Reference Manual, Version 13, Computer Aided Mathematics Group, Symbolics, Inc., 1988.
9. Macsyma User's Guide, Computer Aided Mathematics Group, Symbolics, Inc., 1988.
10. Roach P. and Steinberg S., "Symbolic Manipulation and Computational Fluid Dynamics", *AIAA Journal*, Vol 22, No.10, 1984, pp 1390-1394.
11. Steinberg S. and Roach P., "Automatic Generation of Finite Difference Code", Symbolic Computation in Fluid Mechanics and Heat Transfer, The American Society of Mechanical Engineers, Vol 97, 1988, pp 81-86.
12. South Jr., J.C., Keller, J.D., Hafez, M.M., "Vector Processor Algorithms for Transonic Flow Calculations", *AIAA Journal*, Vol 18, No.7, 1980, pp 786-792.
13. Weed, R.A., Anderson, W.K., Carlson, L.A., "A Direct-Inverse Three Dimensional Transonic Wing Design Method for Vector Computers", AIAA paper No.84-2156.
14. Carlson, L.A. and Weed, R.A., "A Direct Inverse Transonic Wing Design Analysis Method with Viscous Interaction", AIAA paper No.85-4075.
15. Carlson, L.A. and Weed, R.A., "Direct-Inverse Transonic Wing Analysis Design Method with Viscous Interaction", *Journal of Aircraft*, Vol 23, No.9, Sept.1986, pp 711-718.
16. IBM Engineering and Scientific Subroutine Library, Guide and Reference, Rel 3, SC23-0184-3.
17. Saad, Y. and Schultz, M.H., "GMRES: A Generalized Minimum Residual Algorithm for Solving Nonsymmetric Linear Systems", *SIAM Journal of Scientific and Statistical Computing*, Vol 7, No.3, 1986, pp 856-869.
18. Sonneweld, Wesseling, and De Zeeuv, Multigrid and Conjugate Gradient Methods as Convergence Acceleration Techniques in Multigrid Methods for Integral and Differential Equations, pp 117-167, Edited by Paddon, D.J. and Holstein, M., Oxford University Press (Claredon), Oxford.

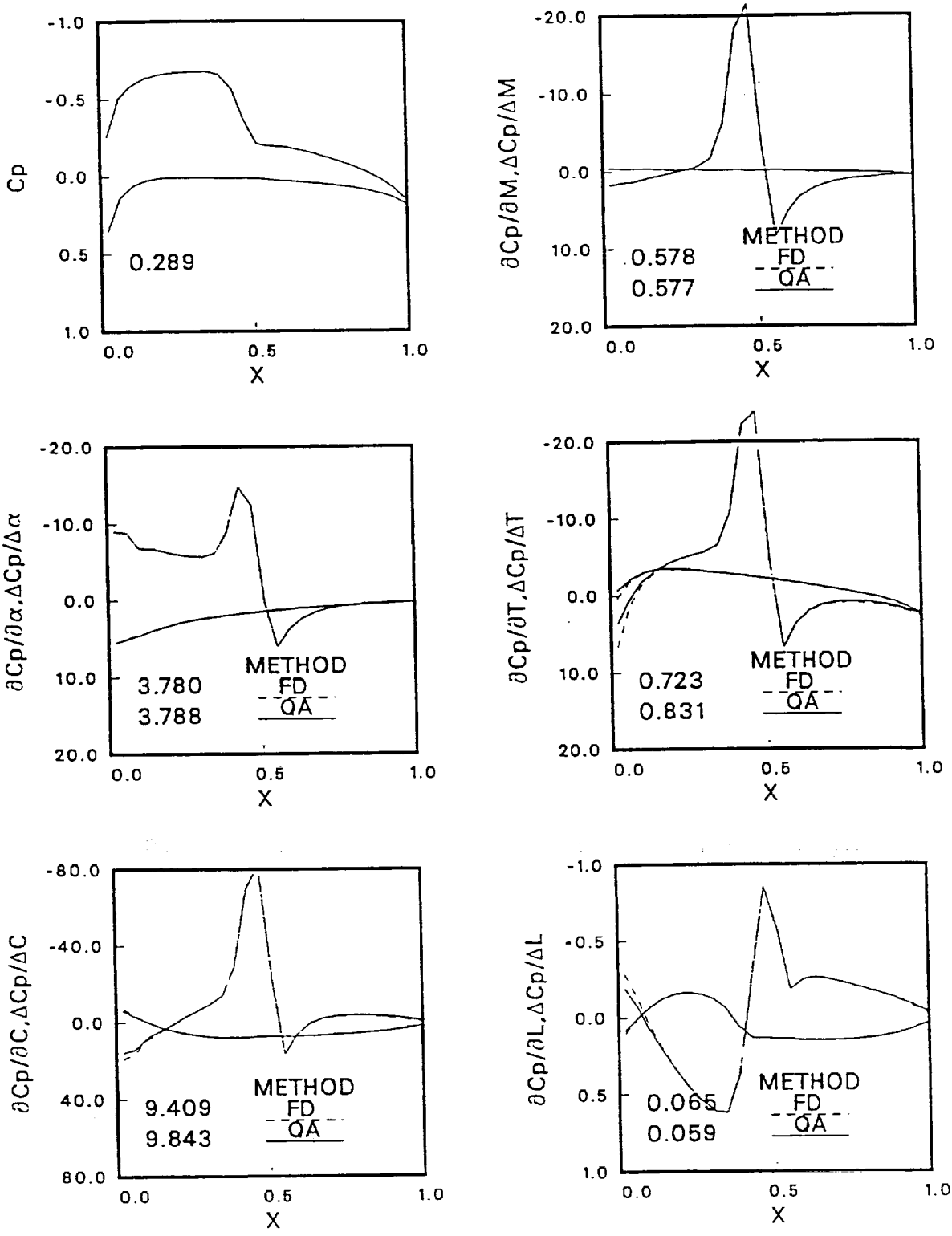

Fig.1 Pressure Coefficient and Pressure Coefficient Sensitivity Derivatives at 56 % Span

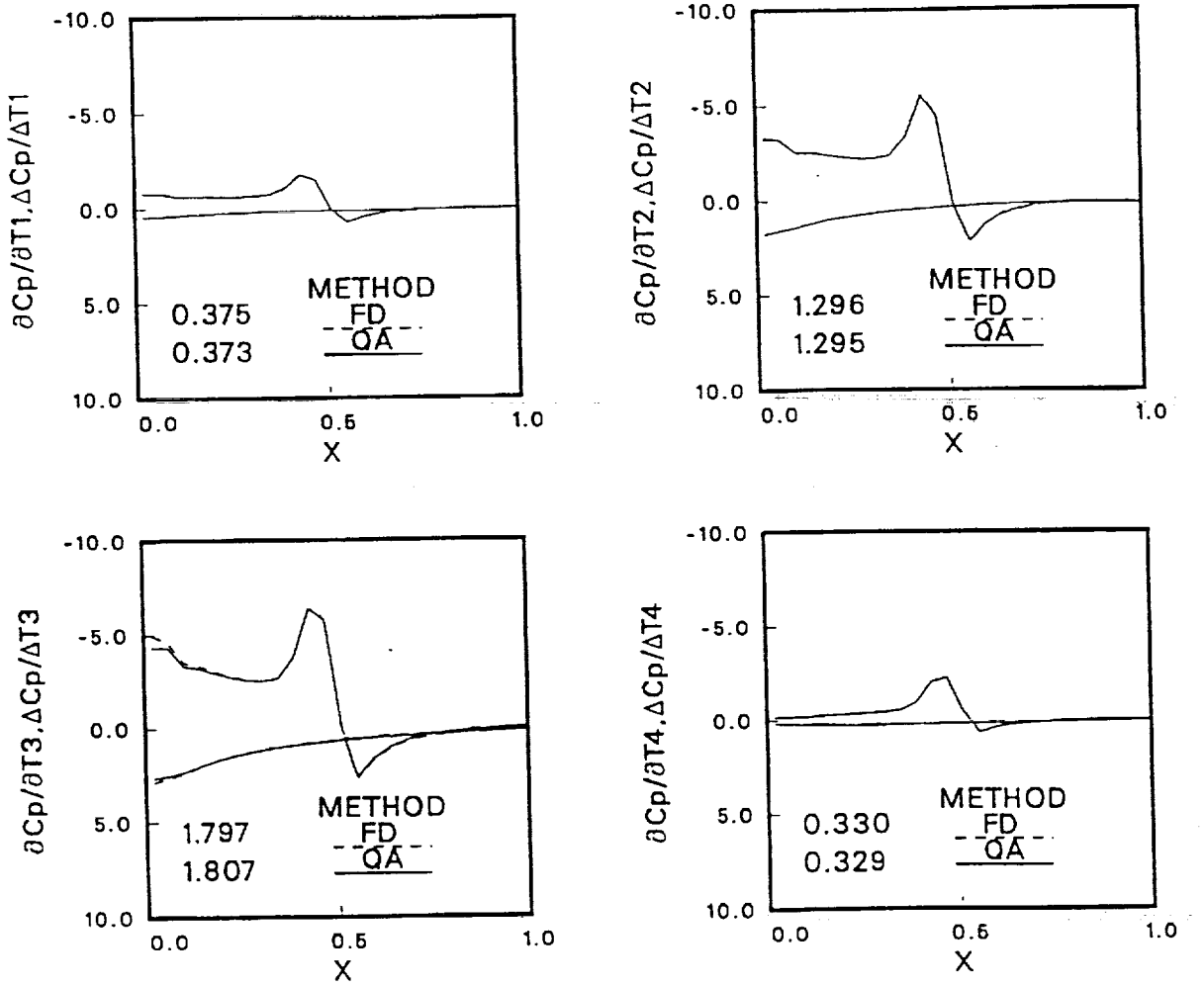

Fig.2 Pressure Coefficient Sensitivity Derivatives at 56 % Span

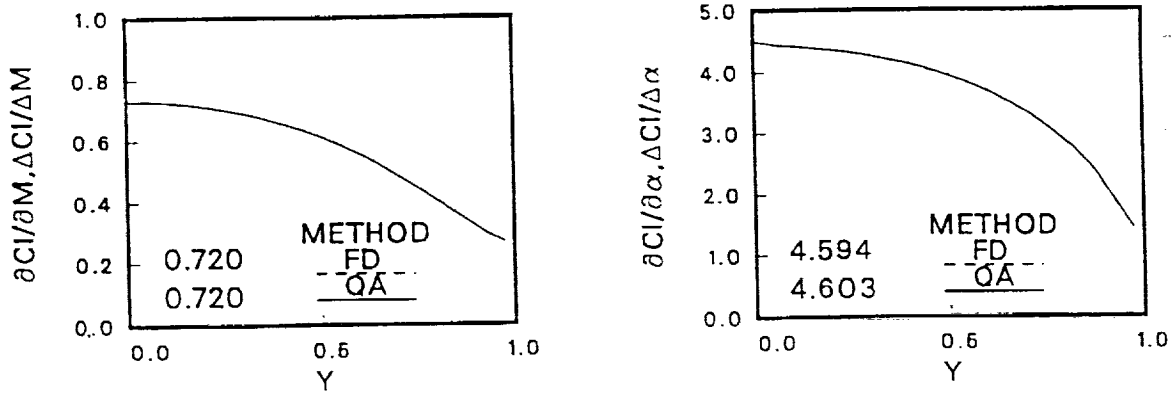

Fig.3 Sensitivity of Cl to M and α

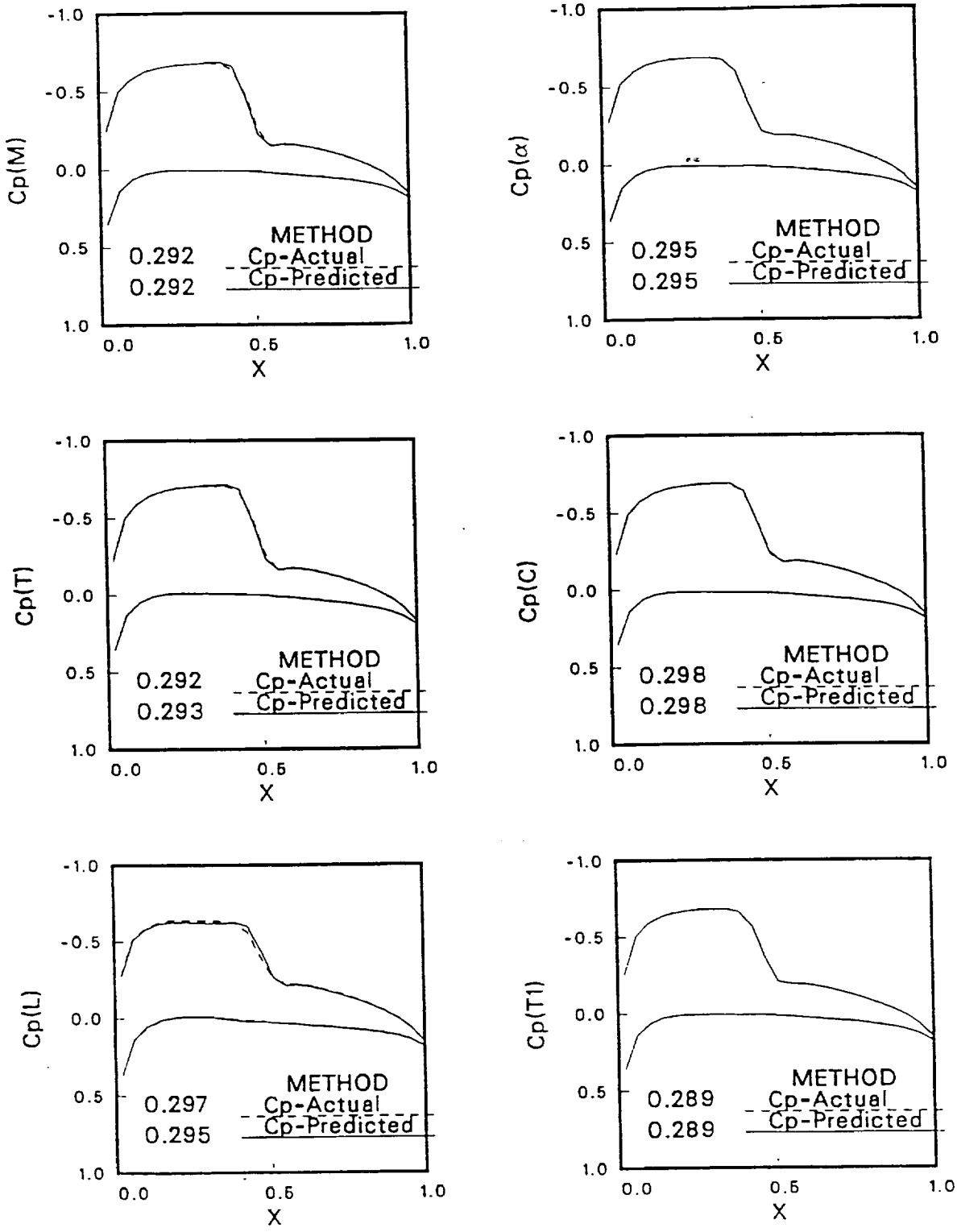

Fig.4 Actual vs Predicted Pressure Coefficients at 56 % Span

DETERMINATION OF AERODYNAMIC SENSITIVITY COEFFICIENTS FOR WINGS IN TRANSONIC FLOW

Leland A. Carlson
Professor of Aerospace Engineering
&
Hesham M. El-banna
Graduate Research Assistant

Texas A&M University
College Station, Texas 77843

PACAM III
3rd Pan American Congress of Applied Mechanics
January 1993

DETERMINATION OF AERODYNAMIC SENSITIVITY COEFFICIENTS FOR WINGS IN TRANSONIC FLOW

Leland A. Carlson
Professor, Aerospace Engineering

and

Hesham M. Elbanna
Graduate Research Assistant
Texas A & M University
College Station, Texas 77843

ABSTRACT

The quasianalytical approach is applied to the three-dimensional full potential equation to compute wing aerodynamic sensitivity coefficients in the transonic regime. Symbolic manipulation is used to reduce the effort associated with obtaining the sensitivity equations, and the large sensitivity system is solved using "state of the art" routines. The quasianalytical approach is believed to be reasonably accurate and computationally efficient for three-dimensional problems.

INTRODUCTION

To design transonic vehicles using codes which utilize optimization techniques requires aerodynamic sensitivity coefficients, which are defined as the derivatives of the aerodynamic functions with respect to the design variables. In most cases, the main contributor to the optimization effort is the calculation of these derivatives; and, thus, it is desirable to have numerical methods which easily, efficiently, and accurately determine these coefficients for large complex problems. The primary purpose of the present study is to investigate the application of the quasianalytical method [1,2] to three-dimensional transonic flows using as the fundamental flow solver the three-dimensional transonic full potential fully conservative code, ZEBRA [3].

PROBLEM STATEMENT

Application of the quasianalytical method to the full potential equation yields the sensitivity equation

$$\left[\frac{\partial R_{i,j,k}}{\partial \phi_{ii,jj,kk}}\right]\left(\frac{\partial \phi_{ii,jj,kk}}{\partial XD}\right) = -\left(\frac{\partial R_{i,j,k}}{\partial XD}\right) \tag{1}$$

where XD is the vector of design variables and the residual expression, $R_{i,j,k}$, of the full potential equation in the computational plane, X, Y, Z, in terms of backward differences is

$$R_{i,j,k} = \bar{\delta}_X(\frac{\bar{\rho}U}{J})_{i+1/2,j,k} + \bar{\delta}_Y(\frac{\bar{\rho}V}{J})_{i,j+1/2,k} + \bar{\delta}_Z(\frac{\bar{\rho}W}{J})_{i,j,k+1/2} \tag{2}$$

Here, the retarded density $\bar{\rho}$ and the contravariant velocity components U, V, and W, are lengthy functions of the reduced potential function, ϕ. The boundary conditions for Eq.(2) are the surface condition, $W = U\frac{\partial z}{\partial X} + V\frac{\partial z}{\partial Y}$, the Kutta condition along the wing semispan, $\Gamma = \Delta\phi, \quad x_{TE} < x \leq \infty$, and the farfield condition. Additional conditions are the downstream boundary potential $\phi_x = 0$ and the wing symmetry condition, $V = 0$.

The discretized form of Eq.(2) contains lengthy expressions, and mathematical symbolic manipulation [4-6] was used to determine the functional dependencies of the residual, the analytical forms of the derivatives, and to generate the corresponding computer code. The basic approach used to differentiate the residual expression was to treat the main expression in terms of smaller subexpressions, each of which was examined in terms of its constituents. This process was extended until simple functional forms for the derivatives were obtained. This subdivision and chain rule differentiation by symbolic manipulation efficiently generated source code for the jacobian and vectors in Eq.(1). The resultant large sparse system, typically 17500 * 17500, of algebraic equations is then efficiently solved for $\frac{\partial\phi}{\partial XD}$ using either the iterative conjugate gradient method or the generalized minimum residual algorithm [7-8]. From these, the pressure and lift coefficient sensitivities to the design variables can be computed. Notice that the effort associated with this approach is essentially independent of the number of design variables considered on the right-hand-side of Eq.(1).

EXAMPLE AND DISCUSSION

Consider the ONERA M6 wing planform with NACA 1406 airfoil sections at a supercritical condition of $M_\infty = 0.84$ and $\alpha = 3\,\text{deg}$, which has subcritical lower surface flow and exhibits an upper surface shock wave located at 70 % chord at the root to 10 % chord at the tip that increases in strength from the root to a point near the wing tip. Basic design variables for the current problem include freestream design variables, Mach number M_∞ and angle of attack α; cross-section design variables of maximum thickness, T, maximum camber, C, and location of maximum camber, L; variables that define wing twist, $T1, T2, T3$, and $T4$; and planform tip coordinates, XLE_{tip}, XTE_{tip}, and Y_{tip}. Knowing the sensitivities to these basic design parameters permits subsequent evaluation of the derivatives with respect to the nonbasic variables taper ratio, aspect ratio, wing area, and sweepback angles. Thus, the present method determines sensitivity coefficients for twelve design variables and five derived design variables.

As part of the solution $\partial\phi/\partial XD$ values are obtained for every grid point in the flowfield. Also, the method automatically computes $\partial C_p/\partial XD$ at twenty-five chordwise locations at each of the twenty semi-span stations on the wing as well as $\partial C_l/\partial XD$ at each of the span stations. Typical results for the example case are shown in Fig.1 for a midspan station. As expected, the sensitivity derivative profiles for the lower surface are typical of subcritical flow [2]; and the upper surface results exhibit large variations in the vicinity of the shock wave. The latter reflect the influence on the aerodynamic coefficients of the sensitivity of the upper surface shock wave location to the various design parameters. Currently, efforts are in progress to validate the present method by comparison with the finite difference

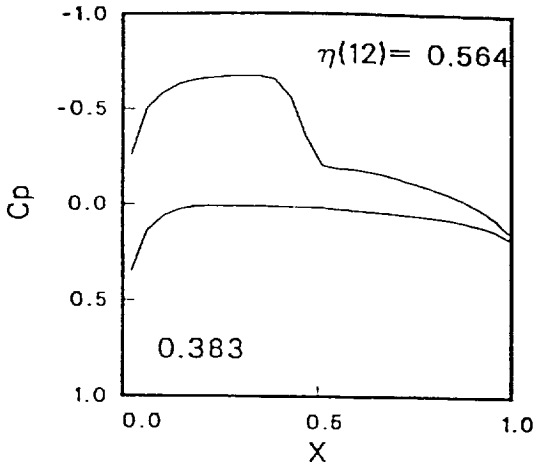

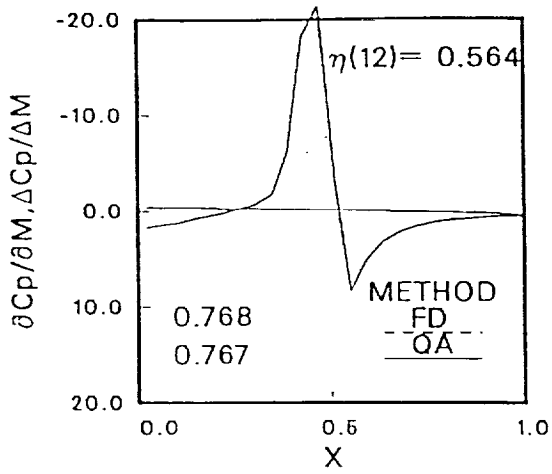

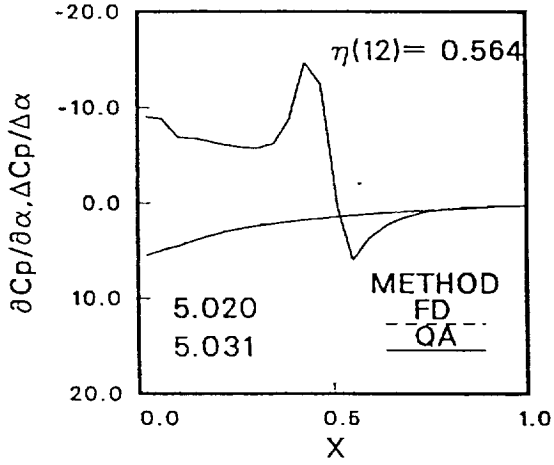

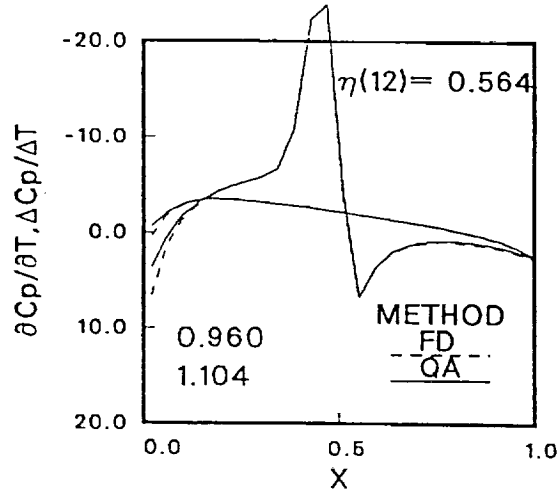

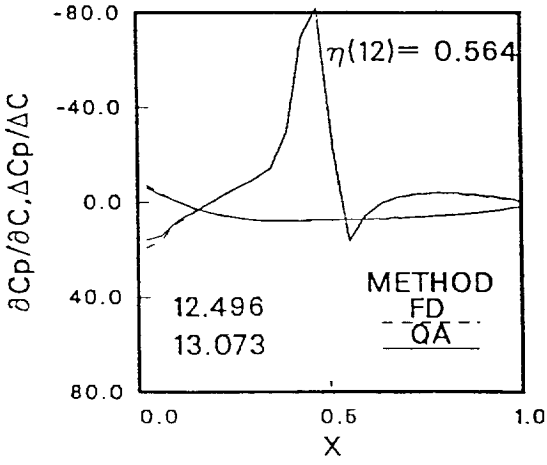

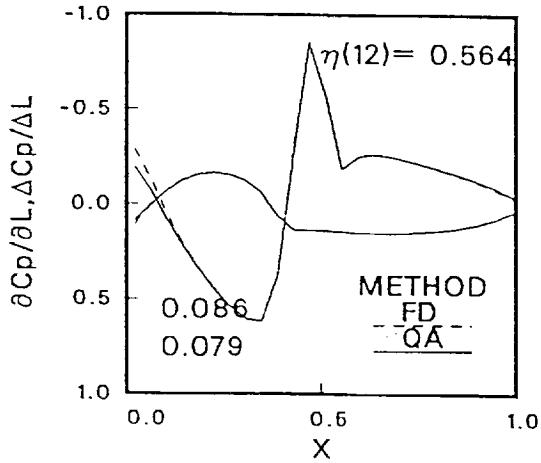

PRESSURE COEFFICIENT AND PRESSURE COEFFICIENT
SENSITIVITY DERIVATIVES AT 56% SPAN

NACA 1406, $M_{oo} = 0.84$, $\alpha = 3^o$

approach, which calculates sensitivities by perturbing a design variable from its previous value, obtaining a new solution, using the differences between the new and old solutions to obtain the sensitivity coefficients. While this direct technique is computer intensive and inefficient, it should serve as a check on the present method.

Based upon the present results, it is concluded that the quasianalytical method is a viable and efficient concept for the determination of three-dimensional transonic aerodynamic sensitivity coefficients. In addition, use of symbolic manipulation to evaluate the elements of the sensitivity equation is believed to be an efficient approach to the development of such methods. Finally, further studies are needed to determine the accuracy and range of applicability of the quasianalytical approach.

ACKNOWLEDGMENT

This project was supported by the National Aeronautics and Space Administration under grant No. NAG 1-793, Dr. E. Carson Yates, Jr., and Dr. Woodrow Whitlow, Jr., NASA Langley Research Center, as technical monitors.

REFERENCES

1. Sobieski, J.S. "The Case for Aerodynamic Sensitivity Analysis", Paper presented to NASA/VPI&SU Symposium on Sensitivity Analysis in Engineering, September 25-26, 1986.
2. Elbanna, H.M. and Carlson, L.A., "Determination of Aerodynamic Sensitivity Coefficients Based on the Transonic Small Perturbation Formulation", Journal of Aircraft, Vol 27, No.6, June 1990, pp 507-515.
3. Carlson, L.A. and Weed, R.A., "Direct-Inverse Transonic Wing Analysis-Design Method with Viscous Interaction", Journal of Aircraft, Vol 23, No.9, Sept.1986, pp 711-718.
4. Bau, H.H., "Symbolic Computation - An Introduction for the Uninitiated", Symbolic Computation in Fluid Mechanics and Heat Transfer, The American Society of Mechanical Engineers, Vol 97, 1988, pp 1-10.
5. Roach P. and Steinberg S., "Symbolic Manipulation and Computational Fluid Dynamics", AIAA Journal, Vol 22, No.10, 1984, pp 1390-1394.
6. Steinberg S. and Roach P., "Automatic Generation of Finite Difference Code", Symbolic Computation in Fluid Mechanics and Heat Transfer, The American Society of Mechanical Engineers, Vol 97, 1988, pp 81-86.
7. Saad, Y. and Schultz, M.H., "GMRES: A Generalized Minimum Residual Algorithm for Solving Nonsymmetric Linear Systems", SIAM Journal of Scientific and Statistical Computing, Vol 7, No.3, 1986, pp 856-869.
8. Sonneweld, Wesseling, and De Zeeuv, Multigrid and Conjugate Gradient Methods as Convergence Acceleration Techniques in Multigrid Methods for Integral and Differential Equations, pp 117-167, Edited by Paddon, D.J. and Holstein, M., Oxford University Press (Claredon), Oxford.

Aerodynamic Sensitivity Coefficients Using the 3-D Full Potential Equation

by H. M. El-banna and L. A. Carlson

Accepted for publication in the ***Journal of Aircraft***

Aerodynamic Sensitivity Coefficients Using The 3-D Full Potential Equation

Hesham M. El-banna* and Leland A. Carlson**
Texas A&M University, College Station, Texas 77843

Abstract

The quasi-analytical approach is applied to the three-dimensional full potential equation to compute wing aerodynamic sensitivity coefficients in the transonic regime. Symbolic manipulation is used and is crucial in reducing the effort associated with obtaining sensitivity equations, and the large sensitivity system is solved using sparse solver routines such as the iterative conjugate gradient method. The results obtained are almost identical to those obtained by the finite difference approach and indicate that obtaining the sensitivity derivatives using the quasi-analytical approach is more efficient than computing the derivatives by the finite difference method, especially as the number of design variables increases. It is concluded that the quasi-analytical method is an efficient and accurate approach for obtaining transonic aerodynamic sensitivity coefficients in three dimensions.

Nomenclature

C	Maximum camber in fraction of chord
CG	Conjugate gradient
CI	Section lift coefficient
CL	Wing lift coefficient
Cp	Pressure coefficient
c(y)	Chord function
FD	Finite difference
GMRES	Generalized minimum residual
L	Chordwise location of maximum camber in fraction of chord
M	Local Mach number M
M_c	Cutoff Mach number $0.94 \leq M_c \leq 1.0$
M_∞	Freestream Mach number
P_∞	Freestream pressure, nondimensionalized by $\{2\gamma/(\gamma + 1)]P_0$
QA	Quasi-analytical

Based on AIAA Paper 92-2670

* Graduate Research Assistant; currently Assistant Professor, Cario University, Egypt.

** Professor, Aerospace Engineering Department, College Station, TX, 77843-3141, Associate Fellow AIAA.

q_∞	Freestream velocity, nondimensionalized by V^*
T	Maximum thickness in fraction of chord
$T_{1..4}$	Twist angles at 0, 20, 60, and 100% semispan
U,V,W	Contravariant velocity components
V^*	Critical speed
x,y,z	Physical grid system
X,Y,Z	Computational coordinates
xle(y)	Leading edge function
XL_T, XLET	x-Coordinate of leading edge of wing tip
XT_T, XTET	x-Coordinate of trailing edge of wing tip
Y_T, SSPAN	y-Coordinate of wing tip
XD	Vector of design variables
ρ	Density, nondimensionalized ρ_0
ρ_∞	Freestream density, nondimensionalized by ρ_0
ρ_0	Stagnation density
$\overline{\rho}$	Retarded density
$\overline{\delta}\,()$	First order backward difference operator
ν	Switching function
α	Angle of attack
γ	Ratio of specific heats
ϕ	Reduced potential function
Φ	Full potential function
Γ	Circulation

Introduction

To design transonic vehicles using optimization techniques requires aerodynamic sensitivity coefficients, which are defined as the derivatives of the aerodynamic functions with respect to the design variables. In most cases, the main contributor to the optimization effort is the calculation of these derivatives; and, thus, it is desirable to have numerical methods which easily, efficiently, and accurately determine these coefficients for large complex problems. At present[1-8], there are two primary approaches for calculating transonic aerodynamic sensitivity derivatives. In the first approach, the sensitivities are calculated by perturbing a design variable from its previous value, a new complete solution is obtained, and the differences between the new and the old solutions are used to obtain the sensitivity derivatives. This brute force direct technique is computer intensive for complex governing equations that

include a large number of design variables. In the second approach, termed the quasi-analytical method, the sensitivities are obtained by solving a large sparse system of algebraic sensitivity equations. While the matrix elements in these algebraic sensitivity equations are obtained analytically, they are obtained by analytically differentiating the discretized or numerical forms of the equations governing the flowfield. Further, the aerodynamic and sensitivity solutions are obtained numerically. Thus, the method is termed a quasi-analytical rather than a numerical or analytical method. It should be noted that the differentiations to obtain the coefficients for the algebraic sensitivity equations, while being straightforward in principle, are usually lengthy and tedious. However, once obtained, the sensitivity equations can be very efficient and accurate for computing large numbers of sensitivity coefficients.

In the first phase of this research[2], the quasi-analytical approach was developed and applied to two-dimensional airfoils. Based upon these proof-of-concept investigations, it was concluded that the quasi-analytical method was a feasible approach for accurately obtaining transonic aerodynamic sensitivity derivatives in two dimensions and was often more accurate and efficient than the finite difference method as the number of design variables was increased. Further, the algebraic forms of the matrix elements in the two-dimensional sensitivity equations were determined by hand, which involved extensive effort associated with differentiating the discretized residual with respect to the various design variables and the dependent unknowns. Today, such operations could be carried out using symbolic manipulation programs[9], such as MACSYMA[10,11], but present symbolic manipulators are incapable of automatically performing all the necessary simplification, combinations, and cancellations of terms associated with algorithmic simplification of expressions. Consequently the user must be familiar with the commands available for the organization of expressions and conduct various trials and experiments to identify a symbolic procedure which is efficient. As a result of these two-dimensional studies, it was decided to continue the research. Consequently, the primary objectives of the present effort have been to apply the quasi-analytical method to three-dimensional transonic flow, investigate the use of symbolic manipulation programs [12,13] for obtaining the matrix elements of the sensitivity equations, and to determine the efficiency and accuracy of the quasi-analytical approach for determining transonic aerodynamic sensitivities.

For this extended effort, it was decided to use for the flow solver a modified version of the three-dimensional direct-inverse analysis-design transonic full potential fully conservative code, ZEBRAII[14-17]. The full potential equation was selected because it can be solved rapidly and is robust and accurate for engineering purposes[17]. Further, it can be formulated using a stretched Cartesian grid system that can be rapidly generated and which has simple metrics. Also, such a grid permits the variation of several design parameters without changing the physical or computational grids. For the present work, the analysis portions of ZEBRAII have been rearranged and unneeded portions deleted. In addition, the capability of calculating the sensitivity derivatives via the finite difference approach has been added.

Problem Statement

Application of the quasi-analytical method to the full potential equation yields the sensitivity equation

$$\left[\frac{\partial R_{i,j,k}}{\partial \phi_{ii,jj,kk}}\right]\left(\frac{\partial \phi_{ii,jj,kk}}{\partial XD}\right) = -\left(\frac{\partial R_{i,j,k}}{\partial XD}\right) \tag{1}$$

where the residual expression in the computational plane in terms of backward differences is

$$R_{i,j,k} = \overline{\delta}_x\left(\frac{\overline{\rho} U}{J}\right)_{i+1/2,j,k} + \overline{\delta}_y\left(\frac{\overline{\rho} V}{J}\right)_{i,j,+1/2,k} + \overline{\delta}_z\left(\frac{\overline{\rho} W}{J}\right)_{i,j,k,+1/2} \tag{2}$$

The retarded density coefficients in Eq. (2) are

$$\overline{\rho}_{i+1/2,j,k} = (1 - \nu_{i+1/2,j,k})\,\rho_{i+1/2,j,k} + \nu_{i+1/2,j,k}\,\rho_{i-1/2,j,k} \tag{3}$$

$$\overline{\rho}_{i,j+1/2,k} = \frac{1}{4}\left(\overline{\rho}_{i+1/2,j,k} + \overline{\rho}_{i+1/2,j+1,k} + \overline{\rho}_{i-1/2,j,k} + \overline{\rho}_{i-1/2,j+1,k}\right) \tag{4}$$

$$\overline{\rho}_{i,j,k+1/2} = \frac{1}{4}\left(\overline{\rho}_{i+1/2,j,k} + \overline{\rho}_{i+1/2,j,k+1} + \overline{\rho}_{i-1/2,j,k} + \overline{\rho}_{i-1/2,j,k+1}\right) \tag{5}$$

where

$$\rho = \left[1 - \frac{\gamma - 1}{\gamma + 1}\left(U\Phi_X + V\Phi_Y + W\Phi_Z\right)\right]^{\frac{1}{\gamma - 1}} \tag{6}$$

and

$$\nu = \min\left[1, \max\left(1 - \frac{M_c}{M^2}, 0\right)\right] \tag{7}$$

In Eq. (7), the Mach number is obtained from

$$\frac{1}{\rho} = \left(\frac{T_0}{T}\right)^{\frac{1}{\gamma-1}} = \left(1 + \frac{\gamma-1}{2} M^2\right)^{\frac{1}{\gamma-1}} \tag{8}$$

and thus

$$M^2 = \frac{2}{\gamma-1}\left(\rho^{1-\gamma} - 1\right) \tag{9}$$

where ρ is nondimensionalized by ρ_0. From Eqs. (7) and (9),

$$\nu = \begin{cases} 0, & M < 1 \\ 1 - \dfrac{(\gamma-1)M_c/2}{\rho^{1-\gamma} - 1}, & M > 1 \end{cases} \tag{10}$$

The contravariant velocities are

$$U = (X_x^2 + X_y^2)\,\Phi_x + X_y\,\Phi_Y \tag{11}$$

$$V = X_y \Phi_X + \Phi_Y \tag{12}$$

$$W = \Phi_Z \tag{13}$$

and the full potential is split into perturbation and freestream components as

$$\Phi_{i,j,k} = \phi_{i,j,k} + Xq\_Cos(\alpha) + Zq\_Sin(\alpha) \tag{14}$$

Note that the angle of attack enters the formulation thru the above equation and that the physical grid system (x,y,z,) is transformed into the wing aligned computational grid (X,Y,Z) by

$$X(x,y) = \frac{x - xle(y)}{c(y)} \tag{15}$$

$$Y(y) = y \tag{16}$$

$$Z(z) = z \tag{17}$$

The boundary conditions are the surface boundary condition,

$$W = U\frac{\partial z}{\partial X} + V\frac{\partial z}{\partial Y} \tag{18}$$

the Kutta condition along the wing semispan,

$$\Gamma = \Delta\phi, \quad x_{TE} < x \leq \infty \tag{19}$$

and the farfield boundary condition. Additional conditions include updating the potential on the downstream boundary ($\phi_x = 0$) and implementing the wing symmetry condition by setting $V = 0$.

Once the unknown sensitivities $\partial\phi/\partial XD$ are obtained, the sensitivities of the pressure coefficient, Cp, with respect to the design variables can be computed. From the pressure coefficient expression

$$Cp = \frac{P - P_\infty}{\rho q_\infty^2/2} \tag{20}$$

substitution for the pressure using the isentropic relations yields,

$$Cp = \frac{(\gamma + 1)/\gamma}{\rho q_\infty^2}(\rho^\gamma - \rho_\infty^\gamma) \tag{21}$$

where ρ is given by Eq. (6) and where the freestream values q_∞, ρ_∞, and P_∞ in Eqs. (20) and (21) are

$$q_\infty = \left[\frac{\gamma + 1}{\gamma - 1 + 2/M_\infty^2}\right]^{1/2} \tag{22}$$

$$\rho_\infty = \left[1 - \frac{\gamma - 1}{\gamma + 1}q_\infty^2\right]^{1/(\gamma-1)} \tag{23}$$

$$P_\infty = \frac{\gamma + 1}{2\gamma}\rho_\infty^\gamma \tag{24}$$

Design Variables

Design variables can be arbitrarily classified according to whether or not they are coupled. Uncoupled design variable are termed basic variables and are the independent variables that influence the solution of a problem.

Coupled design variables are defined here to be nonbasic and are obtained from the basic design variables usually using simple algebraic expressions. For example, in the current problem, wing planform sweepback angles are defined as nonbasic design variables since they are obtainable from the basic variables, i.e. the coordinates of the corner points of the wing. Other examples of nonbasic design variables are the wing area, aspect ratio, and taper ratio.

The basic design variables for the current problem include freestream variables, airfoil cross-section variables, and planform parameters. The freestream design variables include the freestream Mach number, M_∞, and the angle of attack, α. The Mach number enters the formulations thru Eq. (22) while the angle of attack shows up in Eq. (14). The airfoil section design variables include maximum thickness, maximum camber, location of maximum camber, and four angles that define at each spanwise station the amount of geometric twist. These variables enter the problem via the wing surface boundary condition, Eq. (18). The basic planform design variables define the geometry of the wing planform and are comprised of the coordinates of the wing corner points, which enter the formulation via Eq. (15). Evaluation of the sensitivities with respect to these basic planform variables allows the determination of the derivatives with respect to the nonbasic variables. Thus, for the current three-dimensional problem, the vector of design variables consists of twelve basic variables and is given by,

$$XD = \left[M_\infty, \alpha, T, C, L, T_1, T_2, T_3, T_4, XL_T, XT_T, Y_T\right] \tag{25}$$

These variables are used in obtaining the right hand side vectors in Eq. (1).

Note that the design variables listed in Eq. (25) form a complete set of the basic design variables influencing the aerodynamic solution for the wing planform and wing sections considered in the present investigation. If the wing planform were more complicated, having for example a leading edge break, then the coordinates of that break point would have to be included in the vector of design variables. For more complex configurations or for problems involving coupling such as aeroelastic phenomena, the design variable set would be found by examining the solution model(s) and determining which flowfield and geometric parameters appear and consequently affect the aerodynamic solution.

Symbolic and Numerical Treatment

The basic approach used to symbolically differentiate the residual expression was to treat the main expression in terms of smaller subexpressions, each of which was examined in terms of its constituents. This process was extended until the final subexpressions included the appropriate derivative argument, the reduced potential or the design variables, in a simple functional form. The best method to obtain these subexpressions was to consider the governing equation and the involved intermediate expressions in the original form given in Eqs. (2)-(14). This splitting or nesting of expressions with various intermediate dependencies declared in advance allowed each subexpression to be handled efficiently by the symbolic manipulator, in this case MACSYMA. This usage of the

chain rule of differentiation together with the ability of the symbolic manipulator to keep track of various equations resulted in an efficient scheme of analytical differentiation. It is noted that an earlier attempt to obtain the derivatives from a residual expressed as an explicit function of reduced potential thru appropriate substitutions, Eq. (14) into (11), (12) and (13) up to Eq. (2), proved to be a poor strategy since the rapid increase in expression size eventually caused the manipulator program to encounter limitations on memory and manipulative ability. The experience gained from this attempt, however, turned out to be useful in identifying the capabilities and limitations of various symbolic commands and assisted in the development of further symbolic aspects associated with the project.

During this study, various symbolic manipulator codes were developed to assist in the application of the quasi-analytical method. The first code, found all residual reduced potential dependencies. This code was needed prior to carrying out the analytical differentiation of the residual, Eq.(2), with respect to the reduced potential function. Notice that the latter function shows up in Eq. (14), where the details of the dependence of the residual expression on this function are not obvious, since intermediate expressions Eqs.(3) to (13) are involved. As mentioned earlier, handling each intermediate subexpression separately simplifies the operations involved. The result of this code was a file which included various intermediate dependencies obtained in the form of lists. The second code used these lists to perform the symbolic differentiation process to obtain the Jacobian and right hand side vectors for Eq. (1), and the result of this lengthy code was a large 15000 line FORTRAN segment that included three subroutines. This segment is the heart of the quasi-analytical method and is linked into the quasi-analytical sensitivity driver. The third symbolic code generated FORTRAN source code for the derivatives of the pressure coefficient, Eqs. (21) to (25), with respect to the vector of design variables and used the reduced potential sensitivity derivatives as input arrays. This segment of FORTRAN source code was then also linked with the segment obtained from the second symbolic code. Finally, the fourth symbolic code was created during debugging operations to test the evaluation of various residual terms and was very helpful in revealing logic and procedure errors. Finally, it is important to emphasize that each of the above symbolic codes is executed only once followed by a transfer of the resulting source segments to the quasi-analytical sensitivity driver. Details and sample MACSYMA codes for these processes are given in Ref. 4.

Direct solvers that were previously used in the two-dimensional problem[2] failed on the three-dimensional problem due to limitations on memory; while the iterative routines developed earlier worked properly but were very slow. However, library solvers[18] based on the iterative conjugate gradient method and the generalized minimum residual approach have been used with success and have proven to be extremely efficient with respect to memory and execution speed. For these solvers, the exact amount of storage needed depends on the sparsity and band width of the Jacobian matrix which in turn depends on the size of the three-dimensional grid. The present grid of 45 x 30 x 16 yields a large, sparse, banded, and unsymmetric Jacobian matrix of (43 X 29 X 14) X (43 X 29 X 14) or about 17500 x 17500 that is less than one percent dense. An incomplete LU factorization is applied only once to this large matrix, and the sensitivity equations are solved using the iterative CG or GMRES methods[18,19,20].

Following the factorization of the Jacobian matrix, back substitution using the known right hand side vectors generates the unknown sensitivity derivatives with a trivial computational cost. This approach exploits the efficiency of the QA method as the number of design variables is increased.

Program Structure

The analysis-sensitivity program consists of the modified flowfield analysis program, ZEBRA, the finite difference sensitivity driver, and the quasi-analytical sensitivity driver. Execution of the main code starts with an analysis run followed by sensitivity derivative calculations carried out either using the FD method or the QA approach. The FD portion of code uses two consecutive ZEBRA runs to calculate a vector of sensitivity derivatives. This brute force technique, while straight-forward, has the disadvantage of being expensive to implement and exhibits problems when single precision variables are used. The QA driver consists of two main parts. The first part assembles the Jacobian matrix and the right-hand-side vectors thru calls to the large code segment generated via symbolic manipulation. This section of subroutines, as explained earlier, contains source code for the elements of the Jacobian matrix and right-hand-side vectors. Following the numerical assembly step, the second part of the sensitivity driver solves the sensitivity equations using one of the available linear sparse solvers and yields the unknown sensitivity vectors at each point in the flowfield. Finally, the resulting sensitivity derivatives, $\partial\phi/\partial XD$, are processed to obtain the pressure coefficient sensitivity derivatives $\partial Cp/\partial XD$, at twenty-five chordwise locations at each of the twenty wing semispan stations.

Test Cases

For the present study, most of the test cases utilized the four cornered ONERA M6 wing planform [15-17] with a variety of airfoil sections including NACA 1406, 1706, 2406, and 2706 airfoils. This planform has an aspect ratio of 3.8 and a taper ratio of 0.56, with leading and trailing edge sweeps of thirty and 15.76 degrees respectively. Freestream conditions included subcritical cases at Mach 0.8 and an angle of attack of one degree, several supercritical transonic cases, and some supersonic cases up to Mach 1.2. Due to space limitations, most of the results of this paper will be for the ONERA M6 planform with NACA 1406 airfoil sections at freestream conditions of Mach 0.84 and three degrees angle of attack. This case is challenging since it has a subcritical lower surface flow and exhibits an upper surface shock wave located at 70% chord at the root that shifts to 10% chord at the tip and which increases in strength from the root to a point near the wing tip. Thus, the results for this case should be sufficient to demonstrate the capabilities of the present analysis-sensitivity method at transonic conditions. Complete detailed results for all the cases are presented in Refs. 4 and 21.

In the above cases, a coarse-medium grid sequencing was used in the flowfield computations to enhance convergence. For the finite difference method of computing the sensitivities, each design variable was individually perturbed a small amount, typically 1×10^{-6}, and a new flowfield solution obtained. In all cases, double precision arithmetic was utilized and the residual reduced eight orders of magnitude. In addition, the finite difference sensitivity results were computed by restarting each of the perturbed design states from the coarse grid then

proceeding to the medium grid. Different strategies for grid sequencing, such as starting on the medium grid with a previously obtained converged soulution, are all valid options to speed up the finite difference approach; but these were not investigated in this study. In the quasi-analytical method, the sensitivity equation, Eq. (1), was solved with twelve right hand sides representing the vector of design variables, Eq. (25), using one of the sparse solvers. In all cases, $\partial\phi/\partial XD$ values were obtained for every gridpoint in the flowfield. Also, the method automatically computed upper and lower surface $\partial Cp/\partial XD$ values at twenty-five chordwise locations at each of the twenty semispan stations on the wing planform as well as the $\partial Cl/\partial XD$ values at each of the span stations and the overall wing $\partial CL/\partial XD$ results.

Results and Discussion

For the subcritical test cases, the results obtained by the quasi-analytical method were found to be in excellent agreement with results obtained from the finite difference method. In addition, the results followed the trend of the two-dimensional study.[2]

Representative results for the chordwise variation of the pressure coefficient and its sensitivity derivatives for a supercritical case ($M_\infty = 0.84$, $\alpha = 3°$) are shown on Fig. 1 for 56.4 percent semispan. Displayed in the corner in each case are the integrated coefficients, section lift coefficient for the pressure distribution and $\partial Cl/\partial XD_i$ for the rest. In subcritical flow, the sensitivities with respect to the Mach number and the thickness would be small and similar for the upper and lower surfaces while those for angle of attack, camber, and camber location would have larger upper and lower surface values of opposite sign. As expected the sensitivity derivative profiles on Fig. 1 for the lower surface are typical of subcritical flow[2]. However, the upper surface results exhibit large variations in the vicinity of the shock wave that reflect the influence on the pressure of the sensitivity of the upper surface shock wave location to various design parameters. As can be seen by noting the differences in vertical scale, the pressures and lift coefficient at this mid semispan location are most sensitive to camber and least sensitive to camber location. Finally, the agreement between the finite-difference and quasi-analytical predictions is excellent, indicating that accurate three-dimensional transonic results can be obtained using the quasi-analytical approach.

Some results for the spanwise variation of the section lift sensitivity derivatives are shown on Fig. 2, where the numbers in the lower left corner in this case are the total wing lift coefficient sensitivities, $\partial CL/\partial XD_i$. Note that the sensitivity of section lift to freestream Mach number and angle of attack is relatively constant over most of the semispan, but that the lift sensitivity to wing twist at twenty (T2) and sixty (T3) percent semi-span is concentrated in the region near the twist location. While not shown, lift sensitivities to twist at the root and the wing tip are only one-third to one-fourth of those at midspan. In general, primarily due to wing sweep and finite span, all the section sensitivity values are smaller in magnitude than corresponding values for the two-dimensional problem[2]. Finally the agreement between the finite difference and quasi-analytical section sensitivities is excellent.

Figure 3 shows representative section and wing lift sensitivity derivative results for some of the nonbasic

design variables. While the total wing lift sensitivities can often be obtained by other means, the present method also yields spanwise and chordwise information. Note that while the lifts are relatively insensitive to the semispan, the outboard lift and total lift exhibit a strong dependence on area, aspect ratio, and taper ratio, and that the agreement between the quasi-analytical method and the finite difference approach is reasonable. While not shown, the corresponding derivatives with respect to the leading and trailing edge sweep angles were very small. [4, 21]

While both the finite difference and quasi-analytical methods yield similar results, the present results indicate that for twelve design variables the quasi-analytical method is about 2.4 times computationally more efficient than the brute force finite difference approach. However, it is recognized that the costs associated with the finite difference method probably could be reduced by executing the perturbed runs directly on the medium grid starting with the design point solution obtained from the coarse grid. Likewise, the quasi-analytical method could be improved by utilizing various options associated with the sparse system equation solvers; and both methods are probably affected by grid size. Therefore, the stated relative efficiency should only be viewed as an estimate when comparing the two methods.

One application of sensitivity derivatives is solution prediction, and Fig. 4 compares two pressure coefficient distributions at the 56 percent semispan location predicted using a first order Taylor series expansion about the original calculation point with the actual variation. The predicted Cp's were calculated using

$$Cp_{predicted} = Cp_{original} + (\partial Cp/\partial XD_i)\,\Delta XD_i \tag{26}$$

where the $\partial Cp/\partial XD_i$ values were obtained from the quasi-analytical method at Mach 0.84 and α = 3 degrees. For the two results presented, the wing thickness was increased 8.3 percent to 0.065 chord and the wing tip leading edge ordinate was moved aft 0.1 chord respectively. Since the original lift coefficient at this station, as shown on Figure 1(a), was 0.383, both changes resulted in a slight increase in lift coefficient and aft movement of the shockwave at this station. However, the detailed results [4,21] show that the movement of the wing tip ordinate caused a lift coefficient decrease in the inboard sections of the wing. As can be seen on the figure, the agreement between the quasi-analytically predicted and actual pressure distributions is very good, which indicates that the sensitivity derivatives calculated using the quasi-analytical method can be used for predictions. Similar results were obtained for the other design variables.[4]

Since sensitivity derivatives describe the response of the overall solution to changes in design variables, they can be computed over a range of flight conditions to determine the degree and nature of the influence of each design variable on the solution. At transonic conditions, the Mach number strongly influences a wing flowfield; and, thus, sensitivity derivatives were computed for the ONERA M6 planform with NACA 1406 cross sections at an angle of attack of three degrees for Mach numbers ranging from 0.8 to 1.2. For simplicity, only the derivatives of the total wing lift coefficients with respect to each of the twelve basic design variables were considered. Figure 5

shows results for three of these design variables, freestream Mach number, maximum camber location, and wing tip trailing edge ordinate. For all the design variables the largest variation of each derivative occurs in the transonic regime below Mach one. In this range as Mach number increases, the upper surface shock wave is rapidly moving towards the trailing edge with the inboard portions reaching the trailing edge first. Thus, as shown by $\partial CL/\partial M_\infty$ there initially is an increase in wing lift coefficient. However, by Mach 0.92, the inboard portion of the shock wave is at or near the trailing edge, and the effects of lower surface pressure changes due to freestream Mach number increase cannot be compensated by aft shock wave movement, thus resulting in a less rapid (smaller derivative value of $\partial CL/\partial M_\infty$) rise in lift. By Mach 0.96 the entire upper surface shock wave is essentially at the trailing edge and the lift decreases, as indicated by the negative value of $\partial CL/\partial M_\infty$. As can be seen on the figure, the effects of this shock wave movement are captured by the variations in the sensitivity derivatives. Also, notice on Fig. 5 for supersonic freestream Mach numbers that the sensitivities are considerably lower. Additional results[4,21] show that the derivatives of the total lift coefficient exhibit their largest change with respect to M_∞, T, C, α, XL_T, XT_T followed by T_2, T_3, L, Y_T, T_4, and T_1, indicating that a hierarchy of dominance exists among the design variables for the current wing configuration. Finally, again there is good agreement between the results obtained by the quasi-analytical method and the finite difference approach.

Conclusion

Based upon the above results, it is concluded that the quasi-analytical method is a feasible and efficient approach for accurately obtaining transonic aerodynamic sensitivity coefficients in three dimensions. In addition, use of the symbolic manipulation packages to carry out the symbolic evaluation of the elements of the sensitivity equations is crucial in this type of sensitivity study. The results obtained from the quasi-analytical method are almost identical to those obtained by the finite difference approach. Furthermore, the study indicates that:

(1) obtaining the sensitivity derivatives using the quasi-analytical approach and an iterative conjugate gradient method appears to be more efficient than computing the derivatives by the finite difference method, especially when the number of design variables is large, and

(2) the quasi-analytical method shows promise with regard to analysis-sensitivity methodologies applied to large aerodynamic systems.

Acknowledgment

This project was supported by the National Aeronautics and Space Administration under grant No. NAG 1-793, Dr. E. Carson Yates, Jr., and Dr. Woodrow Whitlow, Jr. NASA Langley Research Center, as technical monitors. The authors also appreciate the helpful suggestions and discussions of Dr. Perry Newman of NASA Langley.

References

1. Sobieski, J.S., "The Case for Aerodynamic Sensitivity Analysis," NASA CP-2457, pp. 77-97, January 1987.
2. El-banna, H.M. and Carlson, L.A., "Determination of Aerodynamic Sensitivity Coefficients Based on the Transonic Small Perturbation Formulation", *Journal of Aircraft*, Vol 27, No. 6, June 1990, pp. 507-515.
3. El-banna, H.M., Carlson, L.A., "Determination of Aerodynamic Sensitivity Coefficients Based on the Three-Dimensional Full Potential Equation", AIAA paper No. 92-2670, June 1992.
4. El-banna, H.M., Aerodynamic Sensitivity Analysis in the Transonic Regime, Ph.D. Dissertation, Texas A&M University, College Station, Tx, August 1992.
5. Baysal, O. and Eleshaky, M.E., "Aerodynamic Design Optimization Using Sensitivity Analysis and Computational Fluid Dynamics," *AIAA Journal*, Vol. 30, No. 3, 1992, pp. 718-725.
6. Dulikravich, G.S., "Aerodynamic Shape Design and Optimization", AIAA Paper No. 91-0476, January 1991.
7. Taylor III, A.C., Korivi, V.M., and Hou, G.W., "Approximate Analysis and Sensitivity Analysis Methods for Viscous Flow Involving Variation of Geometric Shape," AIAA Paper 91-1569-CP, *AIAA 10th Computational Fluid Dynamics Conference*, AIAA, New York, NY, 1991, pp. 456-475.
8. Baysal, O., Eleshaky, M.E., Burgreen, G.W., "Aerodynamic Shape Optimization Using Sensitivity Analysis on Third-Order Euler Equations", *Journal of Aircraft*, Vol. 30, No. 6, 1993, pp. 953-961.
9. Bau, H.H., "Symbolic Computation - An Introduction for the Uninitiated", *Symbolic Computation in Fluid Mechanics and Heat Transfer*, The American Society of Mechanical Engineers, Vol 97, 1988, pp. 1-10.
10. *MACSYMA Reference Manual*, Version 13, Computer Aided Mathematics Group, Symbolics, Inc., Burlington, MA, 1988.
11. *MACSYMA User's Guide*, Computer Aided Mathematics Group, Symbolics, Inc., Burlington, MA, 1988.
12. Roach P. and Steinberg S., "Symbolic Manipulation and Computational Fluid Dynamics", *AIAA Journal*, Vol 22, No. 10, 1984, pp. 1390-1394.
13. Steinberg S. and Roach P., "Automatic Generation of Finite Difference Code", *Symbolic Computation in Fluid Mechanics and Heat Transfer*, The American Society of Mechanical Engineers, Vol 97, 1988, pp. 81-86.
14. South Jr., J.C., Keller, J.D., Hafez, M.M.," Vector Processor Algorithms for Transonic Flow Calculations", *AIAA Journal*, Vol 18, No. 7, 1980, pp. 786-792.
15. Weed, R.A., Anderson, W.K., Carlson, L.A., "A Direct-Inverse Three Dimensional Transonic Wing Design Method for Vector Computers", AIAA Paper 84-2156, August 1984.

16. Carlson, L.A. and Weed, R.A., "A Direct Inverse Transonic Wing Design Analysis Method with Viscous Interaction", AIAA Paper 85-4075, Oct. 1985.

17. Carlson, L.A. and Weed, R.A.,"A Direct Inverse Transonic Wing Design Analysis Method with Viscous Interaction", *Journal of Aircraft*, Vol 23, No. 9, Sept. 1986, pp. 711-718.

18. IBM Engineering and Scientific Subroutine Library, *Guide and Reference*, Release 3, Rept. No. SC23-0184-3, IBM Corporation, Kingston, NY, 1990.

19. Saad, Y. and Schultz, M.H., "GMRES: A Generalized Minimum Residual Algorithm for Solving Nonsymmetric Linear Systems", *SIAM Journal of Scientific and Statistical Computing*, Vol 7, No. 3, 1986, pp. 856-869.

20. Sonneweld, A., Wesseling, B., and DeZeeuv, C., "Multigrid and Conjugate Gradient Methods as Convergence Acceleration Techniques," *Multigrid Methods for Integral and Differential Equations*, edited by Paddon, D.J. and Holstein, M., Oxford University Press (Claredon), Oxford, 1985, pp. 117-167.

21. El-Banna, H.M. and Carlson, L.A., "A Compendium of Transonic Aerodynamic Sensitivity Coefficient Data," Texas Engineering Experiment Station Report TAMRF 5802-92-03, College Station, Tx., July 1992.

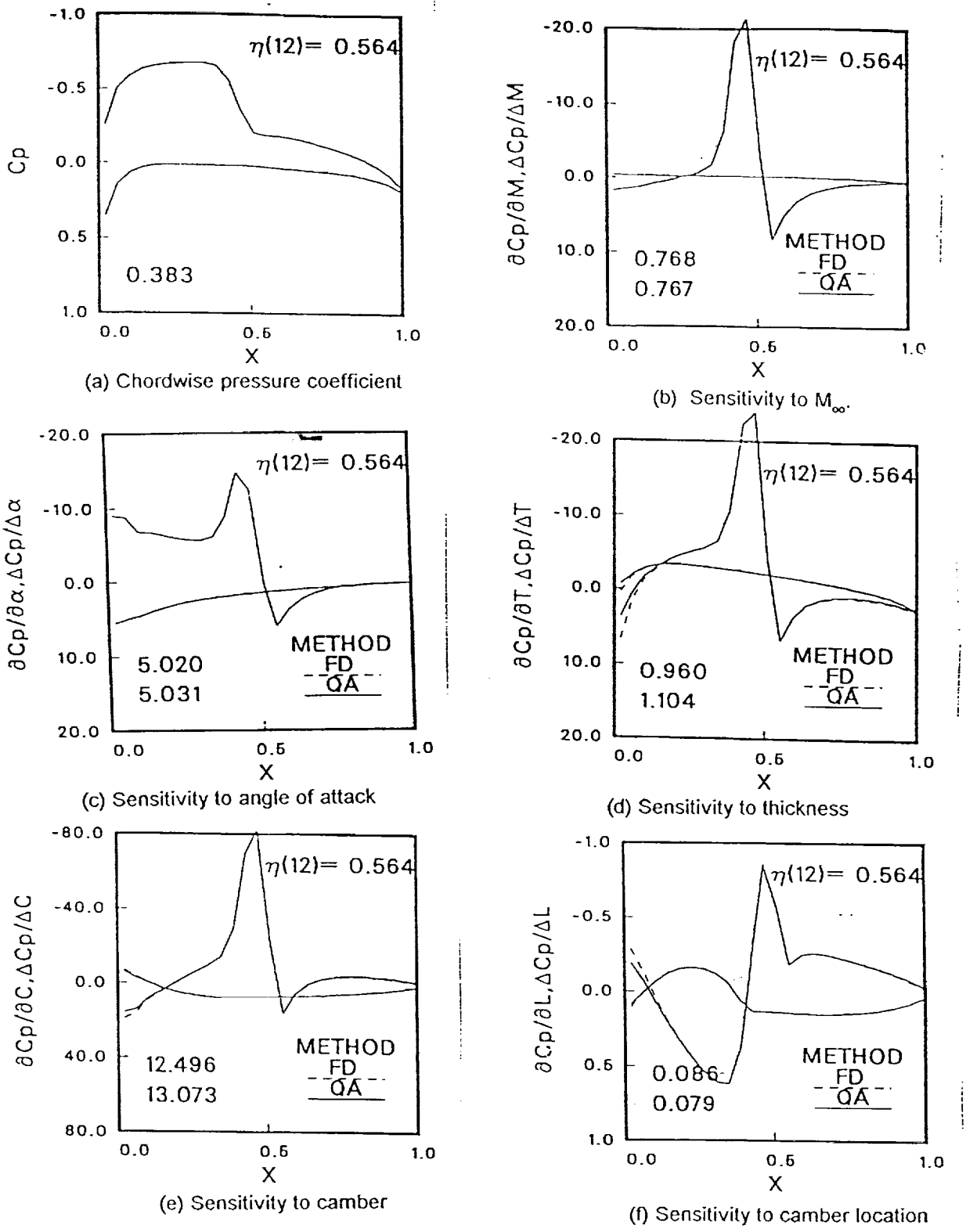

Fig. 1 -- Pressure coefficient and pressure coefficient sensitivity derivatives at 56% semispan, $M_\infty = 0.84$, $\alpha = 3°$. Values in lower left-hand corners are Cl for (a). For (b)-(f), they are the section $\frac{\partial Cl}{\partial XD_i}$ computed by FD and QA methods.

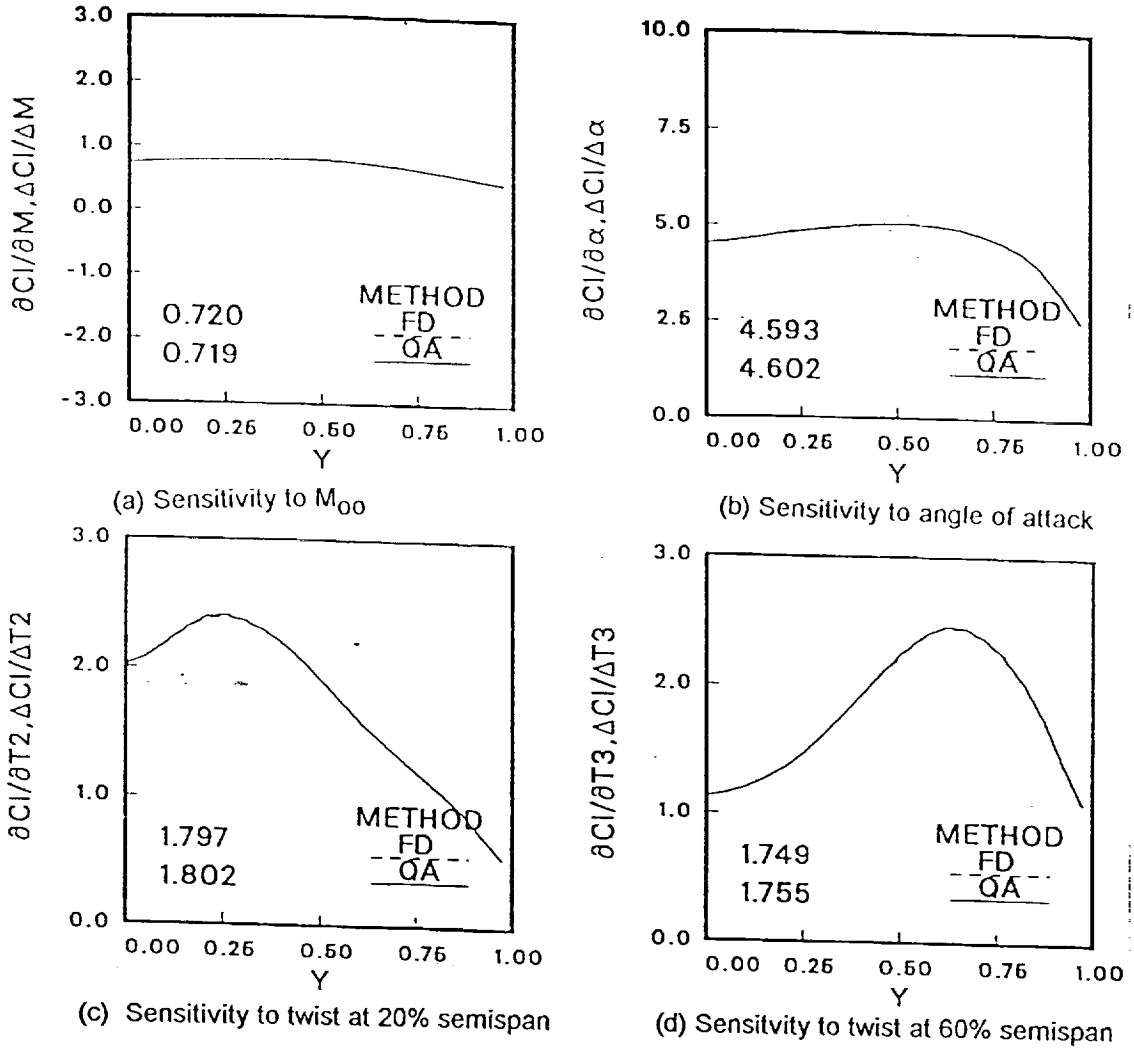

Fig. 2 -- Lift coefficient sensitivity derivatives, $M_{\infty} = 0.84$, $\alpha = 3°$; Values in lower left-hand corners are the wing $\frac{\partial CL}{\partial XD_i}$ computed by FD and QA methods.

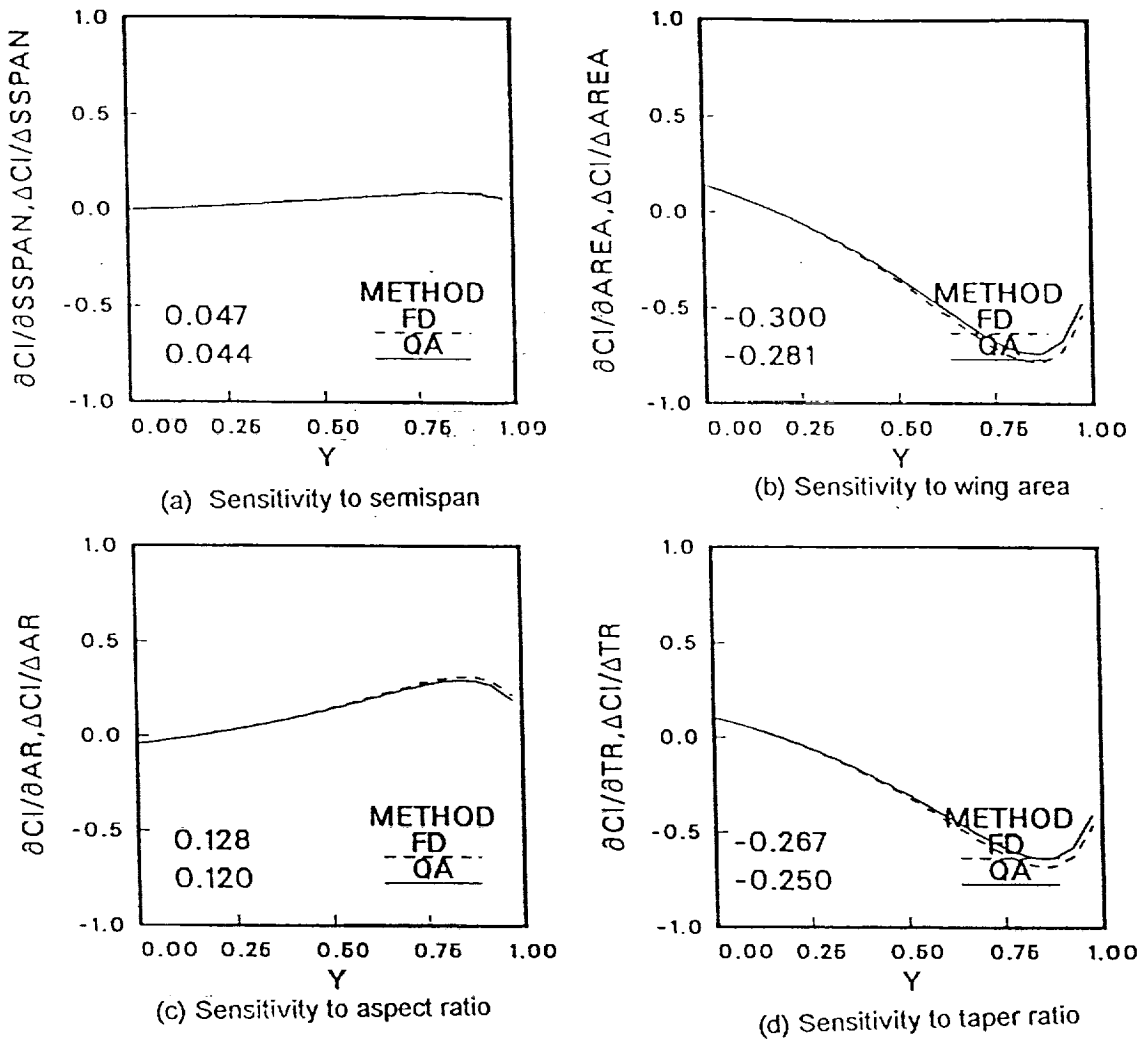

Fig. 3 -- Sensitivity to nonbasic design variables. Values in lower left-hand corners are the wing $\frac{\partial CL}{\partial XD_i}$ computed by FD and QA methods.

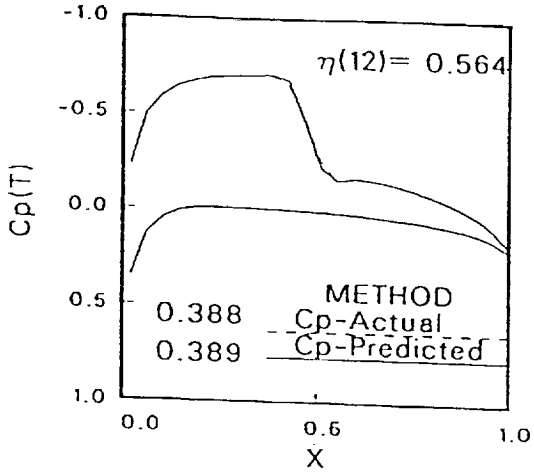

(a) Thickness increased to 0.065 chord

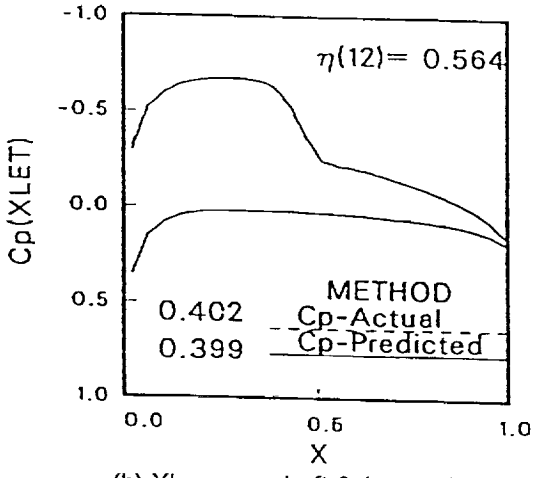

(b) XL_T moved aft 0.1 root chord

Fig. 4 -- Actual versus predicted pressure coefficients at 56% semispan. Values in lower left-hand corners are the actual and predicted section Cl.

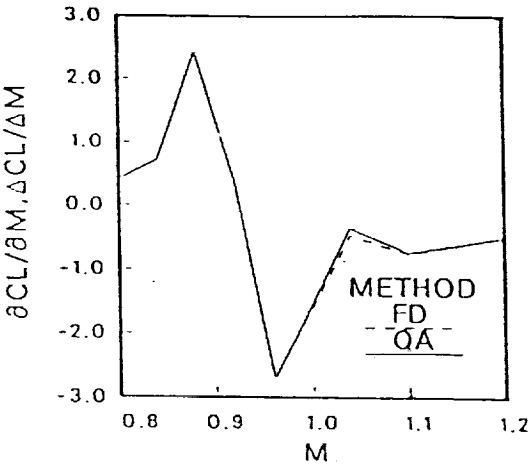

(a) Sensitivity to M_{oo}

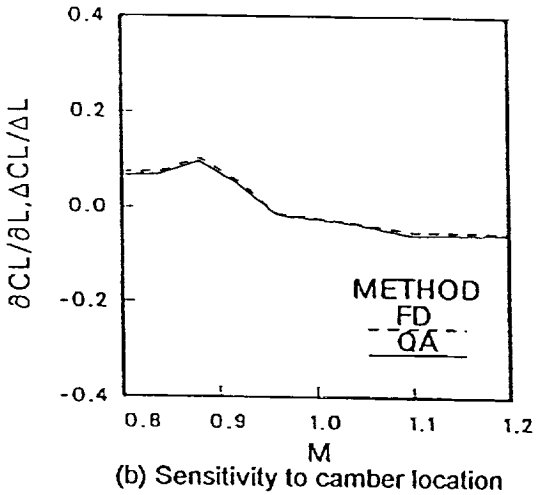

(b) Sensitivity to camber location

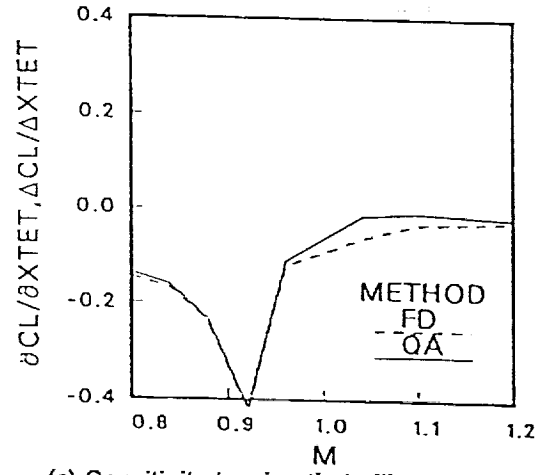

(c) Sensitivity to wing tip trailing edge ordinate

Fig. 5 -- Sensitivity of CL for $0.8 < M_{oo} < 1.2$.

Integrated Determination of Sensitivity Derivatives for an Aeroelastic Transonic Wing

by A. E. Arslan and L. A. Carlson

Submitted to the AIAA/USAF/NASA/ISSMO Symposium on Multidisciplinary Analysis and Optimization

September 1994

INTEGRATED DETERMINATION OF SENSITIVITY DERIVATIVES FOR AN AEROELASTIC TRANSONIC WING

by

Alan E. Arslan, Graduate Research Assistant
and
Leland A. Carlson, Professor

Texas A&M University
Aerospace Engineering Department
College Station, TX 77843
Ph: (409) 845-1426
(409) 845-0720
FAX:(409) 845-6051

AN EXTENDED ABSTRACT

Submitted to the 5th AIAA/USAF/NASA/ISSMO
Symposium on Multidisciplinary Analysis and Optimization

NOMENCLATURE

c	Chord length
C	Maximum camber
C_l	Section lift coefficient
C_L	Wing lift coefficient
C_p	Pressure coefficient
E	Young's modulus of elasticity (non-dimensionalized by 10^7 Psi)
f, g, h	Grid stretching factors
ILE, ITE	Leading and trailing edge index in the x direction
LC	Location of maximum camber
M_∞	Freestream Mach number
R	Residual of the aerodynamic equation
T_{tip}	Twist angle at the tip
TH	Maximum thickness
tw	Twist angle at a given section
t	Thickness of the plate(non-dimensionalized by the chord)
T	Residual of the structural equation
TU	Residual for the U equation
U_∞	Freestream velocity(also U_{inf})
u, v, w	Perturbation velocity Cartesian components
XD	Vector of design variables
x,y,z	Cartesian coordinates directions

α	Angle of attack
δ	Structural deflections non-dimensionalized by the chord
ϕ	Small perturbation velocity potential function
γ	Ratio of specific heats
Γ	Circulation at a given station along the wing
ν	Poisson's ratio
ρ_∞	Freestream density

Subscripts

∞	Free stream condition
A	Obtained from aerodynamic variables alone
b	Body
i,j,k	Grid point
ii,jj,kk	Counters for the residual dependencies
iii,jjj,kkk	Counters for the selected deflections and loads for the coupling
LE	Leading edge
l	Lower side of the wing
p	Pressure
root	At the root
S	Obtained from the structural variables alone
TE	Trailing edge
tip	At the wing tip
u	Upper side of the wing

INTRODUCTION

In the transonic regime, due to the non-linearity of the governing flow equations, the determination of optimum aerodynamic loads is one of the main difficulties facing the aircraft designer. Since most present day commercial aircraft operate transonically, computational methods which use optimization techniques are being developed to improve current designs. However, in order for these advanced computational codes to become more useful as design tools, it is necessary to develop methods for the computation of the sensitivity of the different parameters, such as aerodynamic forces or structural deflections, to the different design variables. With a sensitivity derivative being defined as a system response of interest with respect to a given independent design variable, it is desirable that such sensitivity coefficients be easily obtained.

In the past, sensitivity methodology has been used in structural design[1] and optimization programs[2] and in some aerodynamic studies.[3-8] However, the predominant contributor to cost and computational time in the optimization procedure has always been the calculation of sensitivity derivatives. Hence, efficient numerical

methods for computing such derivatives are needed for the integration of advanced computational codes into systematic design methodology, where the computational cost of a single flow analysis can be extremely high, particularly in three dimensions.

Consequently, the primary objective of this research is to investigate the concept that it is possible to use similar, perhaps identical, incremental iterative, solution approaches to efficiently couple for three dimensional transonic flow an aerodynamic solution for the pressure distribution with a structural solution for the corresponding deflections and to simultaneously use the same solution algorithms and the quasi-analytical method to obtain the aerodynamic as well as the structural discipline sensitivity derivatives for the fully coupled system with the input coefficients necessary to determine system sensitivities. Since the entire method is complex and requires an efficient flowfield as well as structural solver and since the present study is essentially proof-of-concept, it was decided for the present work to base the aerodynamics on the transonic small perturbation potential equation and the structural solver on the small deflection plate equation. Because of their simplicity, these equations are practical tools for the present proof-of-concept study where rapid solutions are essential. Previous experience with this approach has indicated that it is robust and reasonably accurate for engineering purposes. Finally, in order for an optimization process to be accurate, it must take into account the system sensitivity derivatives in which the effects of each discipline on the other is considered. Thus, the solver also computes the coupling derivatives relevant to the calculation of the system sensitivity derivatives.

Currently, one conceptually simple method for computing sensitivity derivatives is the method of "brute force" finite differencing. Here, a design variable is perturbed from its previous value, a new complete solution is obtained, and the differences between the new and old solutions are used to obtain the sensitivity coefficients. This direct technique has the disadvantage of being very computer intensive, especially if the governing equations are expensive to solve and the number of design variables is large, and the resultant values are often very sensitive to the magnitude of the design variable perturbation. As a less costly alternative, sensitivity derivatives can, in principle, be computed by direct differentiation of the governing equations. In the case where the continuous governing equations are differentiated prior to their numerical discretization, the method is known as the "continuum" or the analytical approach[3]. On the other hand, if the governing equations are differentiated after their discretization, the method is known as the "discrete" or the "quasi-analytical" approach.

Investigations concerning the feasibility of the quasi-analytical approach for the computation of the aerodynamic sensitivity derivatives have been undertaken by many researchers[4,5,6] and several methods have proven to be very successful. However, the differentiation of the governing discretized equations results in very large systems of algebraic linear sensitivity equations which must be solved to obtain the derivatives of interest. The application of a direct solver method to such a system requires extensive computer storage which for practical three dimensional problems is beyond the capacity of modern supercomputers. Moreover, the sensitivity matrix, sparse in nature, is generally very ill conditioned (or not diagonally dominant) and the convergence by the

use of standard iterative techniques is very slow. To avoid these problems, it is necessary to develop other iterative solution algorithms of the sensitivity equations. One possibility is the incremental iterative technique[4,7] which allows the iterative calculation of the sensitivity derivatives using algorithms similar to those applied to the flowfield..

The incremental iterative technique can be applied through a point semi-implicit algorithm to solve for the flowfield, structural deflections, and their respective sensitivities with respect to the different design variables simultaneously. However, these results are only discipline specific. To obtain a trully optimized solution the effect of one discipline on the other[8] needs to be considered. In other words, system as well as discipline derivatives need to be determined. Consequently, a second objective of the current work is to not only compute the coefficients needed for the system sensitivity equations but to also investigate the number of system sensitivities needed and methods for computing them.

THEORY

Flowfield Model

The equations governing transonic flow are highly nonlinear and range from the Navier-Stokes equations to the small perturbation potential equation. Since this research is a proof-of-concept investigation, the flow modeling is the simplest possible, e.g. the non-conservative transonic small perturbation equation:

$$(1 - M_\infty^2 - (\gamma + 1) M_\infty^2 \phi_x)\phi_{xx} + \phi_{yy} + \phi_{zz} = 0 \qquad (1.a)$$

where

$$\phi_x = u \qquad (1.b)$$

$$\phi_y = v \qquad (1.c)$$

$$\phi_z = w \qquad (1.d)$$

As shown in Fig. 1, the selected geometry is a rectangular wing with the z axis in the spanwise direction.

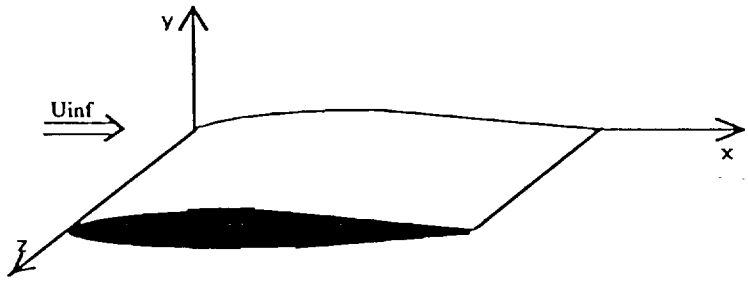

Fig. 1 Geometry Setup

At the wing, the boundary conditions are the inviscid surface boundary conditions for tangent flow:

$$v = (U_\infty + u)\frac{\partial y_{u,l}}{\partial x} + w\frac{\partial y_{u,l}}{\partial z} \tag{2}$$

where $y_{u,l}$ is a function of x and z and certain design variables, such as the angle of attack. In the wake, the Kutta condition along the wing semispan yields:

$$\Gamma = \Delta\phi, \quad x_{TE} < x < \infty \tag{3}$$

while at the farfield, the boundary condition is:

$$\phi_\infty = 0 \tag{4}$$

At the downstream boundary, the Trefftz boundary condition can be approximated by:

$$\text{At} \quad x=\infty : \ \phi_x = 0 \tag{5}$$

Further, the wing symmetry condition is expressed by:

$$w(z=0) = 0 \tag{6}$$

The finite differencing of Eq. (1), requires the use of a residual R written in functional notation at the point i,j,k as:

$$R_{i,j,k} \equiv R_{i,j,k}(\phi_{ii,jj,kk}, XD) \tag{7}$$

Since the structural deflections are included as the boundary conditions, and are not treated as dependent design variables in the above equation, Eq. (7) should be considered a discipline equation.

After taking the total differential of Eq. (7) with respect to a design variable XD, the sensitivity equation is obtained:

$$\frac{dR_{i,j,k}}{dXD} = \left[\frac{\partial R_{i,j,k}}{\partial \phi_{ii,jj,kk}}\right]\left\{\frac{\partial \phi_{ii,jj,kk}}{\partial XD}\right\} + \left\{\frac{\partial R_{i,j,k}}{\partial XD}\right\} = 0 \tag{8}$$

In this equation lies the essence of the quasi-analytical formulation in which the discretized governing equations are differentiated. Here, $\phi_{ii,jj,kk}$ is $\phi(x(ii), y(jj), z(kk), XD, \delta)$; and the system matrix $\partial R/\partial\phi$ is sparse, or non zero at certain points only (mostly the ones neighboring i,j,k). In this equation, the vector of deflections $\{\delta\}$, even though not explicitly shown, is considered to be a vector of independent variables. Near the boundaries, Eq. (8) has been reformulated to include the flowfield boundary conditions. The flowfield sensitivity derivatives $\partial\phi/\partial XD$ that are obtained from solving Eq. (8) above can be used to calculate pressure sensitivities $\partial C_p/\partial XD$ which in turn can be used to calculate the sensitivities of the section and wing lift to the design variables.

Structural Modeling

The structural problem is modeled by representing the wing by an equivalent flat plate with dimensions almost coincident with those of the wing. The equation describing the plate deflections is:[9]

$$D\nabla^4\delta - \Delta p = 0 \tag{9}$$

which assumes a thin plate and small deflections. Here, Δp is the loading due to the difference in pressures between the upper and lower surface:

$$\Delta p = \tfrac{1}{2}\rho_\infty U_\infty^2 \Delta C_p \qquad \text{and} \qquad \Delta C_p = C_{pl} - C_{pu} \tag{10}$$

and D, the flexural rigidity (or equivalent bending stiffness), is given by:

$$D = \frac{Et^3}{12(1-\nu^2)} \tag{11}$$

This model, while simple, will yield both bending and twisting effects.

The boundary conditions[10] for Eq. (9) involve both fixed and the free edges. The root is the only fixed edge and there the boundary condition is:

$$\text{At} \quad z=0 \qquad \delta=0 \tag{12.a}$$

$$\frac{\partial \delta}{\partial z} = 0 \tag{12.b}$$

At the tip, the boundary conditions are written:

$$\text{At} \qquad z = z_{TIP} : \frac{\partial^3 \delta}{\partial z^3} + (2-\nu)\frac{\partial^3 \delta}{\partial z \partial x^2} = 0 \tag{13.a}$$

$$\frac{\partial^2 \delta}{\partial z^2} + \nu \frac{\partial^2 \delta}{\partial x^2} = 0 \tag{13.b}$$

Eq. (13.a) combines the no twisting moment and no shearing force conditions at a free edge while Eq. (13.b) states that the bending moment along the edge is zero. The other two free edges are the leading and trailing edges, and the boundary conditions for those are written:

$$\text{At} \qquad x = x_{LE}, x_{TE} : \frac{\partial^3 \delta}{\partial x^3} + (2-\nu)\frac{\partial^3 \delta}{\partial x \partial z^2} = 0 \tag{14.a}$$

$$\frac{\partial^2 \delta}{\partial x^2} + \nu \frac{\partial^2 \delta}{\partial z^2} = 0 \tag{14.b}$$

Hence, this system of equations establishes a well defined boundary value problem that can be solved by finite differencing.

The residual for Eq. (9) can be expressed as:

$$T_{i,k} = T_{i,k}(\delta_{ii,kk}, XD) \tag{15}$$

Again, this equation is discipline specific since $\delta_{ii,kk}=\delta(x(ii), z(kk), \phi_{iii,kkk}, XD)$; and $\phi_{iii,kkk}$ is the vector of potentials on the upper and lower side of the wing that are related to the calculation of loads. This vector is considered to be composed of independent variables. Unlike the flowfield case, which is three dimensional, the deflection field is a two dimensional variable.

After taking the total derivative of Eq. (15) with respect to a design variable the structural sensitivity equation is obtained:

$$\frac{dT_{i,k}}{dXD} = \left[\frac{\partial T_{i,k}}{\partial \delta_{ii,kk}}\right]\left(\frac{\partial \delta_{ii,kk}}{\partial XD}\right) + \left(\frac{\partial T_{i,k}}{\partial XD}\right) = 0 \tag{16}$$

In this case, also, the system matrix is sparse. Like the flowfield case, Eq. (16) must take into account the appropriate conditions at the boundaries.

Coupling

As a result of aerodynamic loads, the equivalent plate representing the wing will deflect; and such deflections will perturb through bending and twisting of the wing the section angles of attack and camber line shapes. These deflections in turn will induce different load distributions, and the two processes must be interacted until a converged solution is obtained. This interaction is the process of aerodynamic and structural coupling.

The coupling between the structural and the flowfield solutions is achieved through the wing boundary conditions and is included by simply adding the structural deflections to the ordinates of the wing. Hence, after taking the derivatives with respect to the x and z coordinates, the boundary conditions equations are modified by:

$$\frac{\partial y_{u,l}}{\partial x} = \left(\frac{\partial y_{u,l}}{\partial x} \right)_A + \frac{\partial \delta}{\partial x} \tag{17.a}$$

$$\frac{\partial y_{u,l}}{\partial z} = \left(\frac{\partial y_{u,l}}{\partial z} \right)_A + \frac{\partial \delta}{\partial z} \tag{17.b}$$

Note that this coupling is only carried out at the field variables level. In other words, for a linear case (much below the critical Mach number), a case in which the sensitivity matrix $\partial R/\partial \phi$ would not be influenced by the values of ϕ, this aeroelastic coupling would only slightly affect the aerodynamic and the structural sensitivity derivatives. Thus, the coupling is said to be achieved for the sensitivity derivatives at the zero order only.

System Sensitivity

As mentioned, for an optimization process to be accurate, it must take into account the system sensitivity derivatives in which the coupling between the disciplines is included. Thus, the calculation of interdisciplinary sensitivities such as the sensitivity of the pressure distribution to the thickness of the plate or that of the tip deflections with respect to the camber at the tip are needed. In general, the set of equations governing the entire coupled system can be written as:[9]

$$A((XD, \delta), \phi) = 0 \tag{18}$$

$$S((XD, \phi), \delta) = 0 \tag{19}$$

where Eq. (18) represents the aerodynamics and Eq. (19) is for the structures. For the system analysis ϕ can be replaced by ΔC_p since it is the variable involved in the aerodynamic coupling. The vectors grouped in the inner parentheses are the input, while the vectors of unknowns (output) are listed last. The purpose of the analysis is to find the total derivatives dY/dXD of the output vector with respect to the different

design variables. According to the implicit functions theorem, the equations above can be written as[10]:

$$\Delta C_P = \Delta C_{P_A}(XD, \delta) \tag{20}$$

$$\delta = \delta_S(XD, \Delta C_P) \tag{21}$$

After considering $Y=(\{\Delta Cp\},\{\delta\})$, taking its total derivatives with respect to XD, and rearranging the terms, the following system equation is obtained:

$$\begin{bmatrix} I & -J_{AS} \\ -J_{SA} & I \end{bmatrix} \left\{ \frac{dY}{dXD} \right\} = \left\{ \frac{\partial Y}{\partial XD} \right\} \tag{22}$$

where J_{AS} is a Jacobian of the partial "coupling" sensitivity derivatives $\partial\Delta Cp/\partial\delta$ and J_{SA} is the Jacobian of $\partial\delta/\partial\Delta Cp$ for selected points on the wing. For example, the i-th column of J_{AS} comprises the partial derivatives with respect to the i-th displacement. The partial derivatives in the coupling matrix as well as the right hand side are, by definition, calculated using strictly discipline derivatives. Again, the quasi-analytical approach is used. Equations (7) and (15) are rewritten as:

$$R_{i,j,k} \equiv R_{i,j,k}((XD, \delta), \phi_{ii,jj,kk}) \tag{23}$$

$$T_{i,k} = T_{i,k}((XD, \Delta C_P), \delta_{ii,kk}) \tag{24}$$

where δ is considered an independent variable for Eq. (23) and ΔCp is considered independent for Eq. (24). This approach is valid since it is discipline specific. Differentiating Eq. (23) with respect to a given deflection and Eq. (24) with respect to a given ΔCp on the wing yields the system of linear coupling sensitivities equations:

$$\frac{dR_{i,j,k}}{d\delta} = \left[\frac{\partial R_{i,j,k}}{\partial \phi_{ii,jj,kk}} \right] \left\{ \frac{\partial \phi_{ii,jj,kk}}{\partial \delta} \right\} + \left\{ \frac{\partial R_{i,j,k}}{\partial \delta} \right\} = 0 \tag{25}$$

$$\frac{dT_{i,k}}{d\Delta C_p} = \left[\frac{\partial T_{i,k}}{\partial \delta_{ii,kk}} \right] \left(\frac{\partial \delta_{ii,kk}}{\partial \Delta C_p} \right) + \left(\frac{\partial T_{i,k}}{\partial \Delta C_p} \right) = 0 \tag{26}$$

which when solved yields the coupling sensitivity derivatives, i.e. the elements of the J_{AS} and J_{SA} matrices, necessary for the calculation of the system sensitivities via Eq. (22).

DESIGN VARIABLES

Design variables are classified into two groups, the aerodyanmic variables termed XDA and the structural variables called XDS. One variable (M_∞) is common to both vectors. A design variable is termed to be aerodynamic or structural depending in which expression of the discipline residuals it appears. For example, the angle of attack would be an aerodynamic variable while the plate thickness, which only appears in the deflection equation would be a structural variable. However, all the design

variables used are basic variables in that they are uncoupled and independent. For the current problem the vector of design variables consists of twelve variables and is given by:

$$XD = (XD1, \ldots, XD12) \tag{27}$$

These design variables can be classified into three groups:

(a) Freestream design variables: These include the freestream Mach number and the angle of attack. The Mach number enters the formulation through Eq. (1) while α appears in the boundary conditions in Eq. (2).

(b) Cross section design variables: These include the variables that define the airfoil. For the present study only NACA four-digit airfoils are considered. Thus the relevant design variables are maximum thickness, maximum camber, and location of the maximum camber, at both the root and tip. Another variable defining each spanwise section would be the geometric twist, usually defined in terms of the relative twist of the wing tip to that of the root. The airfoil sections as well as the aerodynamic twist at a given span station are obtained by linear lofting between the root and tip the values for TH, C, and LC, each expressed as a fraction of the chord, i.e.:

$$TH = TH_{root} + z/z_{tip} (TH_{tip} - TH_{root}) \tag{30}$$

$$C = C_{root} + z/z_{tip} (C_{tip} - C_{root}) \tag{31}$$

$$LC = LC_{root} + z/z_{tip} (LC_{tip} - LC_{root}) \tag{32}$$

It should be noted that this formulation is not a point by point lofting in which the vertical coordinate is interpolated linearly from root to tip. Nevertheless, this approach was chosen to simplify the analytical derivations as well as the coding. The section twist is also obtained by linear interpolation between the wing root and the wing tip:

$$tw = z/z_{tip} T_{tip} \tag{33}$$

When taking the derivative of $y_{u,l}$ with respect to x, the following is obtained:

$$\left(\frac{\partial y_{u,l}}{\partial x} \right)_A = \frac{\partial y_c}{\partial x} \pm \frac{\partial y_{TH}}{\partial x} - \alpha - tw \tag{34}$$

$$\left(\frac{\partial y_{u,l}}{\partial z} \right)_A = \frac{\partial y_c}{\partial z} \pm \frac{\partial y_{TH}}{\partial z} - \frac{T_{tip}\, x}{z_{tip}} \tag{35}$$

With this formulation, the vector of the aerodynamic design variables can be written:

$$XDA = (\alpha, TH_{root}, TH_{tip}, C_{root}, C_{tip}, LC_{root}, LC_{tip}, T_{tip}, M_\infty) \tag{36}$$

(c) The structural variables: These include the parameters involved in the plate deflection equation. The first, M_∞, comes from the dynamic pressure term, second is the thickness of the plate t, followed by Poisson's ratio ν, and Young's modulus of elasticity E. In the present study, the dynamic pressure is calculated using the sea level conditions. Thus, the vector of structural design variables is:

$$XDS = (M_\infty, t, \nu, E) \tag{37}$$

These two vectors are combined to form a single vector of design variables:

$$XD = (\alpha, TH_{root}, TH_{tip}, C_{root}, C_{tip}, LC_{root}, LC_{tip}, T_{tip}, M_\infty, t, \nu, E) \tag{38}$$

DISCRETIZATION APPROACH AND NUMERICAL PROCEDURE

Aerodynamic Analysis

As previously stated, the aerodynamic analysis is based on the transonic small perturbation potential formulation in Eq. (1), formulated using a Cartesian grid and a finite computational domain. Hence, the transformation utilized maps the infinite physical domain into a finite computational grid.

In the present formulation, the infinite physical plane is transformed via tangent functions into the finite computational space shown in Fig. 2. Thus, the i=1, i=IM, j=1, j=JM, and k=KM planes physically correspond to infinity and k=1 is the wing symetry plane. Further, the wing is located between two grid lines, JB and JB-1.

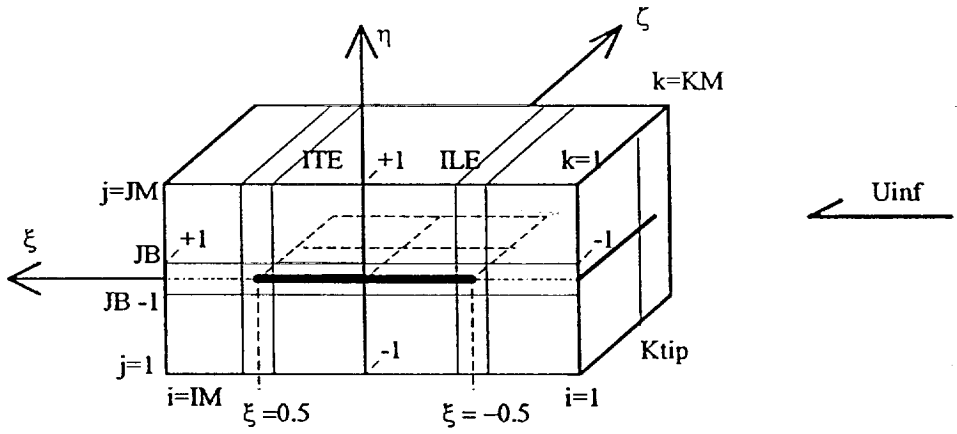

Fig. 2 Computational and Physical Domains

Since there is a potential jump across the trailing edge cut, which extends to downstream infinity, and since the jump depends upon the trailing edge potentials, the sensitivity matrix, $\partial R/\partial \phi$, while banded, contains elements far from the central band. Consequently, the rapid and efficient solution of the sensitivity equation by direct methods is difficult. However, the sensitivity equation can be solved by the same iterative method as the flowfield, by the introduction of a new residual $S_{i,j,k}$ corresponding to Eq. (8).

For the sensitivity portion of this analysis, the residual expressions, $R_{i,j,k}$, are differentiated analytically with respect to the flowfield variable ϕ. Similarly, the right hand side of the sensitivity equations is determined by analytical differentiation of the residuals with respect to each design variable. Unfortunately, the size of the sensitivity matrix is tremendous for fine grids and storing such a matrix is beyond the capability of many computers. In the present study, the storage problem is solved by the use of a more efficient solver, namely the incremental iterative technique. The additional

available memory space allows the use of finer grids and the inclusion of other disciplines as well.

Once the potentials are obtained, the C_p's are obtained through the small perturbation relation:

$$C_p = -2\phi_x \tag{62}$$

which requires the extrapolation (first order) of the ϕ values above and below the plane of the wing. The section lift coefficient is then computed directly from the circulation around every airfoil section:

$$C_l = 2\Gamma_k = 2(\phi_{ITE,JB,k} - \phi_{ITE,JB-1,k}) \tag{63}$$

which gives faster and more accurate results than those obtained by integration of the C_p's difference between the lower and upper surfaces. The wing lift coefficient C_L is calculated by integration over the span. The corresponding sensitivity derivatives are then determined from:

$$\left(\frac{\partial C_l}{\partial XD}\right)_k = 2\frac{\partial \Gamma_k}{\partial XD} \tag{64}$$

and $\partial C_L/\partial XD$ can be calculated by numerical integration of the above coefficient along the span.

Structural Analysis

Since Eq. (9) is a fourth order partial differential equation, its solution can be significantly simplified by splitting it into two equations to be solved simultaneously:[11]

$$\nabla^2 u - \frac{\Delta p}{D} = 0 \tag{65}$$

$$\nabla^2 \delta - u = 0 \tag{66}$$

In non-dimensional form, Eq. (65) is:

$$\nabla^2 u - \bar{k}\Delta C_p = 0 \tag{67}$$

where

$$\bar{k} = k_0 E(1-\nu^2)\frac{M_\infty^2}{t^3} \tag{68}$$

and

$$k_0 = \frac{6\gamma p_\infty}{E_0} \tag{69}$$

After splitting the governing equations, the next step should be to split the eight boundary conditions written in Eqs. (12)-(14) into four for the u's and four for the deflections. However, this splitting must be carried out so that the solution scheme does not become unstable. When applying the Laplacian operator to Eq. (12.b) one obtains:

$$\text{At } z=0: \qquad \frac{\partial u}{\partial z} = 0 \tag{70}$$

For the free edges, the situation is more complicated. The first step would be to take, the partial derivative of u in the z direction. When combining the result of this differentiation with Eq. (13.a) the appropriate boundary condition becomes:

$$\text{At } z=z_{tip}: \qquad \frac{\partial u}{\partial z} = (\nu - 1)\frac{\partial^3 \delta}{\partial z \partial x^2} \tag{71}$$

When finite differenced, this formulation is accurate and has better stability characteristics than the formulation with the third order partial derivative with respect to z. Similarly, at the leading and trailing edges of the plate the boundary condition for u can be expressed:

$$\text{At } x=x_{LE},\, x_{TE}: \qquad \frac{\partial u}{\partial x} = (\nu - 1)\frac{\partial^3 \delta}{\partial x \partial z^2} \tag{72}$$

Since the flowfield solver uses a finite differencing technique with a given grid the same technique and the same grid are used to obtain the structural deflections, which simplifies the aerodynamic structural coupling. Hence, both the flowfield and structural solutions can be calculated within the same loops, which is computationally efficient. Consequently, the structural part uses the same grid metrics. Further, the field variable u is first obtained and then used as an input to solve for the deflection at the same point, thus enhancing convergence and stability.

The boundary conditions stated in Eqs. (12)-(14) should be applied at the exact boundaries of the wing which do not coincide with an exact grid point in the computational domain because the leading, trailing, and wing tip edges are located between grid lines. Hence, a Taylor series development should be used at all the boundaries except the root, where the boundary coincides with a gridline. This development would involve higher order partial derivatives which when finite differenced would yield extremely complicated expressions. To avoid that problem, the size of the equivalent plate and the grid were chosen such that the free edge boundaries of the equivalent plate are very close but not coincident to the wing leading, trailing, and tip edges. The boundary conditions corresponding to Eq. (71) and (72) can cause numerical divergence and a possible solution is to simplify them so that numerical stability can be created. Fortunately, the variable u, physically corresponds to the second derivative in one direction at a given edge. For example, at the wing tip, if it is assumed that the loading along the wing is only a distributed loading without concentrated loads or moments to cause discontinuities in the curvature of the plate, the assumption that the second partial derivative with respect to z is constant is acceptable. Similarly, at the tip, the "curvature in the x-direction" or the second partial with respect to x will also be constant in the absence of concentrated loads and moments. Hence, the approximation that u is constant along a free tip is reasonable. In addition, this condition does not have a destabilizing influence on the algorithm. Hence, the partials with respect to z and x respectively for Eq. (71) and (72) are

assumed to be equal to zero. Also, the boundary conditions for the structural deflections equation (Equ. 66), stated in Equ. (12.a), (13.b), and (14.b), are finite differenced and incorporated in the corresponding residual expressions.

The second part of the structural analysis is the structural sensitivity analysis with respect to the four components of XDS, the vector of structural design variables. The approach used is the same as the one used for the deflections. In other words, the sensitivity equation is also divided into two components. Hence, when applying the quasi-analytical approach to Eq. (75) and (78) the following equations are obtained:

$$STU_{i,k} = \left[\frac{\partial TU_{i,k}}{\partial u_{ii,kk}}\right]\left\{\frac{\partial u_{ii,kk}}{\partial XDS}\right\} + \left\{\frac{\partial TU_{i,k}}{\partial XDS}\right\} = 0 \qquad (88)$$

$$ST_{i,k} = \left[\frac{\partial T_{i,k}}{\partial \delta_{ii,kk}}\right]\left\{\frac{\partial \delta_{ii,kk}}{\partial XDS}\right\} + \left\{\frac{\partial T_{i,k}}{\partial XDS}\right\} = 0 \qquad (89)$$

Here, it should be noted that $\frac{\partial T_{i,k}}{\partial XDS}$ is $\left(\frac{\partial u_{i,k}}{\partial XDS}\right)^{(n+1)}$, which shows that, as in the deflection field solution, the output variable of the system of Eq. (88) is used as an input to Eq. (89). At the boundaries, Eqs. (88) and (89) must take into account the appropriate structural boundary conditions.

Aeroelastic Coupling and System Sensitivity Analyses

Aerodynamic-structural coupling can be carried out at two levels; defined here to be zero and first order. The zero order coupling corresponds to an updating of the aerodynamic boundary conditions each time after the structural deflections are calculated and vice versa. However, sensitivities are computed as discipline sensitivities and do not directly include the complete effects of aerodynamic-structural coupling. On the other hand, the first order coupling is defined to mean that the effect of the structure on the flowfield and vice versa is taken into account not only at the flowfield-deflection level but also at the sensitivity level. For example, for the zero order coupling the structural deflections affect the aerodynamic sensitivity derivatives through the spanwise flow component ϕ_z in $\partial R/\partial XDA$ while the first order coupling also affects that expression through a coupling term $\partial\phi_z/\partial\delta$. This term is called a coupling sensitivity. In this second case, the deflections are not considered constant in the aerodynamic residual expressions (Eq. 18), as in the discipline specific analysis, and are considered as design variables. Likewise, in first order coupling, the potentials related to the C_p calculation along the wing are treated as design variables for Eq. (19).

The terms that affect coupling the most are those that appear directly in the residuals expressions. These are the deflections, since they enter directly in the expression of the boundary conditions for the aerodynamic residuals, and the loads ΔC_p, which appear in the expressions of the structural residuals. However, as shown in

Eq. (22), the coupling derivatives, $\partial\Delta Cp/\partial\delta$ and $\partial\delta/\partial\Delta Cp$, are the essential components of the system sensitivity matrix and are used to obtain the system sensitivity derivatives. The equations for determining those coupling derivatives are presented in Eq. (25) and (26). However, frequently not all the deflections or loads can be used in the system matrix since such inclusions would often require extensive memory storage and CPU times that are unrealistic. Hence, the choice of which loads and deflections to include in the system sensitivity equation is subject to judgment and experimentation. However, the more coupling variables are included, the more accurate the system sensitivity derivatives should be.

Numerical Approach

The sensitivity matrix, associated with the linear sensitivity equations, as well as the matrix resulting from the finite differencing of the flowfield and structural solutions, are generally very sparse and ill conditioned, or not diagonally dominant. Thus, the solution of the corresponding linear equations by standard direct solvers is memory inefficient and iterative methods should be considered.[6,7,8] In addition, since the non-linear flowfield equations must be solved iteratively, the use of a similar iterative scheme to obtain the sensitivities would seem to be appropriate.

A possible scheme is the incremental iterative technique,[4,8] which has shown to have better convergence characteristics in many cases than the standard iterative techniques. This method comes from a formulation in which a system of algebraic equations has the general form:[8]

$$[A]\{Z^*\} + \{B\} = \{0\} \tag{90}$$

where $\{Z^*\}$, the solution vector, is obtained by the two step formulation:

$$-[\tilde{A}]\{\Delta^n Z\} = [A]\{Z^n\} + \{B\} \tag{91}$$

$$\{Z^{n+1}\} = \{Z^n\} + \{\Delta^n Z\} \tag{92}$$

Here, n is the iteration index and $[\tilde{A}]$ is a convenient approximation of $[A]$, generally chosen to enhance the diagonal dominance and, thus, the convergence characteristics of the system.

The above formulation, when applied to sensitivity equations, still requires the storage of a relatively large sensitivity matrix. However, the use of a point algorithm to obtain the increments avoids that problem since it only requires the elements of the matrix relevant to the calculation of the increment at point i,j,k. Obviously, such an approach has the possible disadvantage of slower convergence. Nevertheless, since the sensitivity equations are linear, their convergence should be faster than that of the nonlinear flowfield. Unfortunately, the structural equations tend to behave like the nonlinear flowfield equations in terms of convergence.

An example of such a point algorithm is the semi-implicit ZEBRA scheme[12] which mimics point successive over relaxation (SOR). The algorithm marches in the

streamwise (I) direction solving by spanwise planes. In each plane, the points where j+k are odd are denoted black and the ones where j+k are even are denoted white (Fig. 3). Each plane is solved by a two-pass sweep in which new black values are obtained first, followed by the white ones. Convergence is thus accelerated because calculations at the white points use updated values at the black points. Because of its uncoupled formulation, this method is suitable for sequential, vector, and parallel machines.

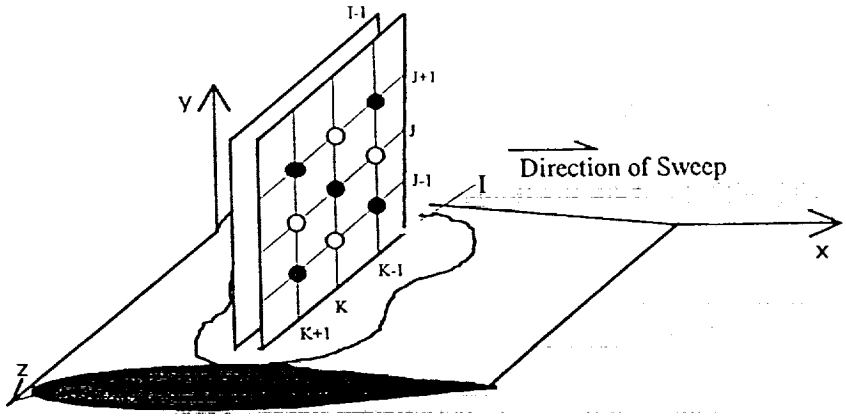

Fig. 3 Point Dependence Illustration

In the ZEBRA algorithm, because of the point semi-implicitness, the matrix $[\bar{A}]$ is reduced to a scalar B. Hence, the incremental changes in the unknowns can be found in the following form for the aerodynamic potential, for example:

$$\Delta\phi_{i,j,k} = \frac{R_{i,j,k}}{B} + DMP \tag{93}$$

where DMP is a damping term added for transonic stability. The same type of formulas can also be used to calculate the increments for the aerodynamic sensitivity field variables, structural deflections, structural sensitivity derivatives and coupling derivatives field variables[16]. The algorithm used is schematically described in the following figure.

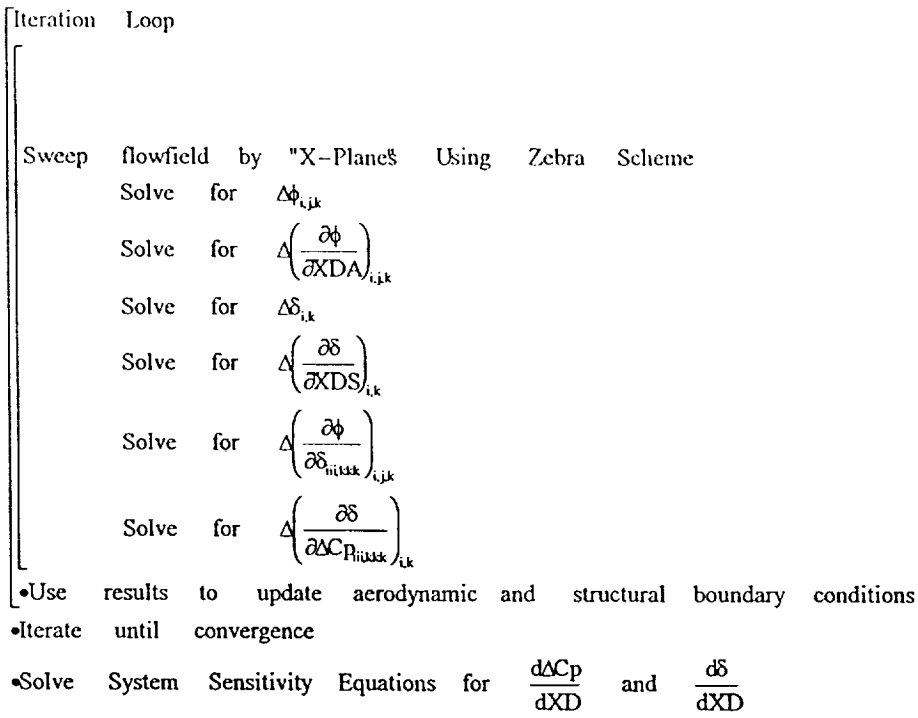

Fig. 4 Integrated Solution Approach

RESULTS AND DISCUSSION

Case Studied

The wing configuration considered in this study has a rectangular planform of constant unit chord. The geometric and structural design parameters describing the wing as well as the nominal freestream conditions are listed in Table 1. It should be noted that the root and tip airfoil sections are NACA 2406 and NACA 1706 respectively.

Table 1 Wing Data

Aspect Ratio	3.17
α	2.0°
z_{tip}	1.58
c	1.0
T_{tip}	-1.0°
TH_{root}	0.06
TH_{tip}	0.06
C_{root}	0.02
C_{tip}	0.01
LC_{root}	0.4
LC_{tip}	0.7
M_∞	0.82
E	1.0
ν	0.33

E leftout

The case presented here used a grid of 97 x 16 x 16 for the flowfield and 49 x 10 for the structural deflections. The freestream Mach number is supercritical and a shock wave is present on the inboard sections of the upper surface of the wing. However, the shock wave disappears on the outboard sections due to three dimensional effects. Thus, this Mach number is interesting because it locally includes both the subcritical and supercritical behavior of the flowfield and the corresponding sensitivities. In all cases, to speed up convergence, a coarse-medium-fine grid sequence halving in the x-direction was used in computing the analysis information. Results were computed for equivalent plate thicknesses of five and two percent but only the two percent results were shown in this paper. It should be noted that a one percent thick case, while attempted, turned out to be aeroelastically divergent. For the coupling variables needed to determine the system sensitivities, five of the ten spanwise stations were selected each involving twenty five of the forty-nine possible points. It is believed, since it is numerically difficult to include every point used in the fine grid, that the deflections and loads selected for the coupling system coefficients in the sensitivites will be representative. However, this choice is under investigation and will be further discussed in the final paper.

Fig. 5 shows the pressure distribution at six of the ten spanwise stations. The upper surface shows a shock wave at approximately the x=0.5 location in the sections near the root. The airfoil section, being non-constant from root to tip, is also drawn on the same diagram and the angle of attack as well as the geometric twist are taken into account when plotting the geometry. The final deflected shape of the airfoil due to aeroelastic coupling is drawn in dashed lines but not to scale. The critical pressure coefficient level C_p^*, is also shown and comparison of C_p^* with the pressures shows that the shock wave weakens progressively when approaching the tip, which is

obviously subcritical. At the tip, the pressure distribution is typical of a subcritical aft cambered NACA section. One should note that due to the change in airfoil sections from root to tip the wing has some inherent aerodynamic twist. However, unlike the thick plate case[16], the lower surface Cp curve at the tip section, goes above the upper one causing the aerodynamic load at the leading edge to be negative.

The results for the discipline sensitivity derivatives are shown in Fig. 6-14 and Fig. 16-19 while the ones for the system sensitivity derivatives are shown in Fig. 20 through 31. Pertinent portions will be selected and discussed in detail in the final paper.

Fig. 15 shows the structural deflections at different span stations. Notice that if a line is drawn from the leading to the trailing edge of the plate at each section, this line would form an "angle of attack" with the x-axis which would be an induced twist due to structural deflections. Further, even though the amplitudes are extremely small, bending exists in the sections toward the wing tip. This "cambering" effect due to chordwise bending is more pronounced as the tip is approached. In fact, the chordwise section of the equivalent plate near the tip looks as a camber line that could cause an increase in lift and could become a dominating component of the tip aerodynamics. Further, the maximum of the structurally induced camber is a little bit aft of center. Note that the spanwise edge of the equivalent plate is loaded due to the ΔCp there, even though no concentrated loads or bending moments exist at the edges of the equivalent plate. If the spanwise edge of the equivalent plate actually corresponded to the wing tip, it would not be loaded and the cambering effect would be attenuated at the tip. Again, pertinent features of the structural sensitivity derivatives shown on Figs. 16-19 will be discussed in the final paper.

For clarity and length reasons, the system sensitivity derivatives plots are only shown for three stations, in Fig. 20 to 31. For the sensitivity of the loads with respect to the design variables the system and discipline curves almost agreed. However, a discrepancy was noticed at the leading and trailing edge locations for the sensitivity of the loads. Moreover, when compared to a case where thirteen stations chordwise were chosen for eight spanwise stations differences were found for the structural system sensitivities with respect to the aerodynamic design variables and for the loads system sensitivities with respect to the structural design variables. This difference is currently under study and will be discussed in the final paper. However, in all cases the system structural sensitivities, $d\delta/dXD$, often differed in magnitude and, more importantly in sign from the discipline sensitivity derivatives, $\partial\delta/\partial XD$. The origins and significance of this behavior will be discussed in the final paper.

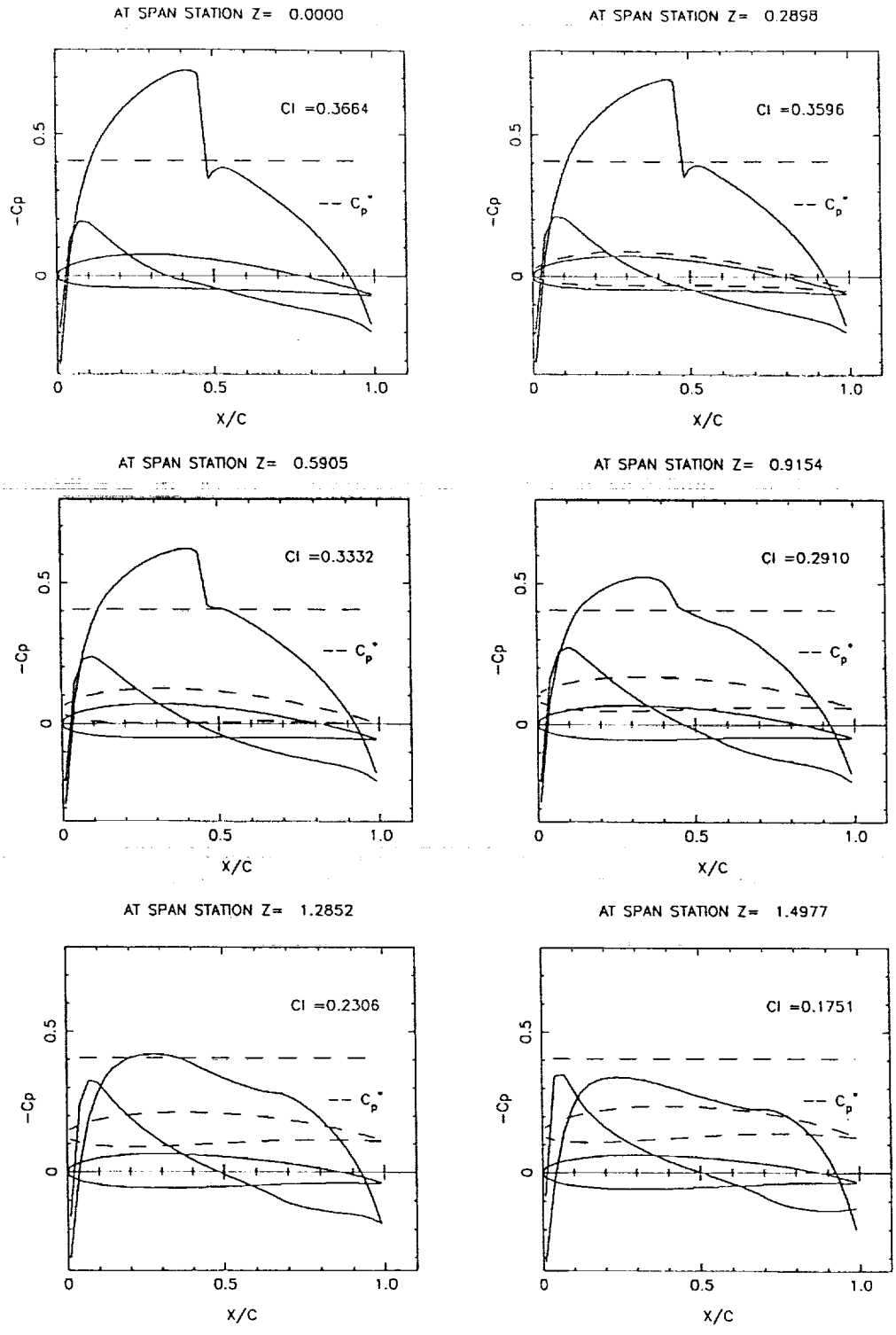

Fig. 5 Pressure Coefficient Distribution.

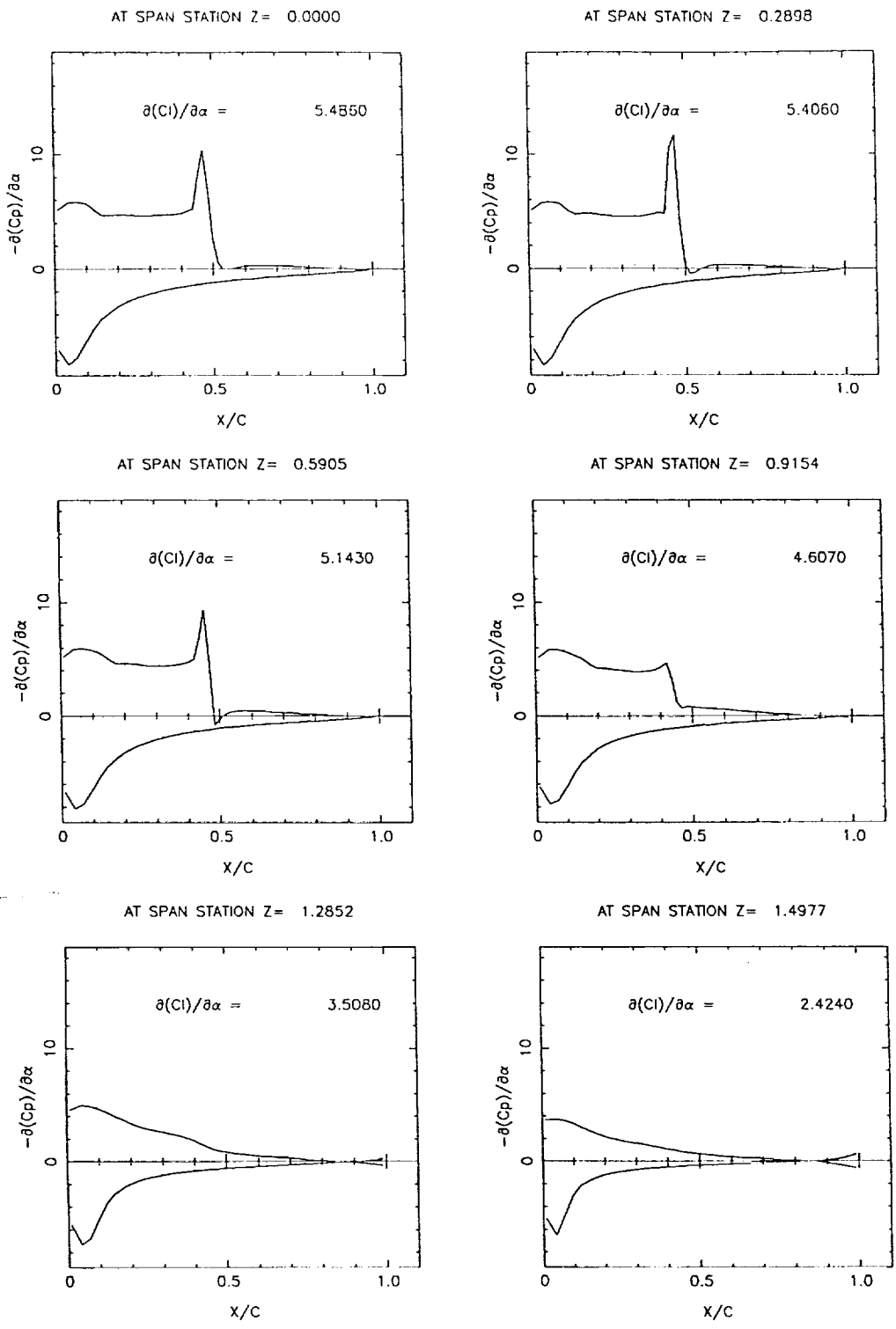

Fig. 6 Pressure Coefficient Sensitivity to the Angle of Attack.

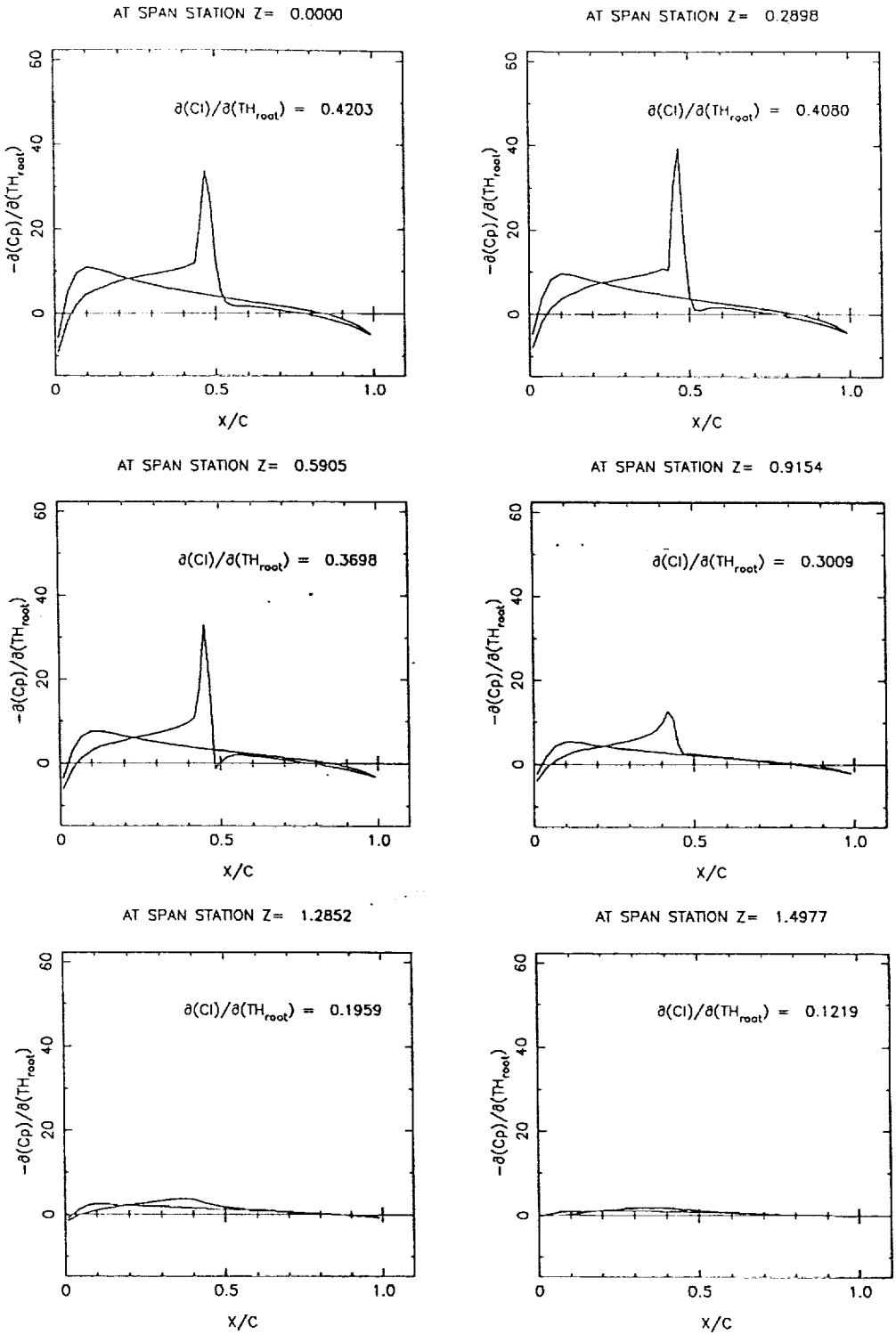

Fig. 7 Pressure Coefficient Sensitivity to the Root Thickness.

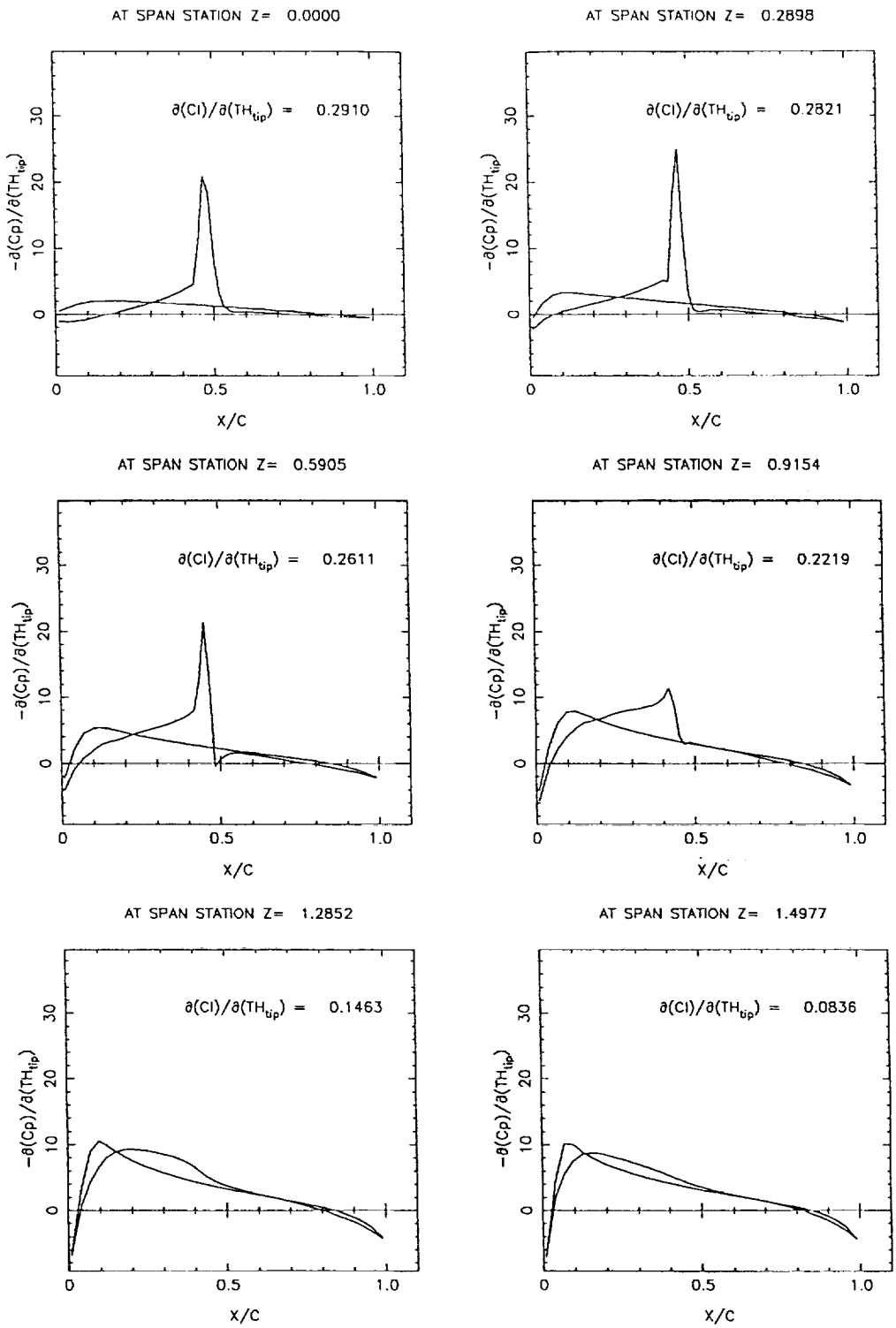

Fig. 8 Pressure Coefficient Sensitivity to the Tip Thickness.

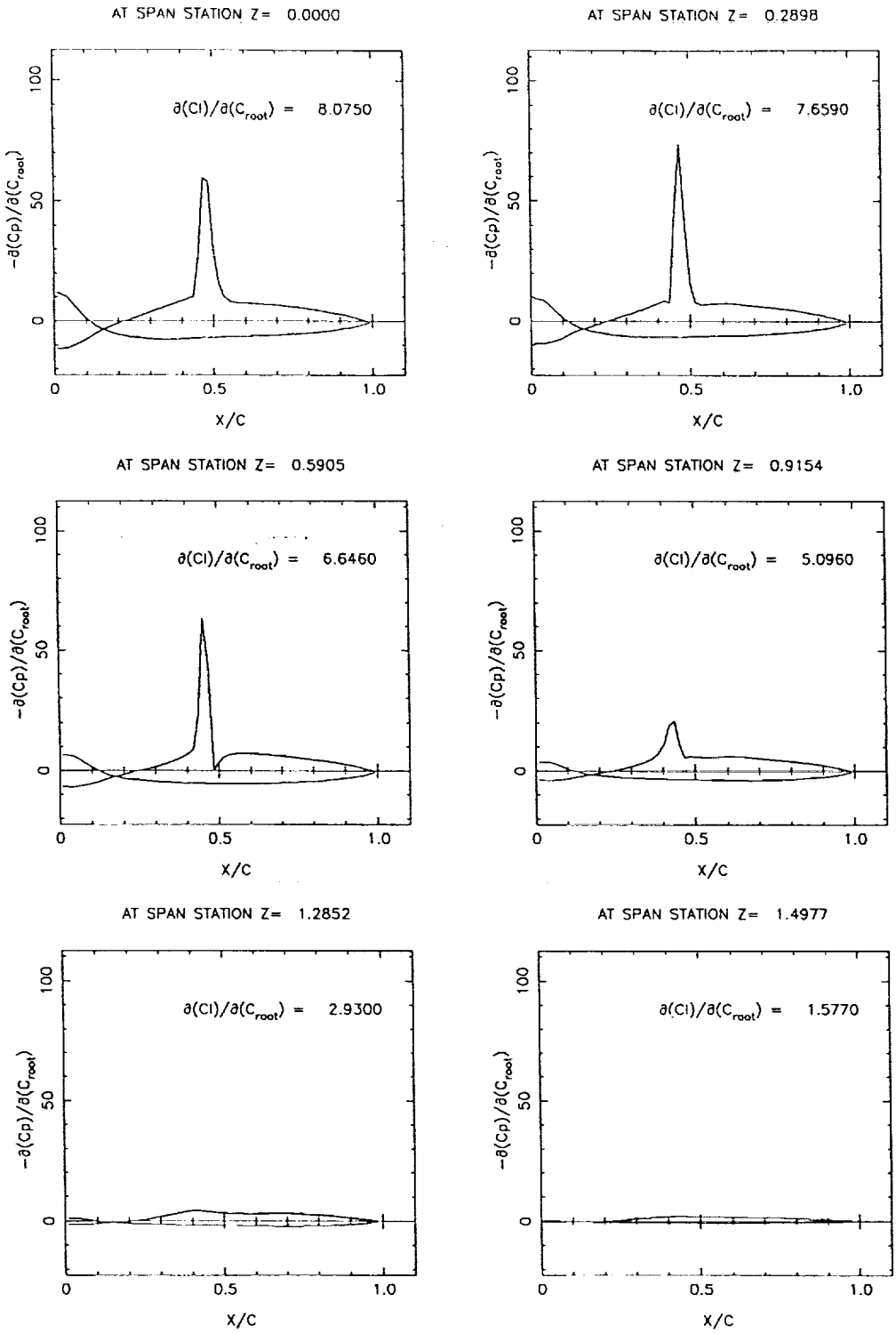

Fig. 9. Pressure Coefficient Sensitivity to the Root Maximum Camber.

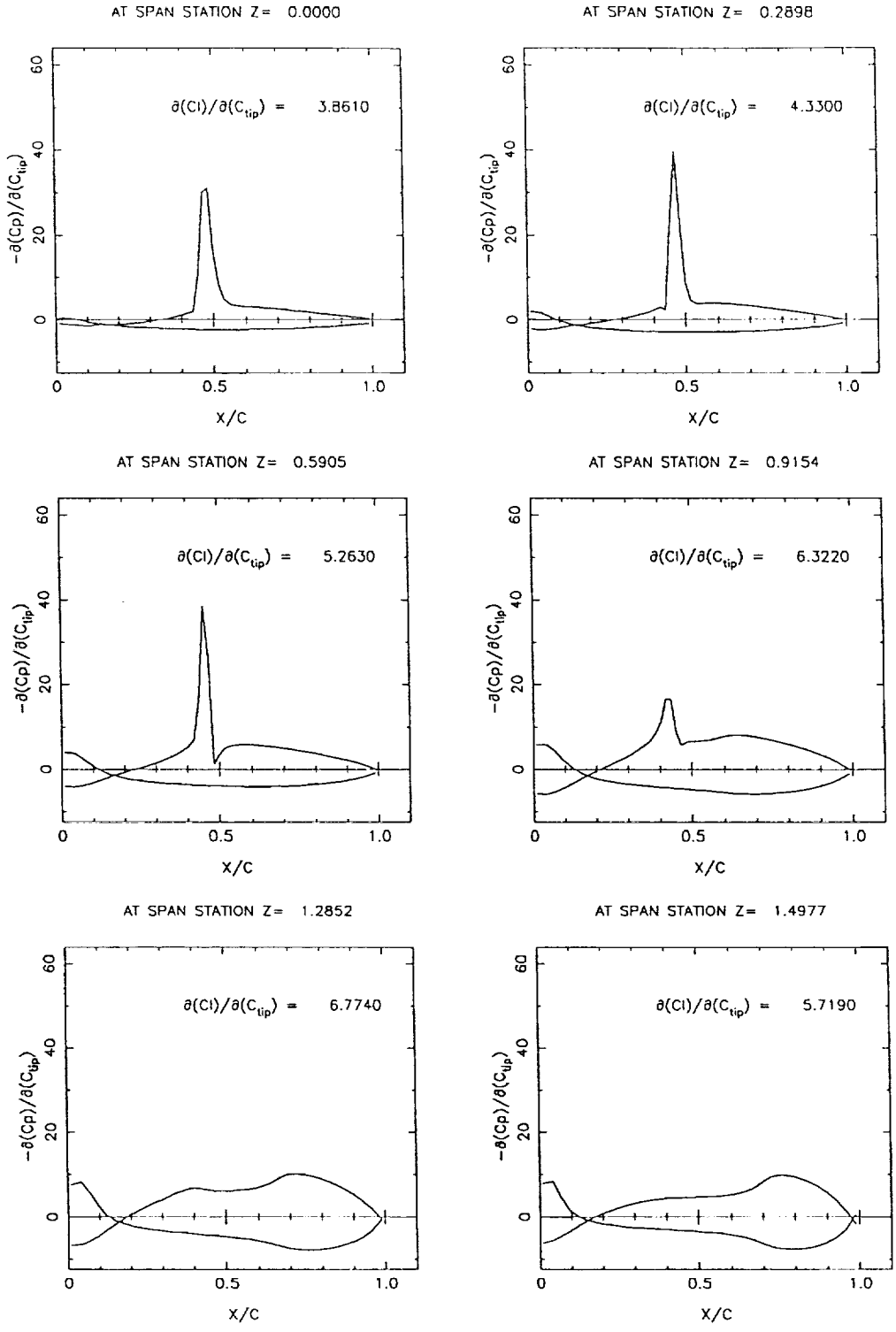

Fig. 10 Pressure Coefficient Sensitivity to the Tip Maximum Camber.

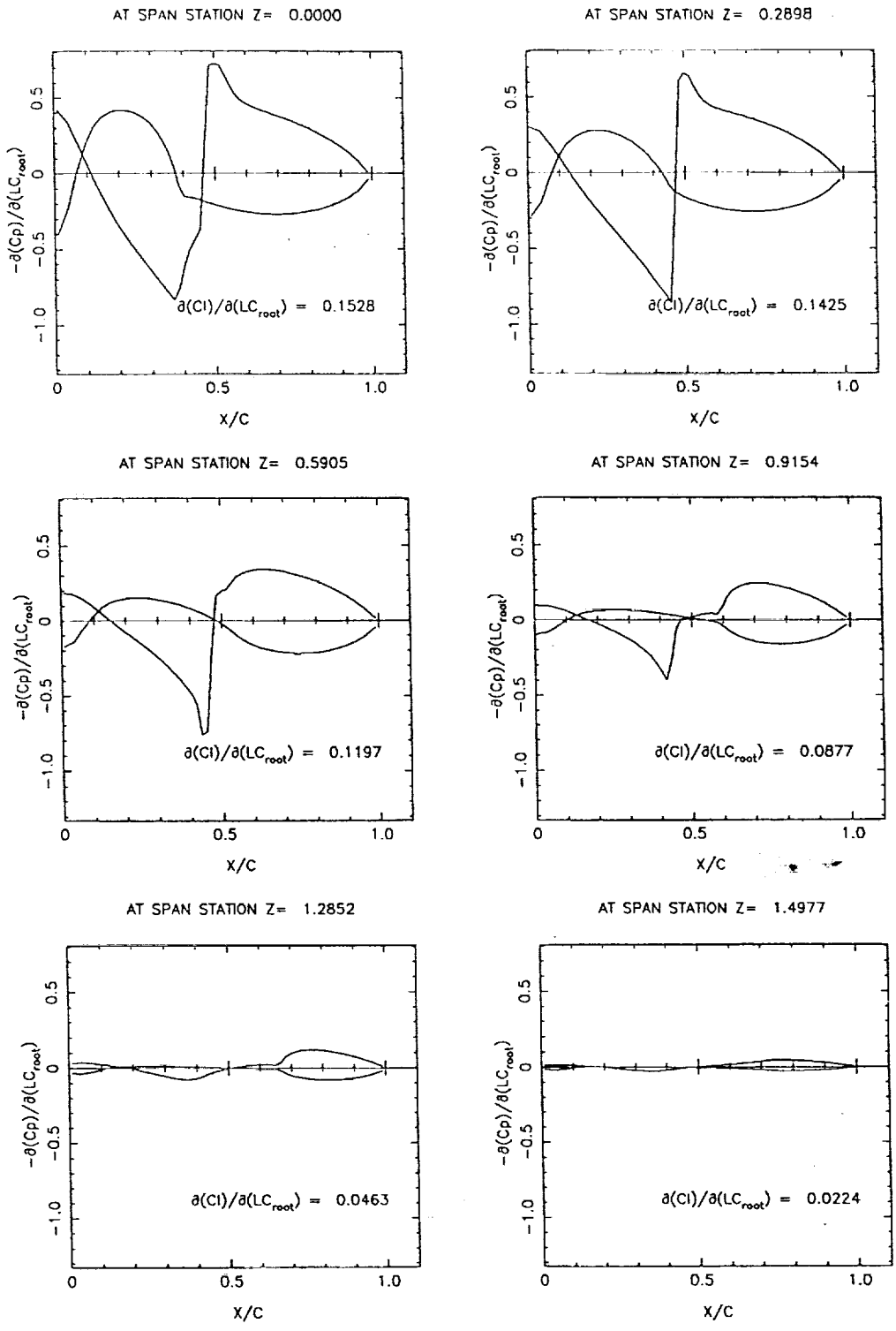

Fig. 11 Pressure Coefficient Sensitivity to LC_{root}.

C-2

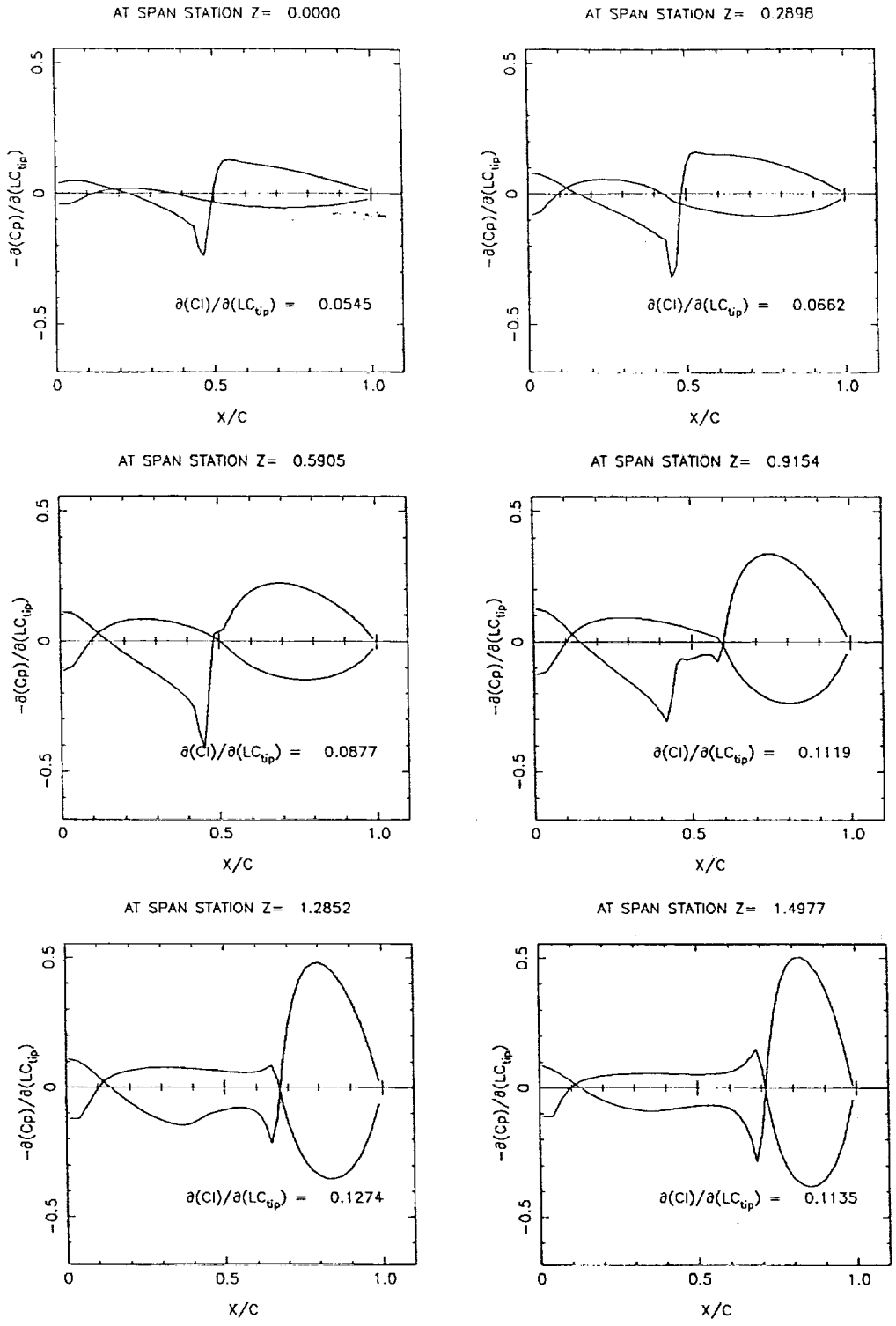

Fig. 12 Pressure Coefficient Sensitivity to LC_{tip}.

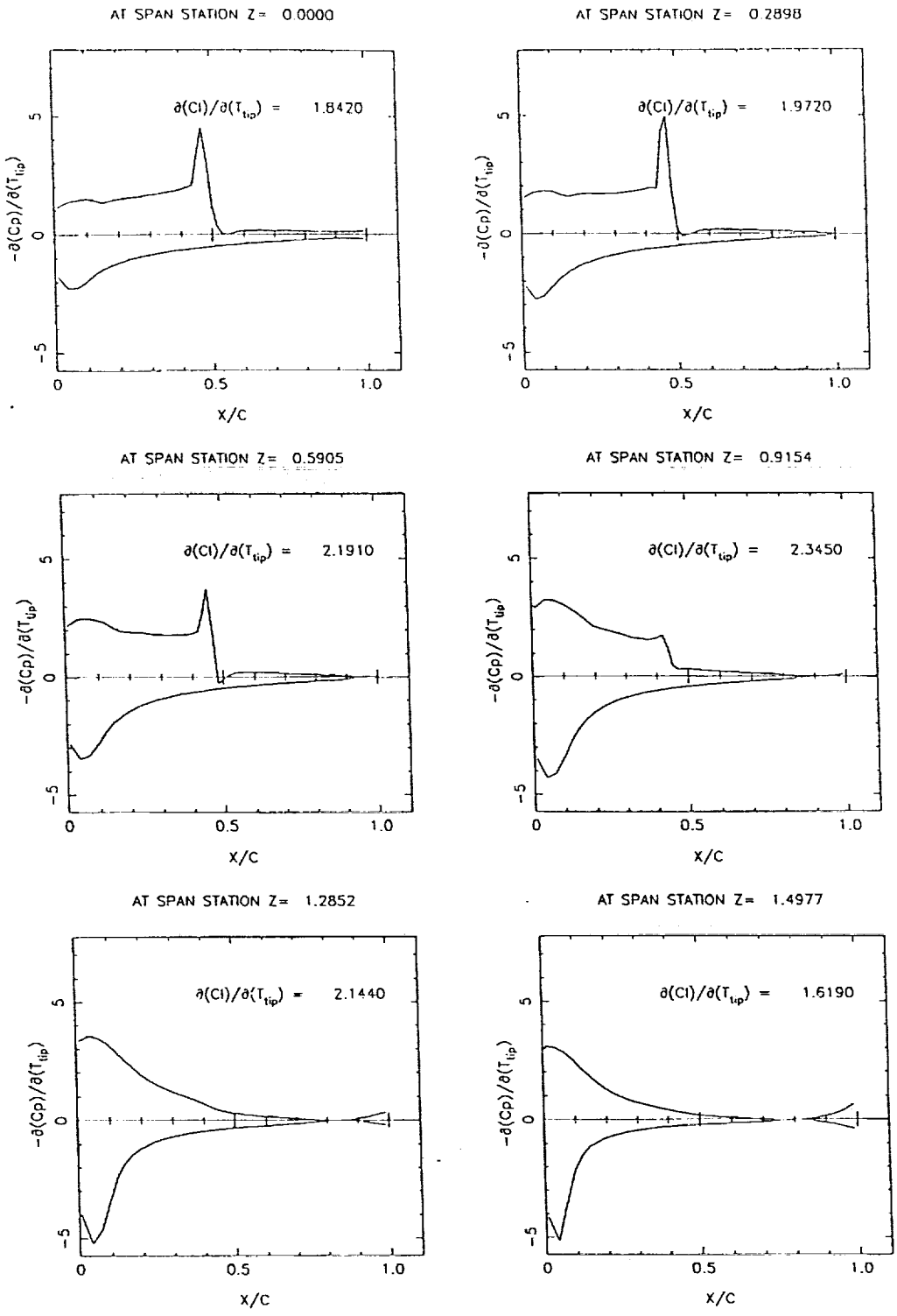

Fig. 13 Pressure Coefficient Sensitivity to the Twist at the Tip.

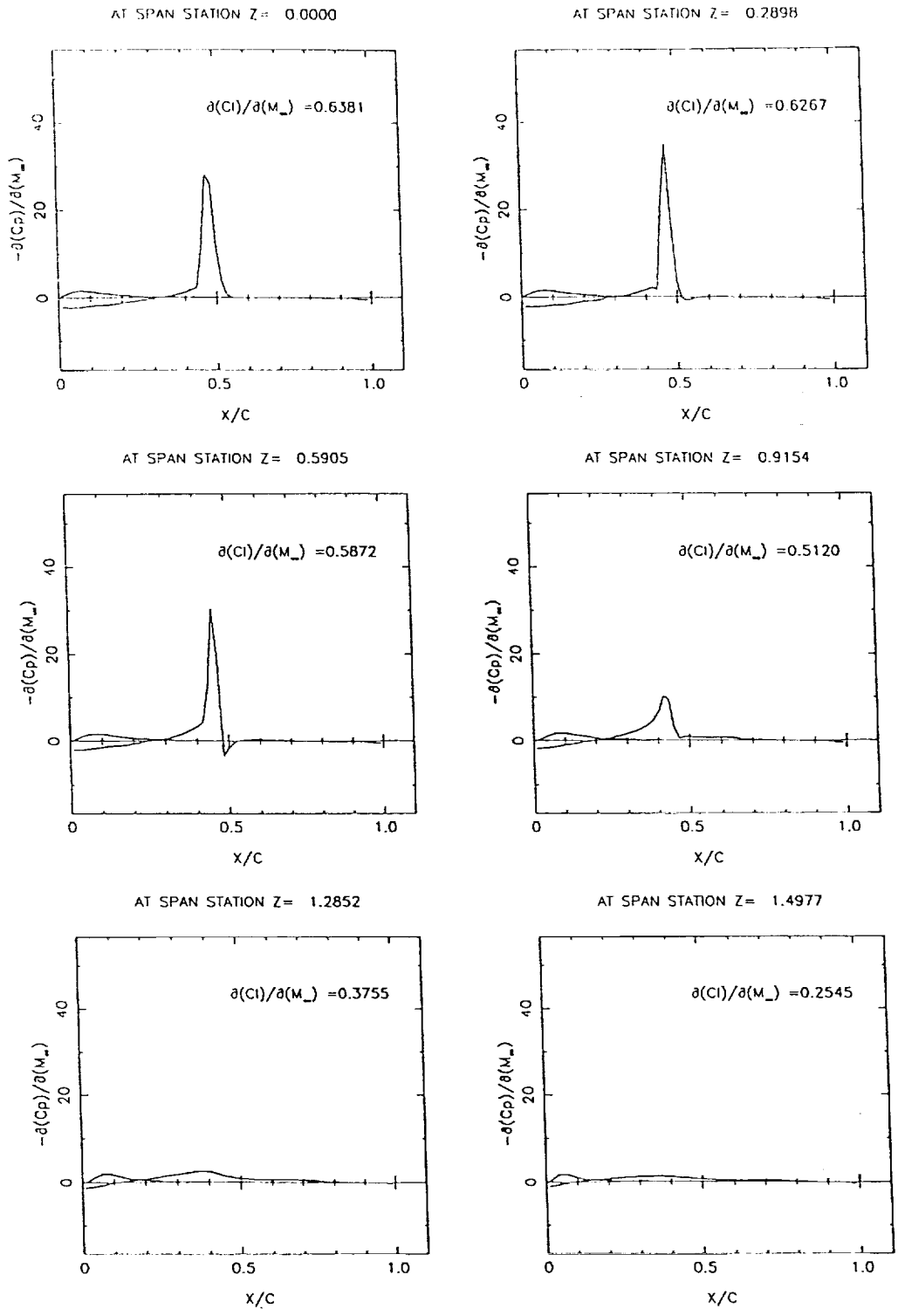

Fig. 14 Pressure Coefficient Sensitivity to the Mach Number.

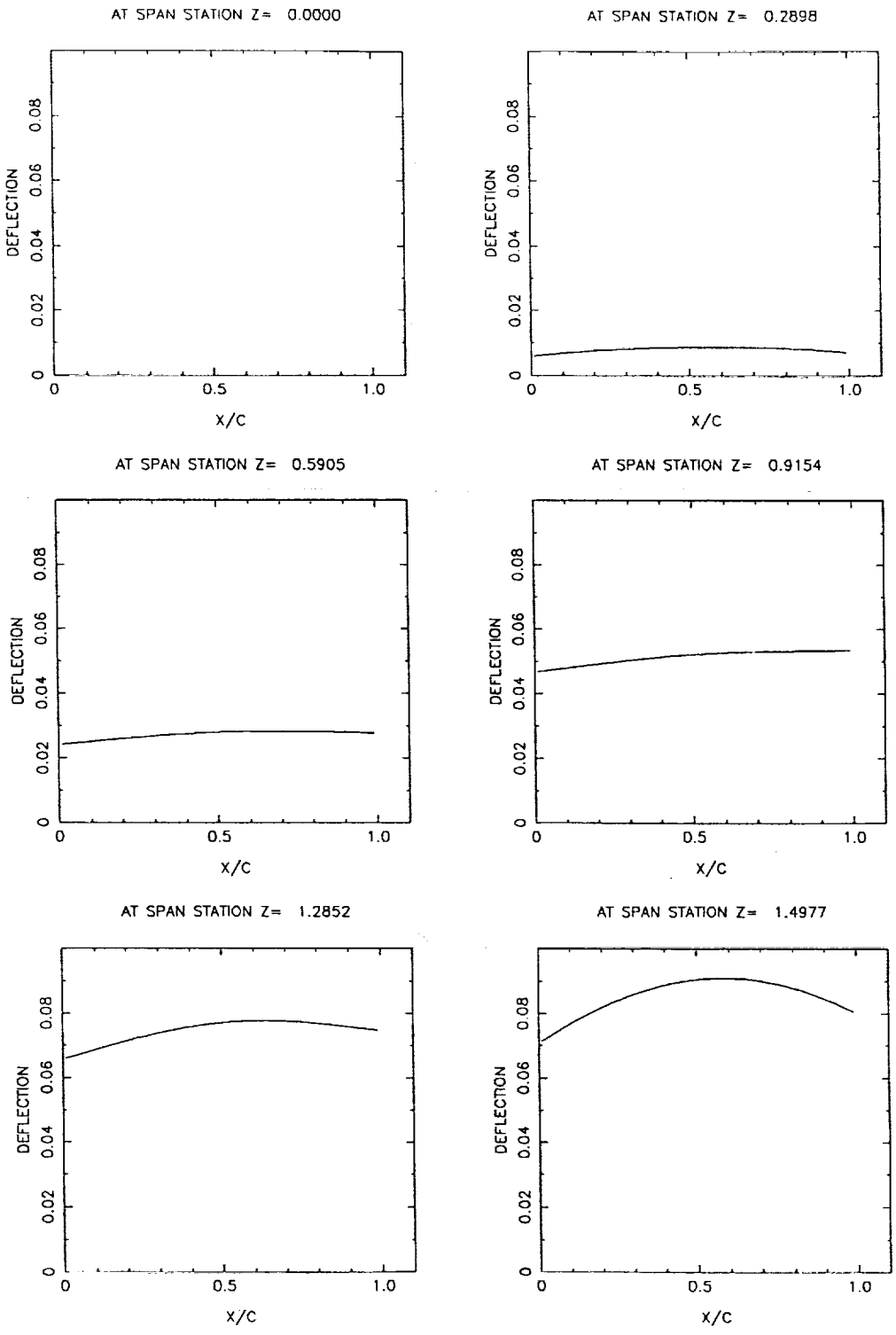

Fig. 15 Structural Deflections of the Modeling Plate.

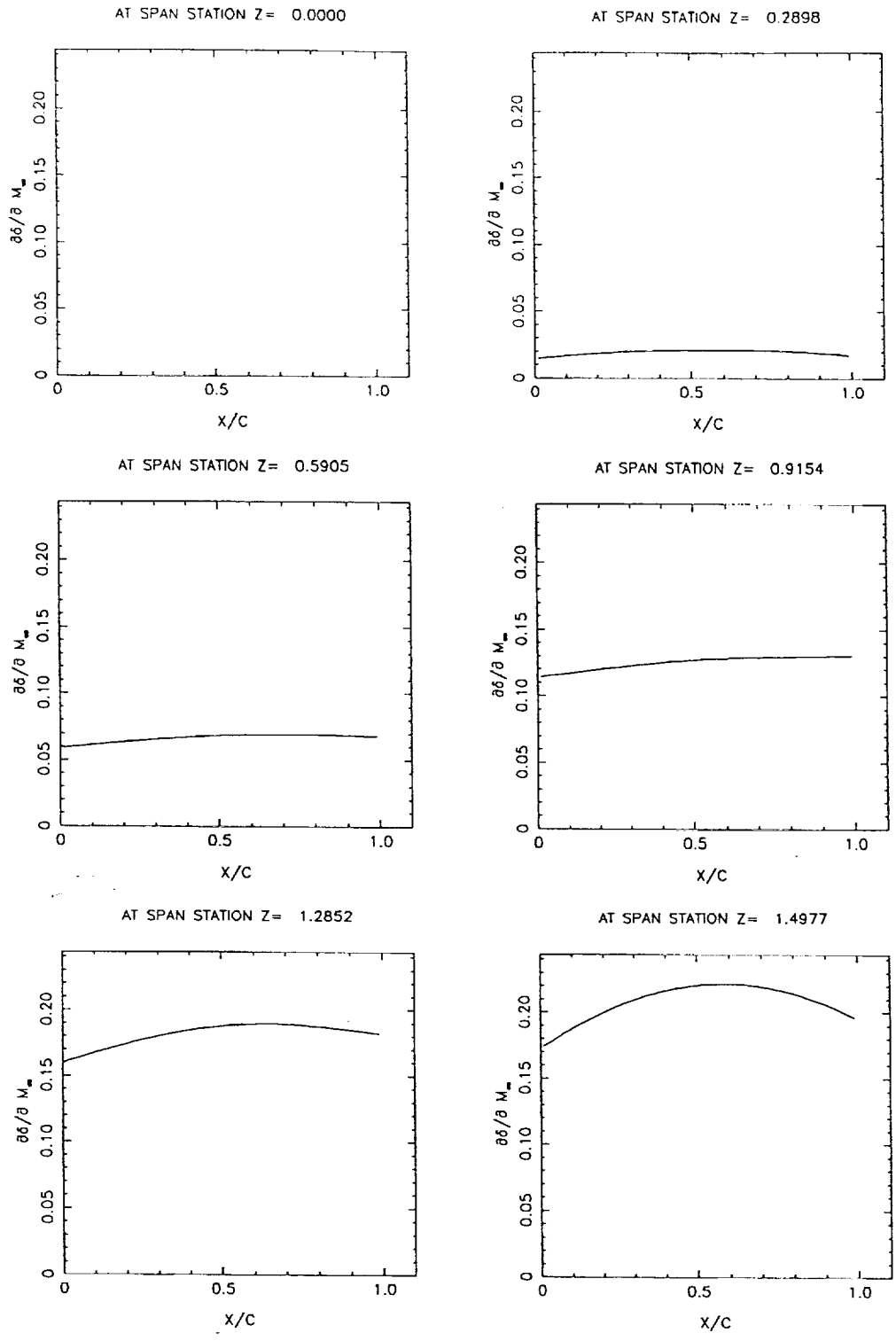

Fig. 16 Structural Deflections Sensitivities With Respect to the Mach Number.

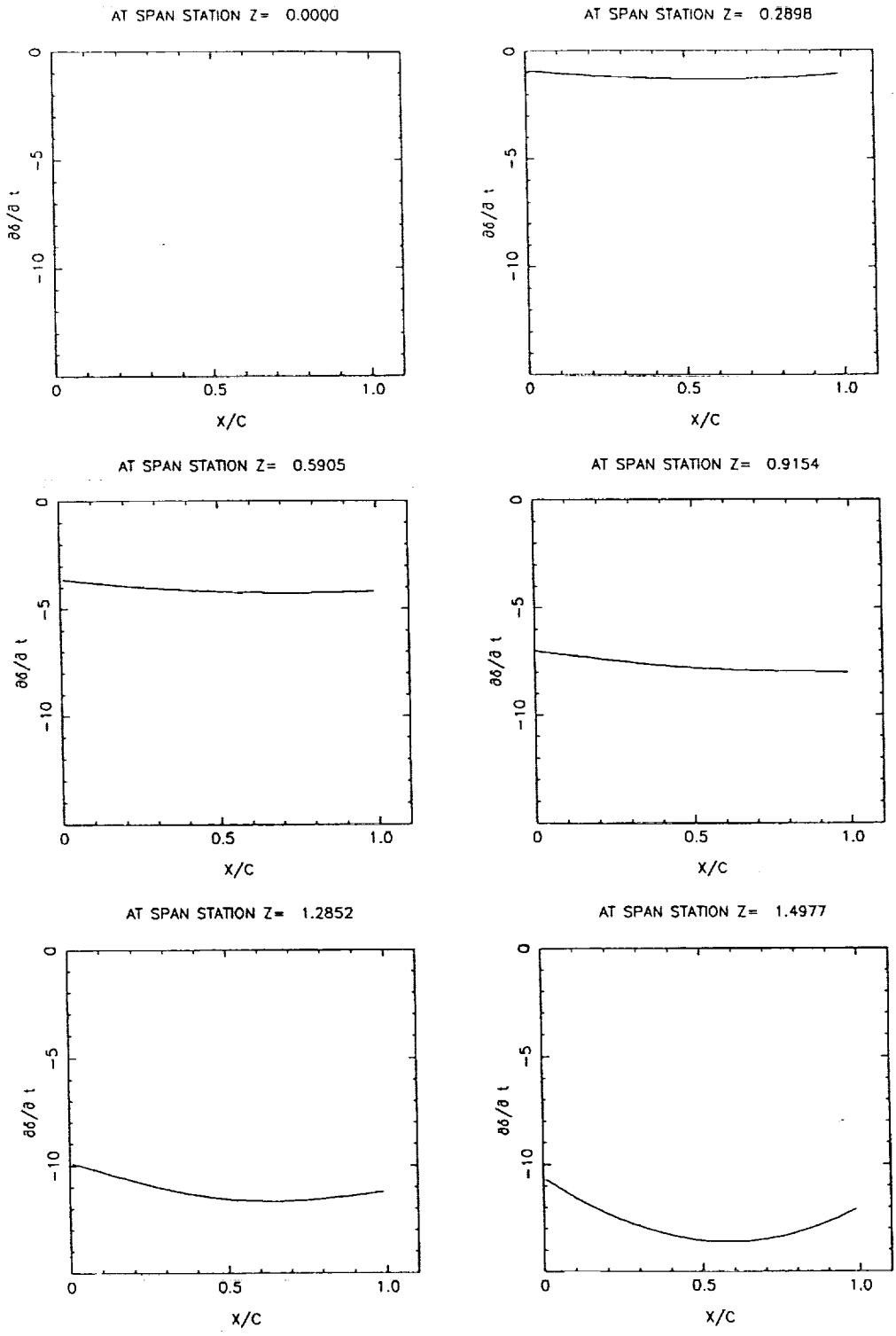

Fig. 17 Structural Deflections Sensitivities With Respect to Plate Thickness.

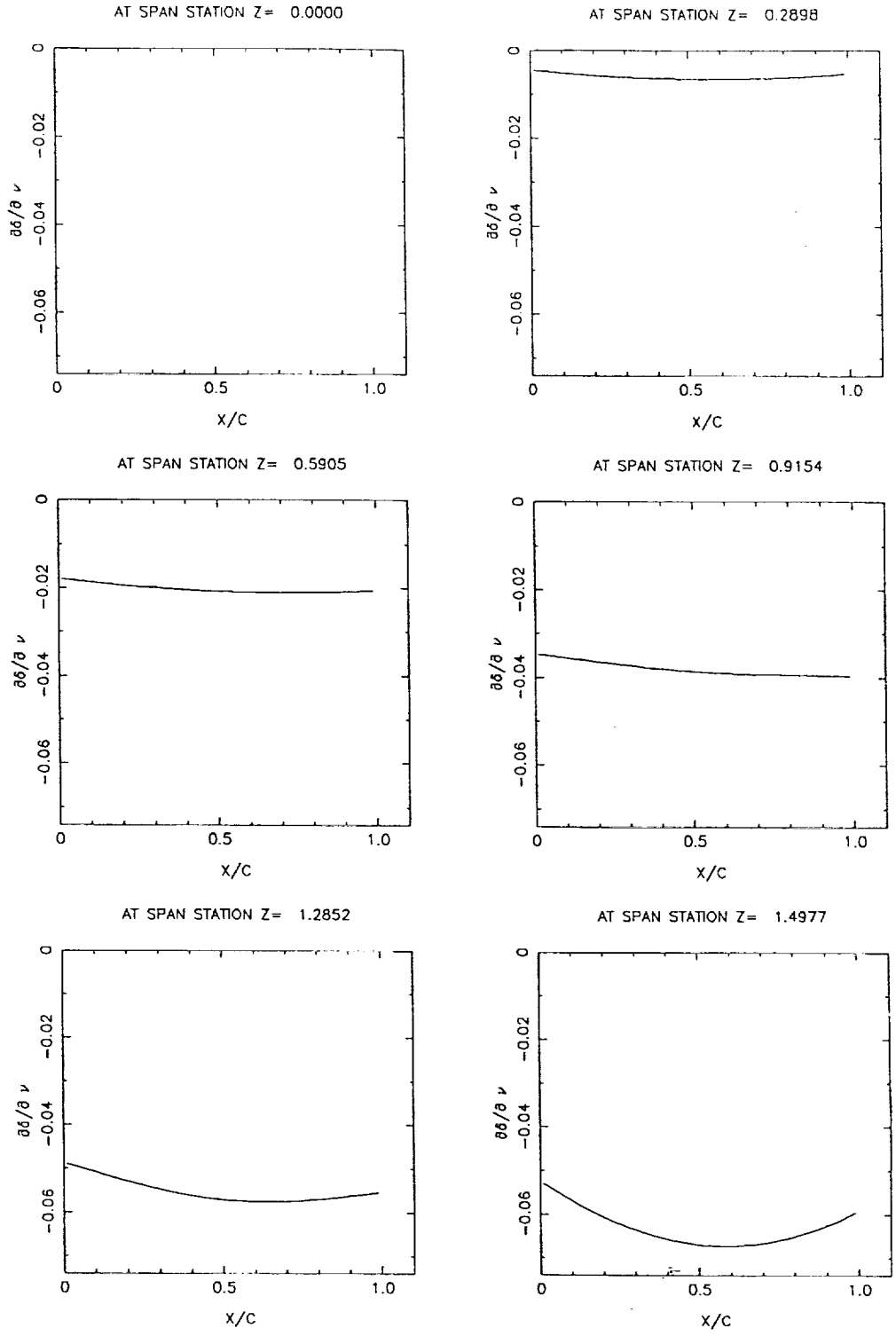

Fig. 18 Structural Deflections Sensitivities With Respect to Poisson's Ratio.

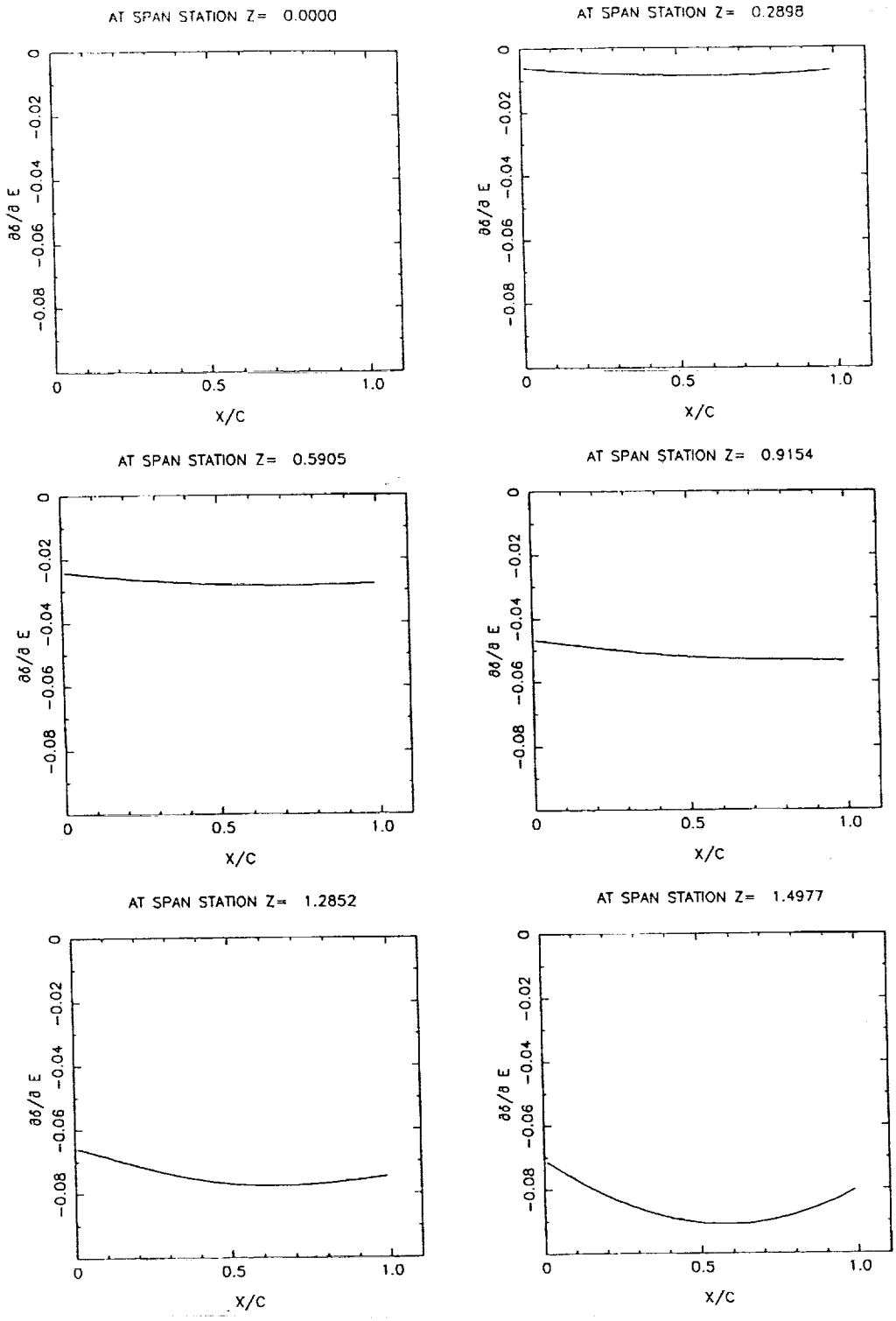

Fig. 19 Structural Deflections Sensitivities With Respect to Young's Modulus.

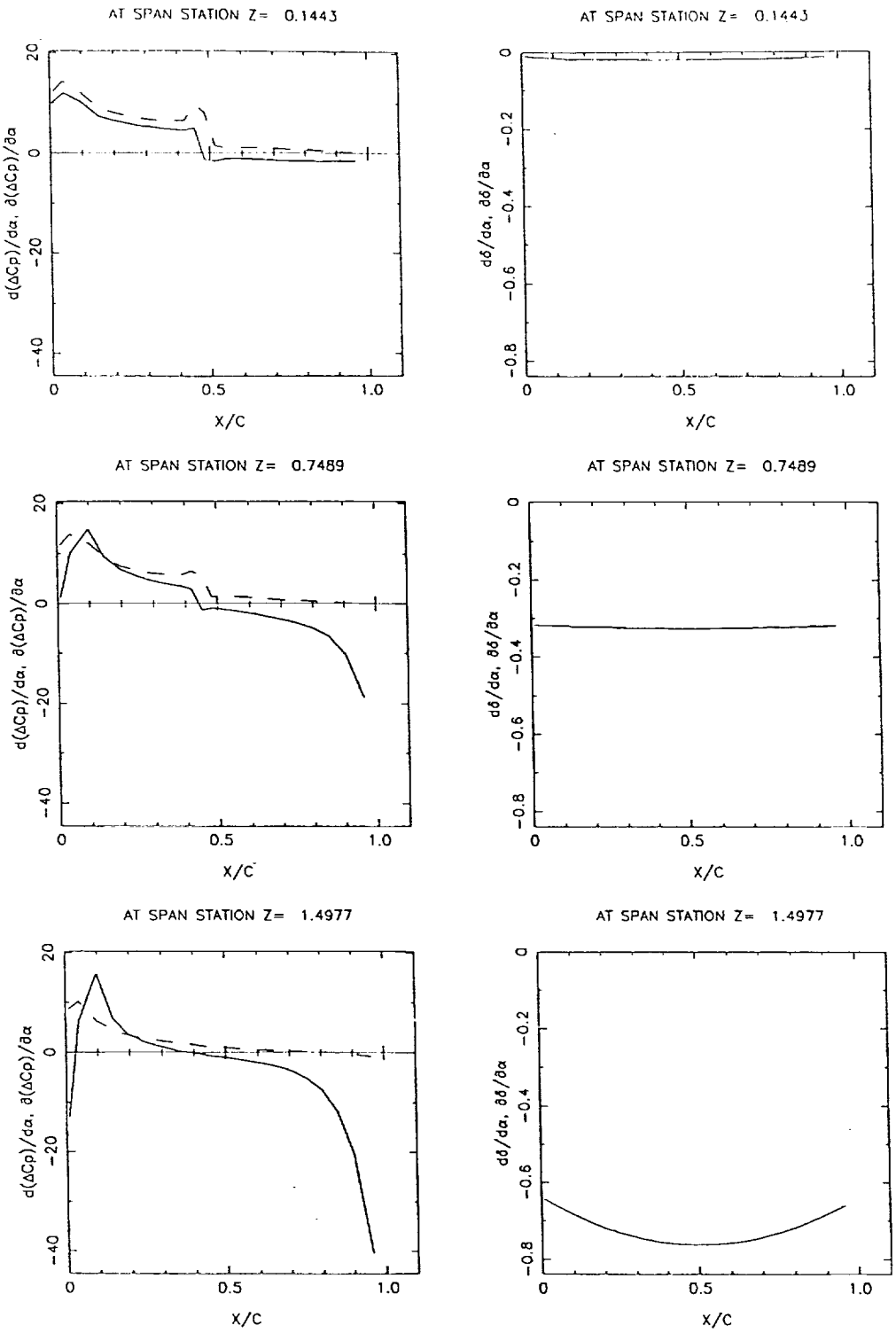

Fig. 20 System Sensitivities to the Angle of Attack.

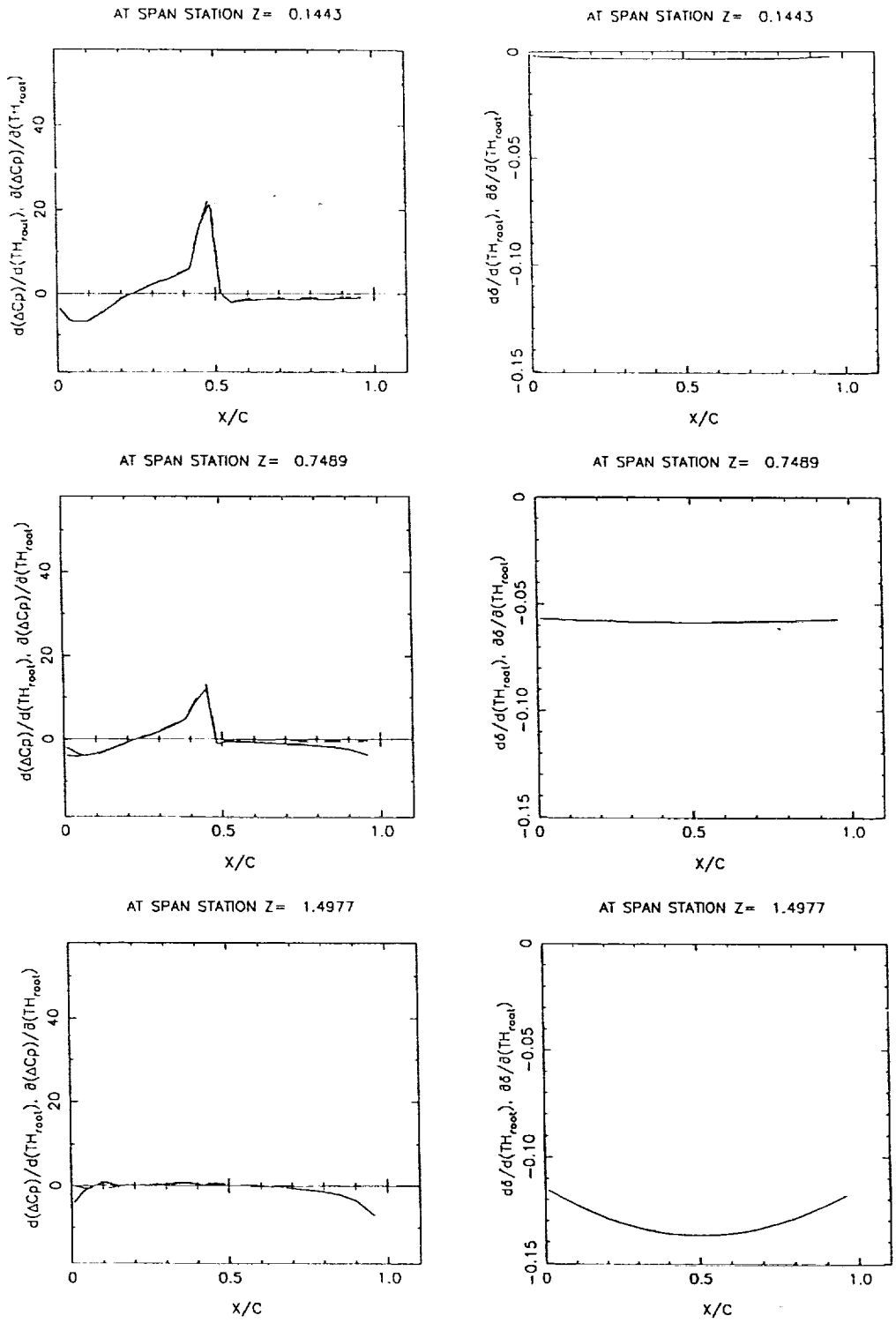

Fig. 21 System Sensitivity Results for the Root Thickness.

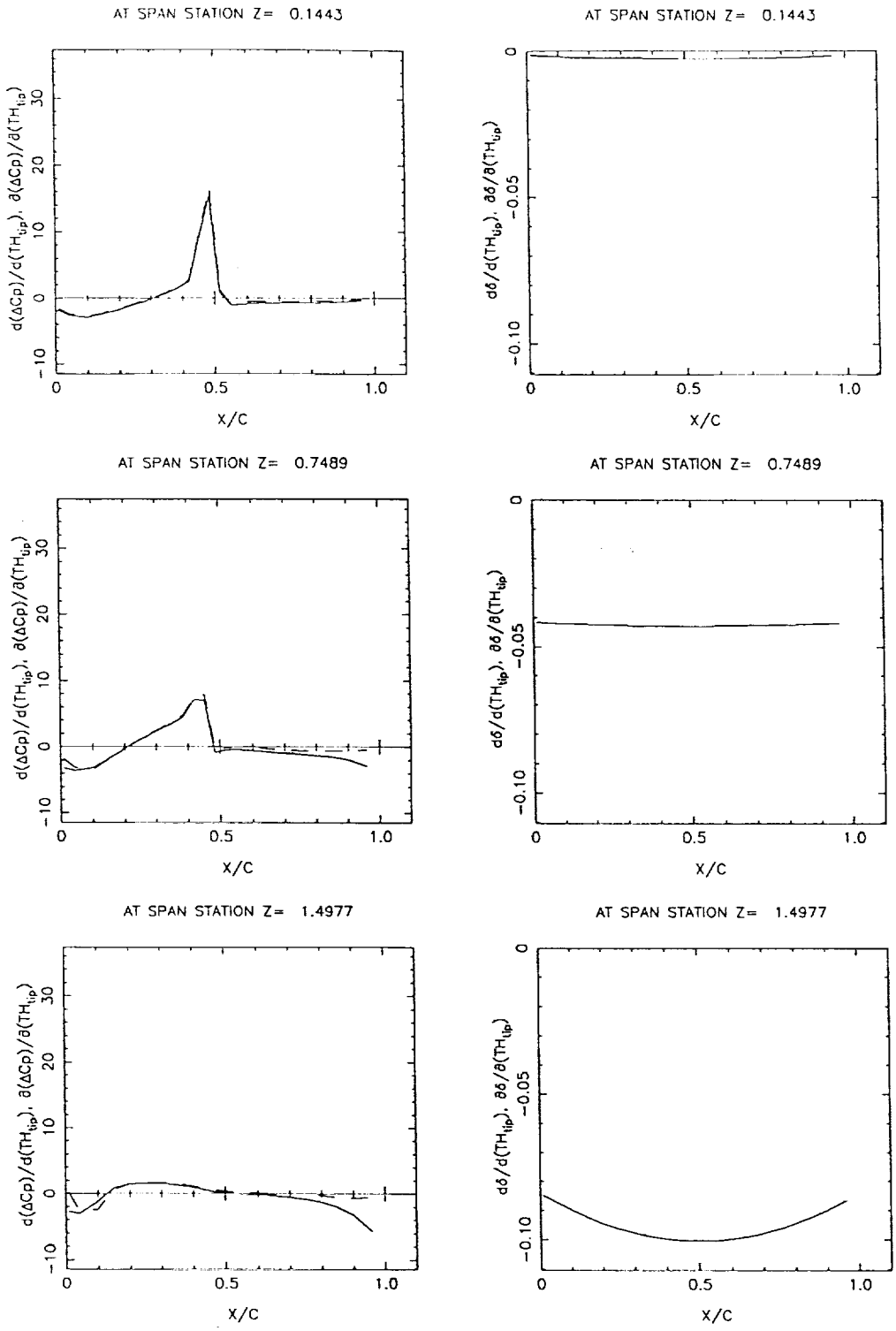

Fig. 22 System Sensitivity Results for the Tip Thickness.

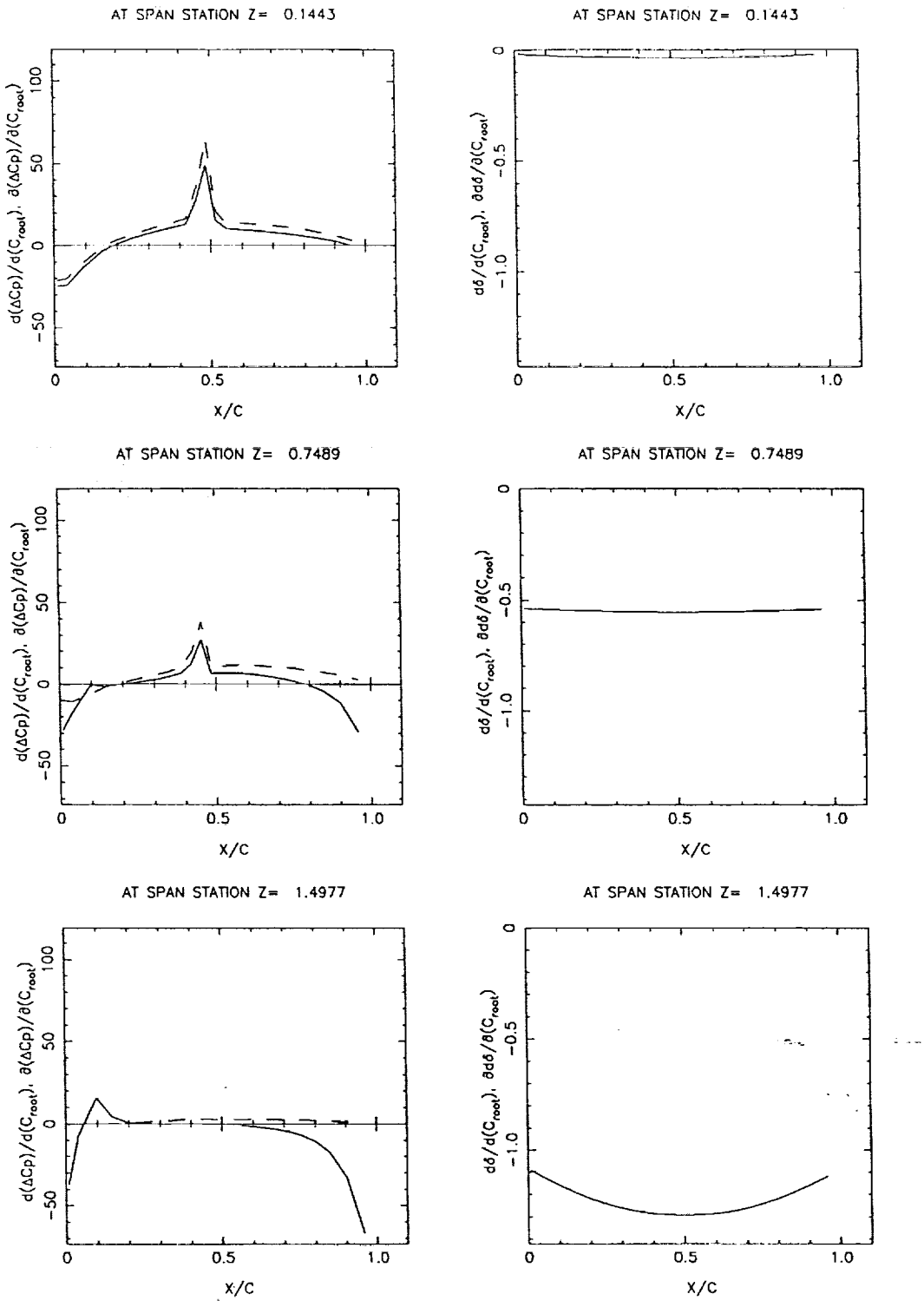

Fig. 23 System Sensitivity Results for the Root Camber.

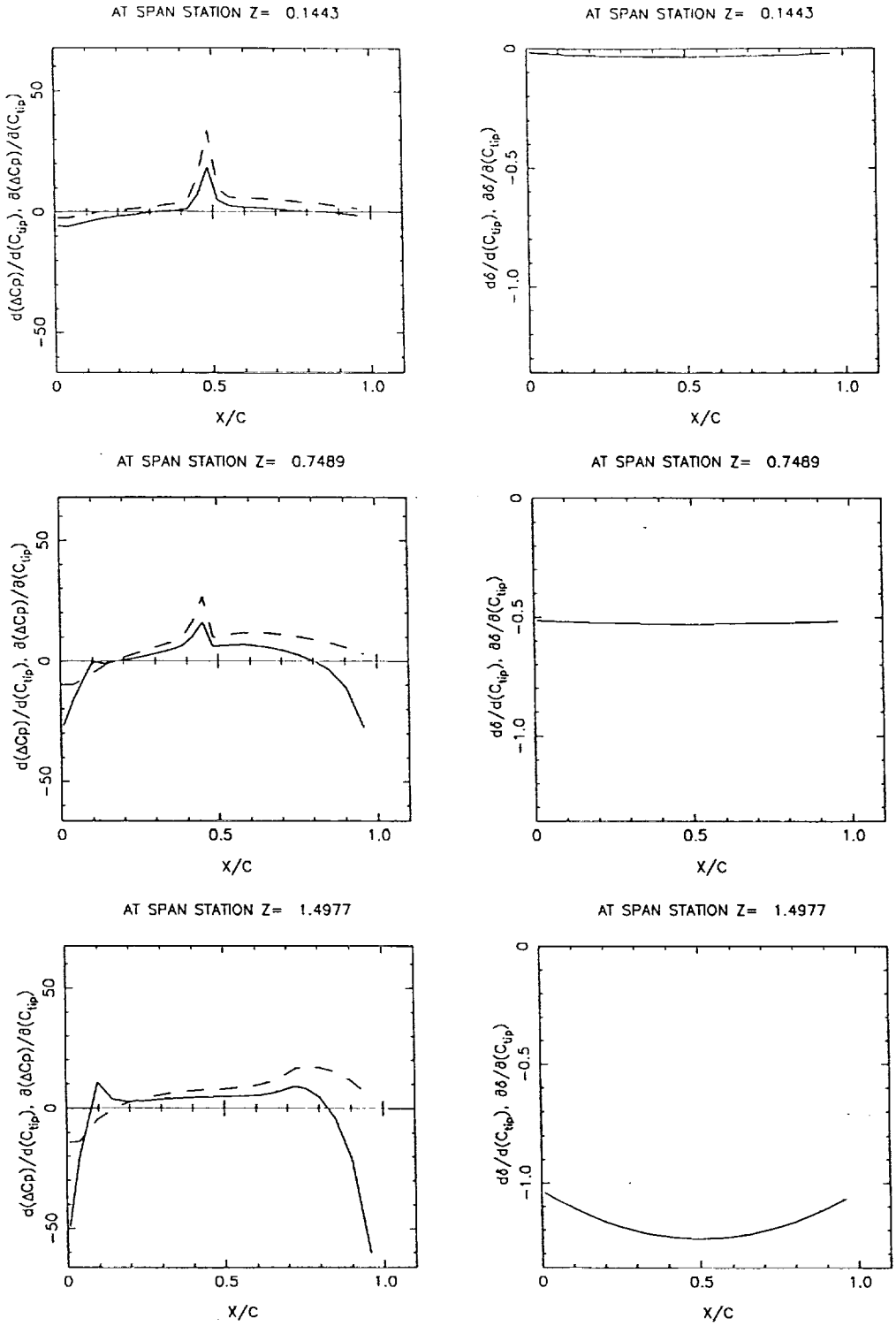

Fig. 24 System Sensitivity Results for the Tip Camber.

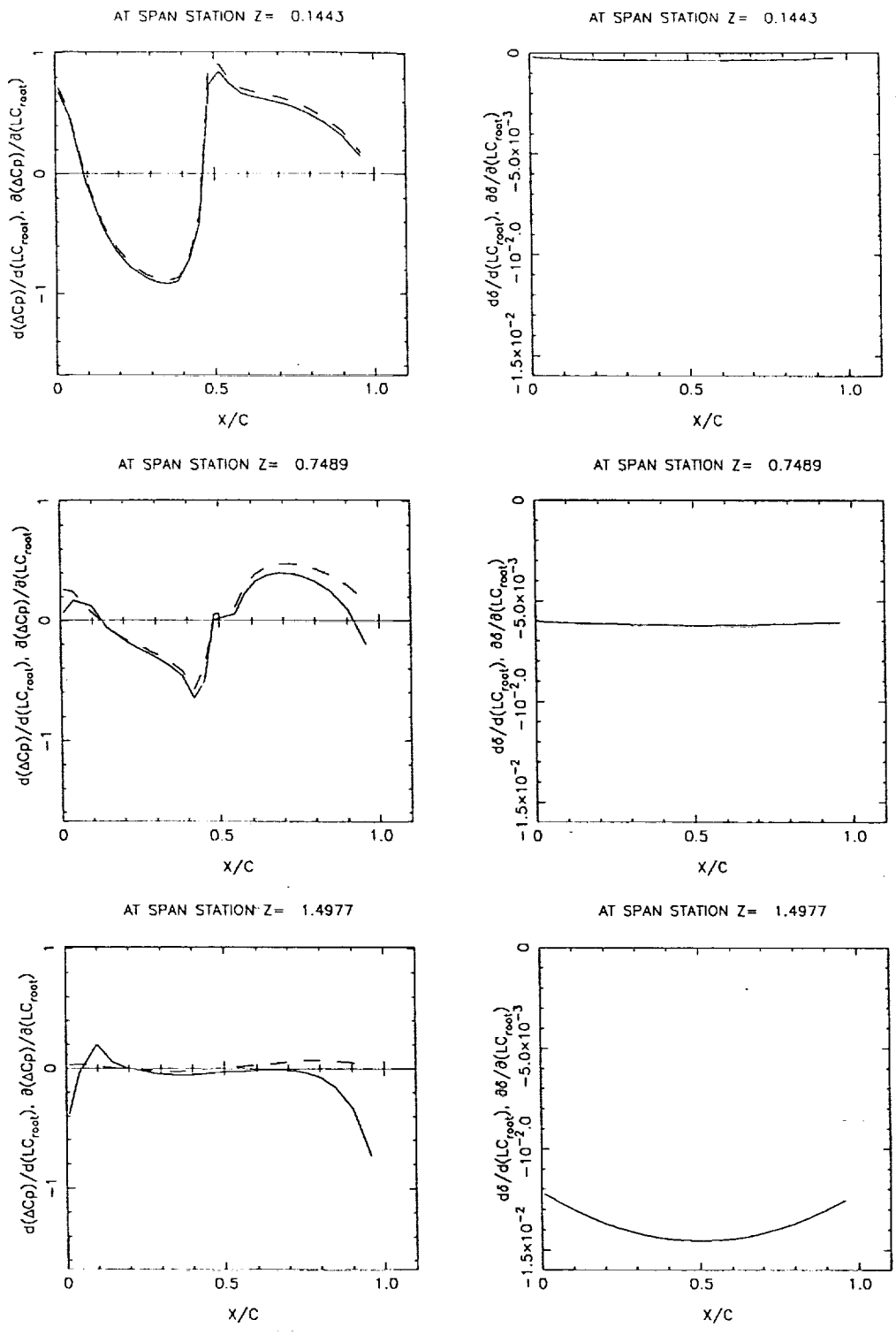

Fig. 25 Results for System Sensitivity to LC_{root}

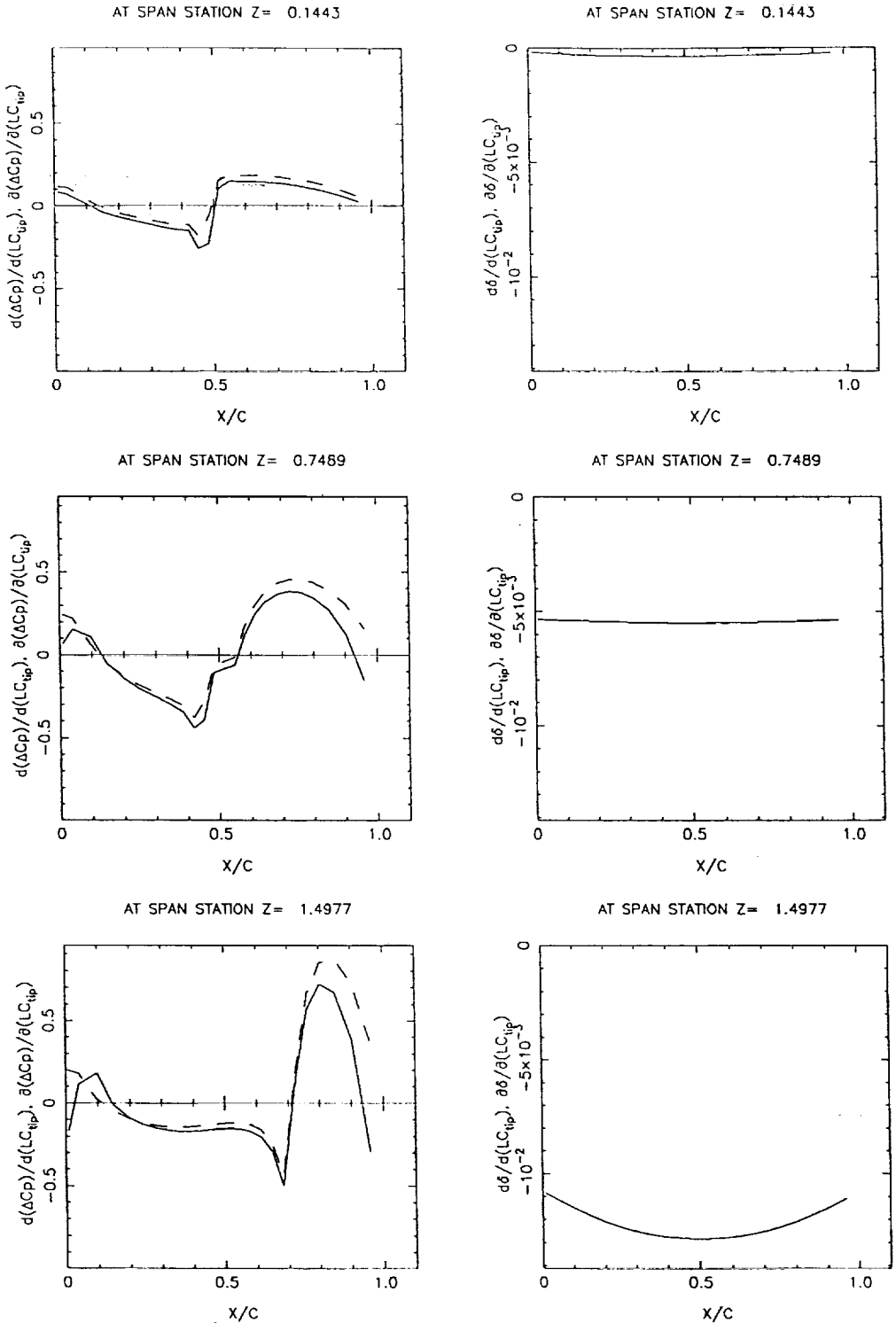

Fig. 26 Results for System Sensitivity to LC_{tip}.

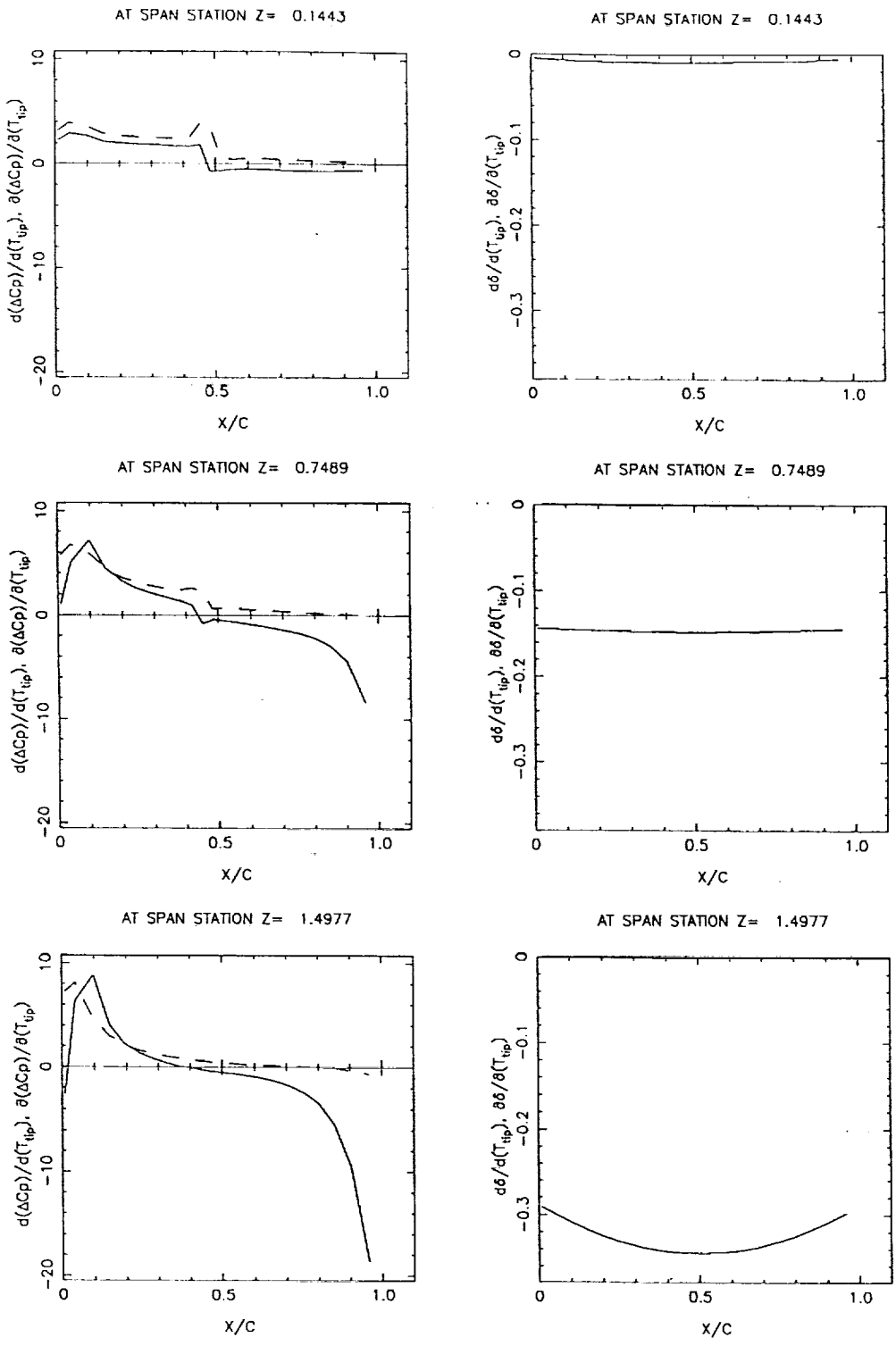

Fig. 27 System Sensitivity Results for the Tip Twist.

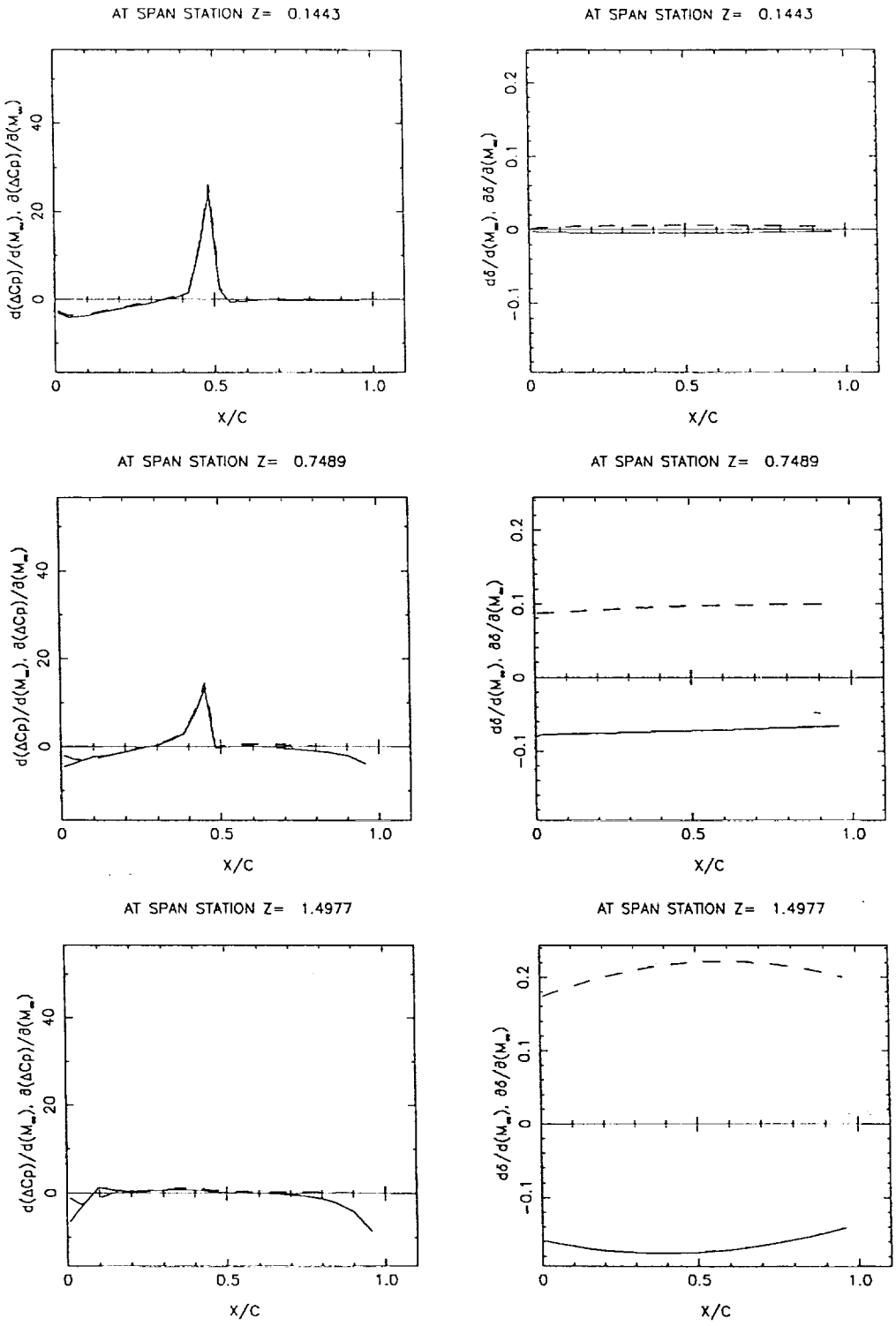

Fig. 28 System Sensitivity Results for the Mach Number.

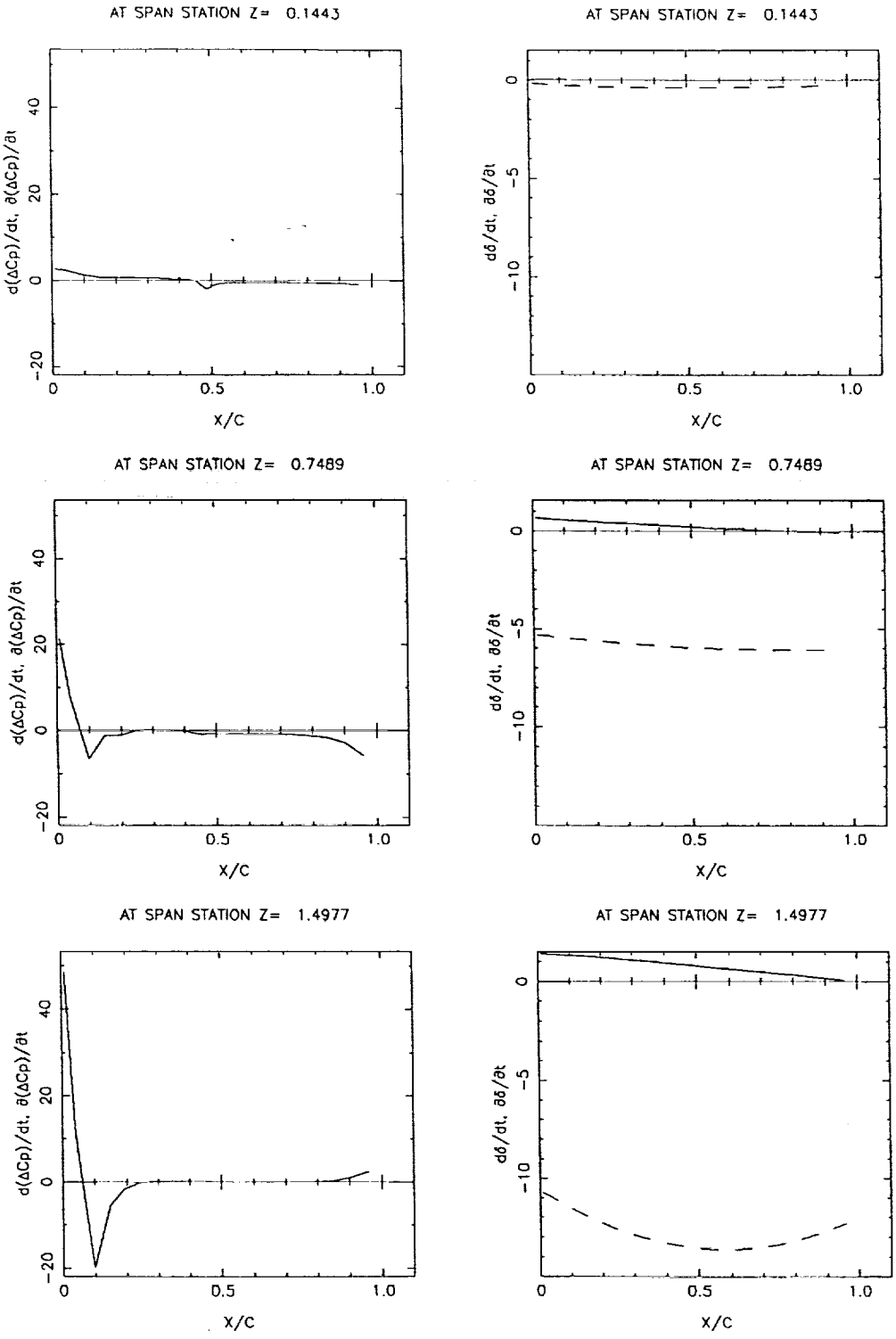

Fig. 29 System Sensitivity Results for the Plate Thickness.

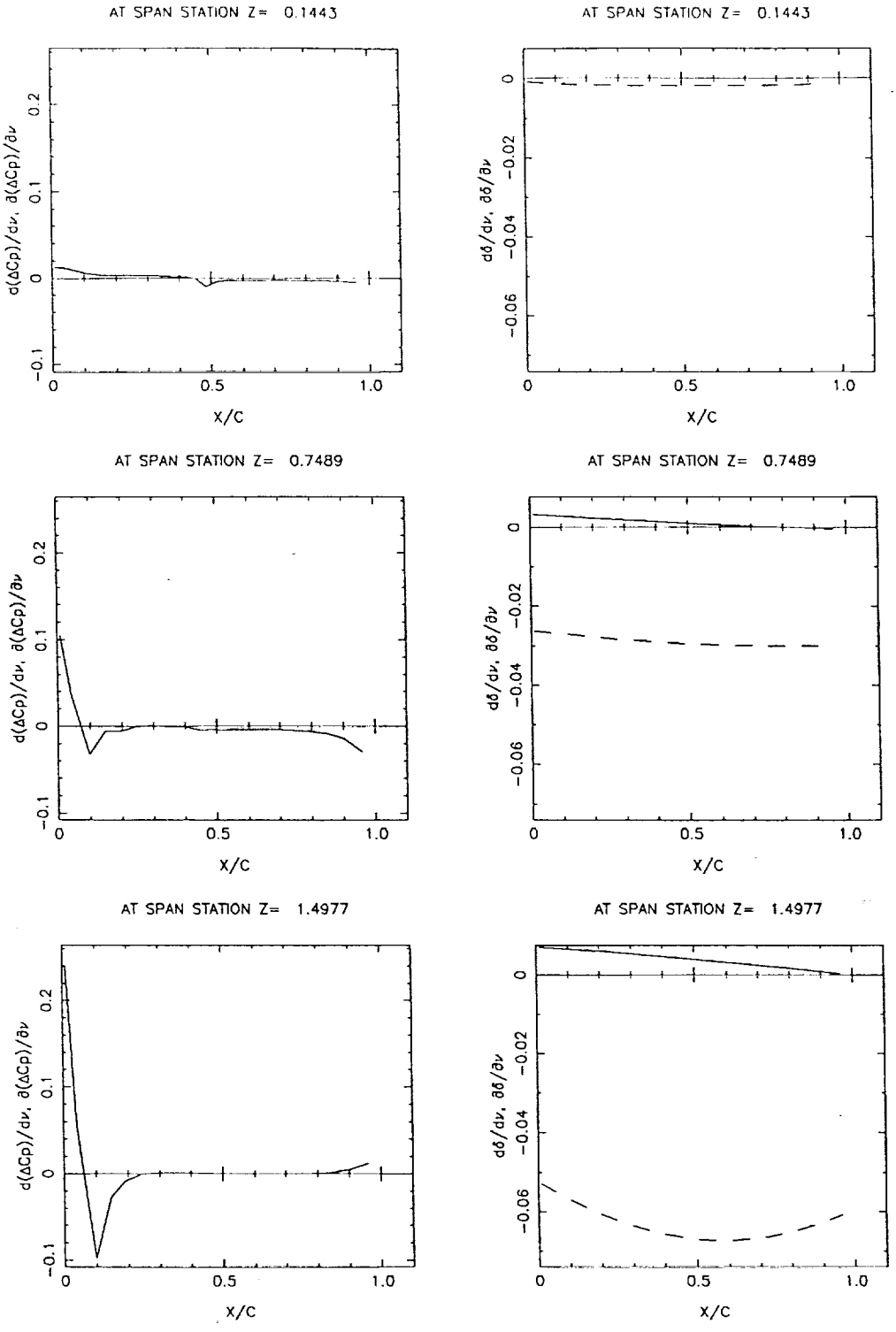

Fig. 30 System Sensitivity Results for the Poisson Ratio.

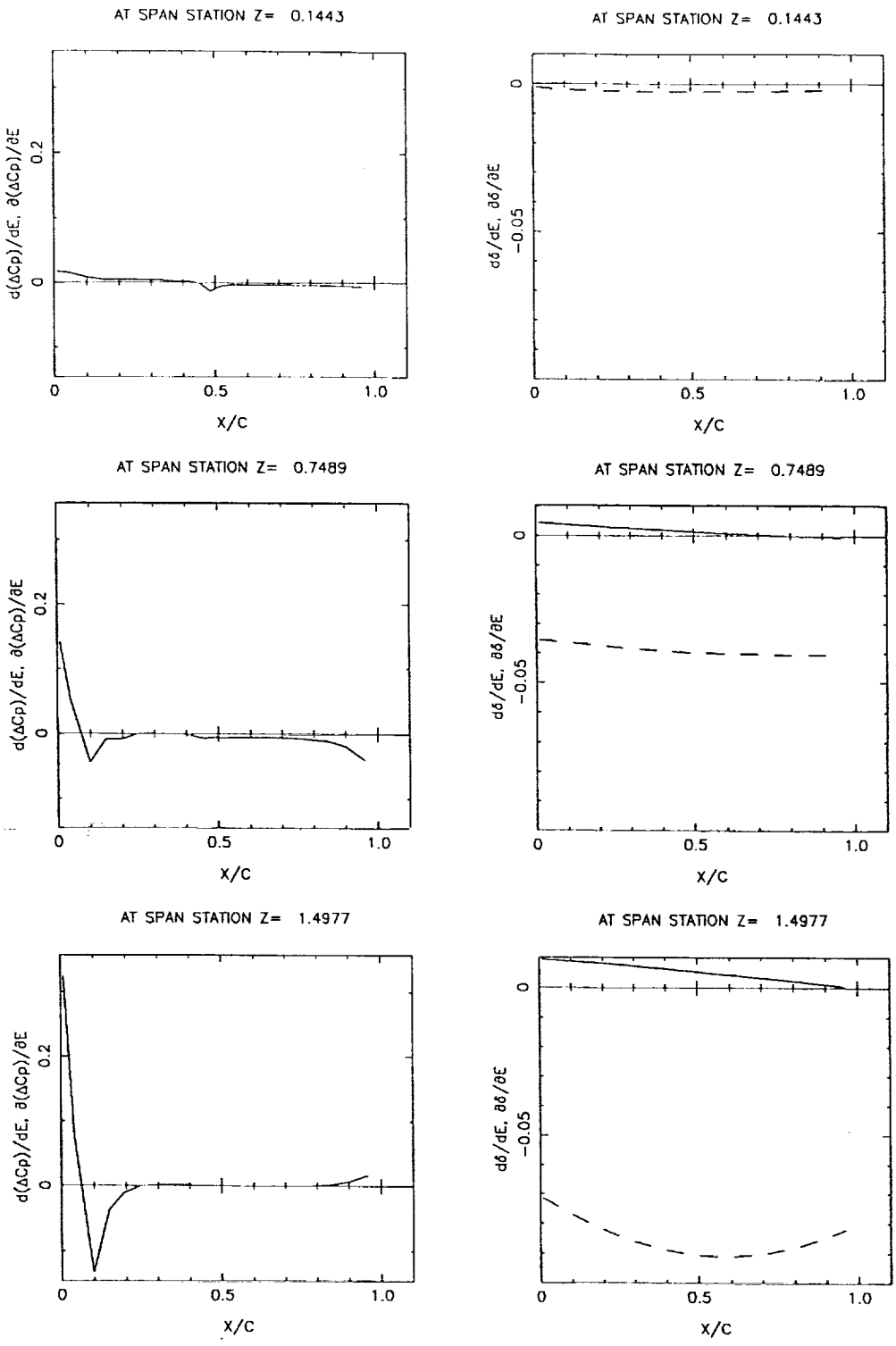

Fig. 31 System Sensitivity Results for Young's Modulus.

Summary

The system sensitivity analysis shows that the deflections at the tip as well as the loads are going to decrease with an increase in α. Likewise, an increase in the values of TH_{root} , TH_{tip}, C_{root}, C_{tip}, LC_{root}, LC_{tip}, T_{tip}, and M_{∞} will cause an unloading of the tip associated with a decrease in the deflections. Further, the structural variables t, ν, and E will cause an increase in the tip loading as well as the associated deflections. The structurally induced camber is essential to the interpretation of these a priori unexpected results.

CONCLUSION

Based on the results presented, the use of the incremental-iterative technique through the semi-implicit ZEBRA scheme to calculate the sensitivity derivatives obtained from the quasi-analytical formulation has proven to be successful and very computationally efficient. A large memory space for the storage of the sensitivity matrix is not needed anymore and the sensitivity derivatives can be calculated at the same time as the flowfield instead of using a converged flowfield solution as an input to a sparse matrix solver.[6]

The saved computational resources can thus be used for finer grids, more design variables, and additional disciplines. Hence, a coupling of the aerodynamic solver with a structural one and its sensitivities has been undertaken. This static aeroelastic coupling is very efficient since the structural calculation and resultant structural sensitivities and coupling sensitivities are computed at the same time as the flowfield. In addition, the use of finite differencing to solve for the structural deflections improves the efficiency of the scheme since no grid transformation is necessary.

Because the system is multidisciplinary, the calculation of the system sensitivity derivatives takes into account the influence of one discipline on the other. This calculation relies on the "coupling" sensitivity derivatives that are not very easy to obtain computationally since their respective convergence (especially for the deflection with respect to load sensitivity) is slow. Results for the system sensitivities will be discussed in the final paper.

ACKNOWLEDGEMENT

This work was primarily supported by the Aerospace Engineering Department of Texas A&M University. Computer support was also provided by the office of the Associate Provost for Computing.

REFERENCES

[1]Adelman, H. M., and Haftka, R. T., "Sensitivity Analysis and Discrete Structural Systems," *AIAA Journal,* Vol. 24, No. 5, May 1986, pp. 823-832.

[2]Bristow, D.R., and Hawk, J.D., "Subsonic Panel Method for Designing Wing Surfaces from Pressure Distributions," NASA CR-3713, 1983. 83N29198

[3] Taylor III, A.C., Korivi, V.M., Hou, G.W.,"Aerodynamic Shape Optimization Using Sensitivity Analysis Methods for Viscous Flow Involving Variation of Geometric Shape", AIAA paper No. 91-1569.

[4]Korivi, V.M., et al.,"An Incremental Strategy for Calculating Consistent Discrete CFD Sensitivity Derivatives,"NASA TM 104207, Feb 1992. 92N24681

[5]Elbanna, H.M., and Carlson, L.A.,"Determination of Aerodynamic Sensitivity Coefficients Based on the Transonic Small Perturbation Formulation,"*AIAA Journal,* Vol. 27, No. 6, June 1990, pp. 507-515.

[6]Elbanna, H.M., and Carlson, L.A.,"Determination of the Aerodynamic Sensitivity Coefficients Based on the Three-Dimensional Full Potential Equation," AIAA Paper No. 92-2670, June 1992.

[7]Baysal, O., Eleshaky, M.E., and Burgreen, G.W.,"Aerodynamic Shape Optimization Using Sensitivity Analysis on Third-Order Euler Equation," AIAA Paper No. 91-1557-CP, June 1991.

[8]Korivi, V.M., and Taylor, A.C. III, et al.,"An Approximately Factored Incremental Strategy for Calculating Consistent Discrete Aerodynamic Sensitivity Derivatives," AIAA Paper No. 92-4746, Sept 1992.

[9]Sobieszczanski-Sobieski, Jaroslaw, "Multidisciplinary Optimization For Engineering Systems: Achievements and Potential,"NASA TM 101566, March 1989. 89N24508

[10]Timoshenko, S., and Woinowsky-Krieger, S., *Theory of Plates and Shells,* Second edition, McGraw-Hill International Book Co., Tokyo-Japan, 1984, pp. 83-84.

[11]Sobieszczanski-Sobieski, J.,"Sensitivity of Complex Coupled Systems,"*AIAA Journal,* Vol. 28, No. 1, January 1990, pp. 153-160.

[12]Abbot, I.H., and Von Doenhoff, A. E., *Theory of Wing Sections,* Dover, New York, 1959.

[13]Carnahan, B., Luther, H.A., and Wilkes, J.O., *Applied Numerical Methods,* John Wiley & Sons, Inc., New York, 1969.

[14]Kapania, R.K., Eldred, L.B., and Barthelemy, J.-F. M.," Sensitivity Analysis of a Wing Aeroelastic Response," *AIAA Journal,* Vol. 30, No. 4, 1992, pp 496-503.

[15]Weed, R.A., Anderson, W.K., and Carlson, L.A.," A Direct-Inverse Three Dimensional Transonic Wing Design Method for Vector Computers,"AIAA paper No. 84-2156, August 1984.

[16] Arslan, A. E.," Analysis and Numerical Computation of Sensitivity Derivatives in the Transonic Regime," M.S. Thesis, Texas A&M University, College Station, Texas, December 1993.